

T.R.
ONDOKUZ MAYIS UNIVERSITY
INSTITUTE OF GRADUATE STUDIES
DEPARTMENT OF NANOSCIENCE AND NANOTECHNOLOGY

**PRODUCTION OF NOVEL $\text{TiO}_2\text{-Ag+ZrO}_2$ - THIN FILMS AS
ANTIMICROBIAL AND MULTIFUNCTIONAL USAGE BY
ELECTROSPRAY DEPOSITION SYSTEM**

Master Thesis

Abdulmohsin AL AIROA

Supervisor

Assist. Prof.Dr. İbrahim İNANÇ

SAMSUN
2020

THESIS APPROVAL

This master thesis study under the name of “**Production of Novel TiO₂–Ag+ZrO₂-Thin Films as Antimicrobial and Multifunctional Usage by Electropray Deposition System**” which is prepared and presented by Abdulmohsin AL AIROA, is approved as Master Thesis in Nanoscience and Nanotechnology Department at Ondokuz Mayıs University by committee members listed below on 16 / 7 / 2020

Thesis Advisor Assist. Prof. Dr. İbrahim İNANÇ
Ondokuz Mayıs University
Metallurgical and Materials
Engineering Department

**Committee Members
Committee
Chairman** Assist. Prof. Dr. İbrahim İNANÇ
Ondokuz Mayıs University
Metallurgical and Materials
Engineering Department

Committee Member Assoc. Prof. Dr. Abdulaziz KAYA
Gaziantep University
Metallurgical and Materials
Engineering Department

Committee Member Assist. Prof. Dr. Sinem ÇEVİK
Ondokuz Mayıs University
Metallurgical and Materials
Engineering Department

Approved in __/__/20__
Prof. Dr. Ali BOLAT
Institute Manager

ETHICAL STATEMENT

I declare that all the information given in this dissertation is true and absolute which is prepared in conformity with the regulations for Ondokuz Mayıs University Graduate School of Science and thesis writing rules, all the information were referred and kept on the right side of the laws according to scientific ethic during in the stage of production of information.

16/07/2020

Abdalmohsin AL AIROA



ABSTRACT

PRODUCTION OF NOVEL $\text{TiO}_2\text{-Ag+ZrO}_2$ THIN FILMS AS ANTIMICROBIAL AND MULTIFUNCTIONAL USAGE BY ELECTROSPRAY DEPOSITION SYSTEM

Abdalmohsin AL AIROA

Ondokuz Mayıs University

Institute of Graduate Studies

Department of Nanoscience and Nanotechnology

M.A., July/ 2020

Supervisor: Assist. Prof.Dr. İbrahim İNANÇ

In the industrial field, as in all other life fields, a huge number of microorganisms exist as fungi or bacteria. Almost of these microorganisms have negative effects on human life. Therefore, for health care in all fields, the effects of bacteria and fungi on the surface of industrial equipments (pharmaceutical and food industry equipments) should be minimized or eliminated. In this study we produced an antimicrobial and multifunctional hybrid thin film of titania (TiO_2), silver nanoparticles (AgNPs) and yttria-stabilized zirconia (YSZ) on stainless steel substrate. Silver nanoparticles have been the antimicrobial agent because of its historic rendering in different medical domains because of its vigorous antimicrobial assessment. Titania plus yttria-stabilized zirconia enhance thermal and corrosion resistance.

In the first step, the colloid silver nanoparticles with six different concentrations (1 mM, 3 mM, 5 mM, 7 mM, 9 mM and 18 mM) were synthesized by sol-gel technique. Colloid silver nanoparticles were produced by a thermal chemical reduction method of silver nitrate salt and trisodium citrate with addition of ethylene glycol as a suspension agent.

In the second step, two different suspensions were prepared for (1% wt.) TiO_2 and (1% wt.) YSZ nanopowder as a coating suspension. Titania suspension prepared by dissolving 1 g of TiO_2 powder with particle size 20 nm in a mixture of distilled water, ethanol, ethylene glycol and a few drops of ammonia. YSZ suspension was prepared by dissolving 1g of YSZ with particle size 25 nm in a 100 ml of isopropanol solution.

Then, the two solutions were coating by Electro spray Deposition process. TiO_2 and YSZ solutions were mixed to produce the final coating solution. Electro spray Deposition device was used as a coating system. After coating of the solutions on steel substrate, sintering was made under Ar gas at 1000°C .

In the final step, 5 mM of synthesized colloid silver nanoparticles was chosen to be the final coating solution. Silver nanoparticles were coated above the samples that were produced in the second step. Then, silver nanoparticles were coated by using electro spray technique and coated steel substrate was sintered under Ar gas at 450°C .

The obtained colloids and thin films were characterized by using (SEM), (EDX), (XRD) and (AFM). The antimicrobial activity of thin films were performed by Diffusion Method and investigated against different types of microorganism.

Key words: Thin Film Coating, Electro spray Deposition, TiO_2 , YSZ, AgNPs, Antimicrobial activity.

ÖZET

ANTİMİKROBİYAL VE ÇOK FONKSİYONLU KULLANIM OLARAK YENİ TiO₂ –Ag + ZrO₂ THIN FİMLERİNİN ELEKTROSPRAY YATIRMA SİSTEMİ İLE ÜRETİMİ

Abdilmohsin AL AIROA

Ondokuz Mayıs Üniversitesi

Lisansüstü Eğitim Enstitüsü

Nanobilim ve Nanoteknoloji Anabilim Dalı

Yüksek Lisans Tezi, Temmuz /2020

Danışman: Yrd. Doç. Dr. İbrahim İNANÇ

Diğer tüm yaşam alanlarında olduğu gibi endüstriyel alanda da mantar veya bakteri olarak çok sayıda mikroorganizma bulunur. Bu mikroorganizmaların hemen hemen insan yaşamı üzerinde olumsuz etkileri vardır. Bu nedenle her alanda sağlık hizmeti için bakteri ve mantarların endüstriyel ekipmanların (ilaç ve gıda sanayi ekipmanları) yüzeyine olan etkileri en aza indirilmeli veya ortadan kaldırılmalıdır. Bu çalışmada, paslanmaz çelik substrat üzerinde antimikrobiyal ve çok işlevli bir hibrit ince film titanya (TiO₂), gümüş nanopartiküller (AgNP'ler) ve itriya ile stabilize edilmiş zirkonya (YSZ) ürettik. Gümüş nanopartiküller, güçlü antimikrobiyal değerlendirmesi nedeniyle farklı tıbbi alanlarda tarihsel olarak yorumlanması nedeniyle antimikrobiyal ajan olmuştur. Titania ve itriya ile stabilize edilmiş zirkonya, termal ve korozyon direncini artırır.

İlk aşamada, altı farklı konsantrasyonda (1 mM, 3 mM, 5 mM, 7 mM, 9 mM ve 18 mM) kolloid gümüş nanopartiküller sol-jel tekniği ile sentezlendi. Kolloid gümüş nanopartiküller, süspansiyon ajanı olarak etilen glikol ilavesiyle gümüş nitrat tuzu ve trisodyum sitratın termal kimyasal indirgeme yöntemi ile üretildi.

İkinci adımda, kaplama süspansiyonu olarak (ağırlıkça% 1) TiO₂ ve (ağırlıkça% 1) YSZ nanotutu için iki farklı süspansiyon hazırlandı. 20 nm partikül büyüklüğüne sahip 1 gr TiO₂ tozunun distile su, etanol, etilen glikol ve birkaç damla amonyak karışımı içinde çözülmesiyle titanya süspansiyonu hazırlandı. YSZ süspansiyonu, 25 nm partikül boyutuna sahip 1 g YSZ'nin 100 ml izopropanol çözeltisi içinde çözülmesiyle hazırlandı.

Ardından, iki çözelti Elektrosprey Biriktirme işlemi ile kaplandı. TiO₂ ve YSZ çözeltileri, nihai kaplama çözümünü üretmek için karıştırıldı. Kaplama sistemi olarak Elektrosprey Çökeltme cihazı kullanıldı. Çözeltilerin çelik alt tabaka üzerine kaplanmasından sonra Ar gazı altında 1000 ° C'de sinterleme yapıldı.

Son aşamada, son kaplama çözümü olarak 5 mM sentezlenmiş kolloid gümüş nanopartiküller seçildi. İkinci adımda üretilen örneklerin üzerine gümüş nanopartiküller kaplandı. Daha sonra gümüş nanopartiküller elektrosprey tekniği ile kaplandı ve kaplanmış çelik substrat Ar gazı altında 450 ° C'de sinterlendi.

Elde edilen kolloidler ve ince filmler (SEM), (EDX), (XRD) ve (AFM) kullanılarak karakterize edildi. İnce filmlerin antimikrobiyal aktivitesi Difüzyon Yöntemi ile yapılmış ve farklı mikroorganizma türlerine karşı araştırılmıştır.

Anahtar kelimeler: İnce Film Kaplama, Elektrosprey Kaplama, TiO₂, YSZ, AgNP'ler, Antimikrobiyal aktivite.

ACKNOWLEDGEMENTS

First of all, I would like to thank my supervisor **Dr. İbrahim İNANÇ** and my co-supervisor **Dr. Mevlüt GÜRBÜZ** for their support, providing the equipment and devices necessary to complete this work and its success and give them the freedom to work for me and for whom without their good advice and guidance, this work would not have been successful. My supervisor , **Dr. İbrahim İNANÇ** has been in contact with me throughout all the stages of work and I have been fortunate to be one of his students

I would also like to express my gratitude and appreciation to **Dr. Hilal AY** for her support and participation in the work of biological tests.

I would also like to thank all the members of the department of nanoscience and nanotechnology and engineering faculty of Ondokuz Mayıs university who helped me during the work.

I thank my friends **Mohammed Abdulwahab, Mohammed Jabbar, Belgihan** and **Rafid** who helped me in the study and work stages.

Finally, I can only offer gratitude and appreciation to my family, without whom I would not have passed all obstacles in my life through their dedicated support to me.

TABLE OF CONTENTS

ABSTRACT	i
ÖZET	iii
ACKNOWLEDGEMENTS	v
TABLE OF CONTENTS	vi
ABBREVIATIONS	ix
FIGURES INDEX.....	x
TABLE LIST	xiii
1. INTRODUCTION	1
2. NANOCOATING	6
2.1. Definition	6
2.2. Classification of Nanocoating	7
2.2.1. Metallic Nanocoating.....	7
2.2.2. Ceramic Nanocoating	8
2.2.3. Nanopolymer Coatings	8
2.2.4. Nanocomposite Coating.....	8
2.3. Nanocoating Applications	9
2.3.1. Antimicrobial Coating	9
2.3.2. Anticorrosion Coatings	10
2.3.3. Self- Cleaning and Biocidal Coatings.....	11
2.3.4. Scratch and Abrasion Resistant Coatings	12
2.3.5. High Thermal Resistant and Fire Resistant Coatings	12
3. NANOMATERIAL	14
3.1. Definition	14
3.2. Silver Nanoparticles (AgNPs).....	17
3.2.1. Antibacterial Activity of AgNPs.....	17
3.3. Titanium Dioxide TiO ₂	19
3.4. Zirconium Dioxides (ZrO ₂).....	20
4. THIN FILMS	22
4.1. Definition	22
4.2. Thin Film Deposition Techniques.....	23

4.2.1. Sol-Gel Deposition	24
4.2.2. Spin Coating	25
4.2.3. Electrospray Deposition (ESD)	26
4.3. Sintering	27
4.4. Agar Diffusion Test.....	28
5. LITERATURE REVIEW.....	29
6. MATERIALS AND METHODS.....	32
6.1. Synthesis of AgNPs.....	32
6.1.1. Materials:	32
6.1.2. Methods	32
6.1.3. Antimicrobial Test of Colloidal AgNPs	34
6.2. Synthesis of TiO ₂ Thin Film.....	34
6.2.1. Material.....	34
6.2.2. Method.....	34
6.3. Synthesis of YSZ Thin Film.....	35
6.3.1. Material.....	35
6.3.2. Method.....	35
6.4. Synthesis of TiO ₂ –YSZ Thin Film	36
6.4.1. Materials and Method	36
6.5. Synthesis of Ag Thin Films	36
6.5.1. Antimicrobial Test of Ag Thin Films	36
6.6. Chemical, Physical and Biogecal Characterization.....	37
6.6.1. SEM and EDX Characterization.....	37
6.6.2. XRD characterization	37
6.6.3. AFM Characterization	38
6.6.4. Antimicrobial Test	38
6.6.5. Image J Program	38
7. RESULT AND DISCUSSION	39
7.1. Characterization of AgNPs.....	39

7.1.1. Antimicrobial Assay of Synthesized AgNPs	39
7.1.2. SEM and EDX Analysis	41
7.2 .Characterization of TiO ₂ , YSZ and TiO ₂ –YSZ Coatings.....	45
7.2.1. XRD Analysis	45
7.2.2. SEM and EDX Analysis	48
7.2.2.1 .TiO ₂ Coating	48
7.2.2.2. YSZ Coating	50
7.2.2.3. TiO ₂ –YSZ Coatings	52
7.2.3. AFM Analysis.....	55
7.2.3.1. TiO ₂ Coating Analysis.....	55
7.2.3. 2. YSZ Coating Analysis	56
7.2.3.3. TiO ₂ –YSZ Coatings Analysis	57
7.3. Ag Thin Films Analysis.....	58
7.3.1. SEM and EDX Analysis	58
7.3.1.1. TiO ₂ –Ag Coating	58
7.3.1.2. YSZ–Ag Coating.....	60
7.3.1.3. TiO ₂ –YSZ–Ag Coating	62
7.3.2. Antimicrobial Assay of Fabricated Thin Films	65
8. CONCLUSION	67
FEATURE WORK	69
REFERENCE.....	70
CURRICULUM VITAE	83

ABBREVIATIONS

AFM	Atomic force microscopy
AgNPs	Silver nanoparticles
ALD	Atomic layer deposition
Ar gas	Argon gas
CVD	Chemical vapor deposition
EDS	Energy-dispersive X-ray spectroscopy
ENs	Engineered nanomaterials
EPD	Electrophoretic deposition
ESD	Electrospray deposition
PVD	Physical vapor deposition
RMS	Root mean square
SEM	Scanning electron microscopy
STM	Scanning tunneling microscope
TiO ₂	Titanium dioxide
UVS	UV-Vis spectrometry
XRD	X-Ray Diffraction
YSZ	Yttria stabilized zirconia
ZrO ₂	Zirconium dioxides
Ra	Average Roughness
Rms	Root mean square

FIGURES INDEX

Figure 2.1. Classes of antibacterial coatings: (a) repelling bacterial attachment or biofilm development; (b) contact killing; (c) releasing of antibacterial agents; and (d) stimuli responsive release in the presence of bacteria....	10
Figure 2.2. Self-cleaning action of nano coating	11
Figure 3.1. Classification of Nanomaterials (a) 0D spheres and clusters, (b) 1D nanofibers, wires, and rods, (c) 2D films, plates, and networks, (d) 3D nanomaterials	16
Figure 3.2. Schematic representation of mechanisms of antimicrobial activity of AgNPs	18
Figure 3.3. Chemical formula of TiO ₂	19
Figure 3.4. Chemical structures of ZrO ₂ and YSZ.....	21
Figure 4.1. Schematic of various routes in the sol-gel process.....	24
Figure 4.2. Schematic illustration of Spin Coating process	25
Figure 4.3. Schematic diagram of Electrospray deposition	24
Figure 4.4. A model explaining the sintering process.....	25
Figure 4.5. Agar diffusion method.....	26
Figure 5.1. chemical preparation of colloidal AgNPs.....	30
Figure 5.2. Colors of synthesized colloidal AgNPs	31
Figure 5.3. Scanning electron microscope Jeol brand JSM7001F model.....	35
Figure 5.4. X-ray diffraction device Rigaku SmartLab model	35
Figure 5.5. Atomic force microscopy (SLOVER NEXT).....	36
Figure 6.1. Result of Antimicrobial activity of AgNPs in (a) <i>Aspergillus niger</i> , (b) <i>Candida albicans</i> , (c) <i>Escherichia coli</i> , (d) <i>Staphylococcus aureus</i> , (e) <i>Bacillus subtilis</i> , (f) <i>Listeria monocytogenes</i> , (g) <i>Salmonella enterica</i> , (h) <i>Enterococcus faecalis</i> and (i) <i>Klebsie</i>	39
Figure 6.2. SEM images of synthesized AgNPs in (a) 1 mM and (b) 3 mM.....	41
Figure 6.3. SEM images of synthesized AgNPs in (a) 5 mM and (b) 7 mM.....	41
Figure 6.4. SEM images of synthesized AgNPs in (a) 9 mM and (b) 18 mM.....	42
Figure 6.5. EDX analysis of fabricated solution in (a) synthesized AgNPs, (b) chemical composition of collidal AgNPs and (c) elemental analysis of collide AgNPs	41
Figure 6.6. XRD patterns of the stainless steel substrate.....	43
Figure 6.7. XRD patterns of the (a) TiO ₂ powder and (b) YSZ powder	44
Figure 6.8. Evolution of diffraction patterns of (a) YSZ powder, (b) TiO ₂ powder (c) TiO ₂ –YSZ coating, (d) YSZ coating and (e) TiO ₂ coating.....	44
Figure 6.9. SEM images of TiO ₂ coating surface in (a) microscale (b) nanoscale ...	48
Figure 6.10. EDX analysis of fabricated TiO ₂ coating in (a) SEM image of TiO ₂ coating surface morphology at 10µm (b) chemical composition of TiO ₂ coating and (c) elemental analysis of TiO ₂ coating.....	47
Figure 6.11. SEM images of YSZ coating surface in (a) microscale (b) nanoscale	508

Figure 6. 12. EDX analysis of fabricated YSZ coating in (a) SEM image of YSZ coating surface morphology at 10 μ m (b) chemical composition of YSZ coating and (c) elemental analysis of YSZ coating.....	49
Figure 6. 13. SEM images of (a) TiO ₂ –YSZ coating surface in microscale (b) TiO ₂ –YSZ coating surface in nanoscale and (c) TiO ₂ –YSZ film cross section	50
Figure 6. 14. EDX analysis of fabricated TiO ₂ – YSZ coating in (a) SEM image of TiO ₂ – YSZ coating surface morphology at 1 μ m (b) chemical composition of TiO ₂ – YSZ coating and (c) elemental analysis of TiO ₂ – YSZ coating	52
Figure 6. 15. AFM images of the TiO ₂ coating samples: (a) 2D image and (b) 3D image	53
Figure 6. 16. AFM images of the TiO ₂ coating samples: (a) 2D image and (b) 3D image	54
Figure 6. 17. AFM images of the TiO ₂ –YSZ coating samples: (a) 2D image and (b) 3D image	55
Figure 6. 18. SEM images of (a) TiO ₂ –Ag coating surface in microscale (b) TiO ₂ –Ag coating surface in nanoscale and (c) TiO ₂ –Ag film cross section....	58
Figure 6. 19. EDX analysis of fabricated TiO ₂ – Ag coating in (a) SEM image of TiO ₂ – Ag coating surface morphology at 1 μ m (b) chemical composition of TiO ₂ – Ag coating and (c) elemental analysis of TiO ₂ – Ag coating..	58
Figure 6. 20. SEM images of (a) YSZ –Ag coating surface in microscale (b) YSZ –Ag coating surface in nanoscale and (c) YSZ Ag film cross section.....	60
Figure 6. 21. EDX analysis of fabricated YSZ – Ag coating in (a) SEM image of YSZ – Ag coating surface morphology at 1 μ m (b) chemical composition of YSZ – Ag coating and (c) elemental analysis of YSZ – Ag coating ..	62
Figure 6. 22. SEM images of (a) TiO ₂ –YSZ–Ag coating surface in microscale (b) TiO ₂ –YSZ–Ag coating surface in nanoscale and (c) TiO ₂ –YSZ–Ag film cross section	62
Figure 6. 23. EDX analysis of fabricated TiO ₂ –YSZ–Ag coating in (a) SEM image of TiO ₂ –YSZ–Ag coating surface morphology at 1 μ m (b) chemical composition of TiO ₂ –YSZ–Ag coating and (c) elemental analysis of TiO ₂ –YSZ–Ag coating.....	64
Figure 6. 24. Result of Antimicrobial activity of (a) TiO ₂ –Ag coating in <i>Escherichia coli</i> , (b) YSZ–Ag coating in <i>Escherichia coli</i> , (c) TiO ₂ –YSZ–Ag coating in <i>Escherichia coli</i> ,(d) TiO ₂ –Ag coating in <i>Pseudomonas aeruginosa</i> , (e) YSZ–Ag coating in <i>Pseudomonas aeruginosa</i> ,(f) TiO ₂ –YSZ–Ag coating in <i>Pseudomonas aeruginosa</i> ,(g) TiO ₂ –Ag coating in <i>Candida albicans</i> ,(h) YSZ–Ag coating in <i>Candida albicans</i> (i) TiO ₂ –YSZ–Ag coating in <i>Candida albicans</i> (f) TiO ₂ –YSZ–Ag coating in	

Pseudomonas aeruginosa (g) TiO₂-Ag coating in *Candida albicans* (h)
YSZ-Ag coating in *Candida albicans* and (i) TiO₂-YSZ-Ag coating in
Candida albicans..... 66



TABLE LIST

Table 1. The weights and molar concentrations of the materials that used in preparing the colloidal AgNPs	33
Table 2. Concentration of colloidal AgNPs vs Inhibition zone on microorganisms .	40
Table 3. The average particle size of AgNPs in AgNO ₃ solutions	42
Table 4. Effect of thin films vs Inhibition zone diameter on microorganisms	66



1. INTRODUCTION

Nanotechnology can be labeled as the survey that dominates and manipulation of the nanoscales materials, commonly that are having dimensions not more than 100 nm (K. Mallikarjuna et al., 2012). Nanomaterials are often having special chemical and physical properties, just by their physical applications in many domains have spurred the look for a replacement fabrication method for material (M. A. Meyers et al., 2006). Metal nanoparticles are enormously investigated due to their unique optical and electrical properties that are various from bulk materials (G. Schimid and L. F. Chi, 1998). Nanoparticles are over a wide range used according to its size, orientation, physical properties; that may change the performance of the fabric (M. C. Daniel and D. Astruc, 2004). Finely strewn nanostructures or nanoparticles are utilized in many foods, medical and technological applications, such as ceramics, metallic and polymer nanocomposites, pigments, filler materials, electronics, fibers, catalysts and lots of others (M. Willert et al., 2001). Also, it's swiftly earning importance over a number of fields like healthcare, cosmetics, food and feed fields, environmental event, device , biomedical application, pharmaceutical applications, chemical corporation, drug delivery, energy, optoelectronics, catalysis, single electron transistors, light emitters, non-linear optical devices and photo electro-chemical applications (V. Colvin et al., 1994).

Colloidal particles are increasingly receiving attention as a crucial start line for the generation of micro and nanostructures (Asta Sileikaite et al., 2006; Yakutik IM et al., 2004). Nanoparticles are increasingly beneath active research because of they possess impressive physical properties that vary significantly from that of the bulk phase. It comes from small sizes and a high ratio of surface/volume (Asta Sileikaite et al., 2006; Ratyakshi ; Chauhan RP, 2009).

AgNPs offer rare physical and chemical properties. They possess perfect conductivity, chemical and optical stability as well as catalytic activity. These properties are straightly hooked into AgNPs size, size distribution and shape of particles (Kimet al., 2006; Xiong. et al., 2007). Additionally, silver materials with one and two dimensional nanostructures of silver materials, involving nanocubes and nanowires, are considered to possess wide prospect applications (Thompson et al., 2008; Takenobu T. et al., 2009).

Since the past, the silver ion has been recognized to be effective versus a wide range of micro-organisms (N. Savithamma et al., 2011). In the present time, silver ions are utilized to controlling the growth of bacterial and fungi during a sort of medical and, health care applications, pharmaceutical applications and food application (Mritunjai Singh et al., 2008; Vyom Parashar et al., 2009). The applications are robustly hooked in to the physical properties of silver nanostructure such as, the crystal structure, dimensions, and morphology. It does describe that the mechanism behind its antimicrobial activity is by targeting to the bacteria cell membrane, disturbing the permeability and intermembrane exchange. Another antimicrobial effect mechanism of silver ions is neatly associated with their reaction with phosphorous and sulfur containing biomolecules involving DNA and proteins by undermining DNA replication and inefficient proteins (N. Savithamma et al., 2011).

Titanium dioxide (TiO_2) may be an inexpensive, non-biodegradable, and non-toxic material, besides their widespread utilizes in diverse industries (Larson S. A and Falconer J. L., 1994). Zirconium dioxide (ZrO_2) has perfect insulation and optical properties it's a high refraction index. In addition, it's a really good translucence on a broad spectral range, an excellent chemical and biogecal stability and a sill of resistance to high laser flow (Zelner M et al., 1997; Wang M.T et al., 2005). Yttria-stabilized zirconia (YSZ) ceramic nanoclusters have wide selection of specific considerable properties like high ionic conductivity, high strength, low thermal conduction, chemical subsidence, excellent chemical and thermal stability, and high refractive index (He et al., 2014; Kumari et al., 2009).

Sol-gel process (Hu L et al., 1992; Brinker C.J and Scherer G.W, 1990; Brinker C.J et al., 1991) is an engaging alternate to other synthesis methods of metals, ceramics and glasses for several reasons: for instance, synthesis of coldness, simple equipment's to be used, thin film configurable then on. Especially, sol-gel process is extremely beneficial for thin film deposition due to the potential to coat materials of varied shapes and/or big area, to regulate the composition easy to gaining solutions of homogeneity and controlled concentrations without using expensive equipment.

Thin film can be described as a skinny layer of fabric, where the thickness is varied from several nanometers to few micrometers. Like all materials, the structure of thin films is split into amorphous and polycrystalline structure counting on the preparation conditions also because the material nature. Thin films are formed by depositing material on a clean suitable substrate to grown up film thickness rather than thinning down the majority material (Wasa K et al., 2004).

Several methods are used for the preparation and production of thin films, like chemical vapor deposition (Aidla A et al., 1997), spin coating (Aegerter and Mennig, 2004; Kohli, 2007), atomic layer deposition (Ponraj J. S., 2013), physical vapor deposition (Mattox, 1998), electrospray deposition (Jaworek A. and Sobczyk, A.T 2008), electrophoretic deposition (Besra L and Liu M 2007), and sol–gel method (Hu L et al., 1992). As compared with other coating methods, the sol–gel method has several advantages like controllability, reliability, reproducibility and may be chosen for the preparations and productions of nanostructured thin films (Hu L et al., 1992; Chrysicopoulou P et al., 1998).

Titanium and zirconium oxides are very propitious nominees for future technology of thin films due to their attractive properties such as mechanical, thermal and chemical. The previous properties lead to miscellaneous applications like laser mirrors, optical filters or barriers layers from the warmth. Titania (TiO_2) thin films are widespread under the active studied due to their attractive chemical, physical and biogecal properties (Zheng S.K et al., 2001). TiO_2 film in anatase phase could achieve the photocatalytic degradation of organic components under the radiation of UV. Therefore, it's an expansion of application possibility within the field of environmental preservation (Takeda S. et al., 2001). Zirconia (ZrO_2) films are used as block layer for high conducting ceramics (Wendel H et al. 1990; Fork D.K et al. 1990), like biomaterial for prostheses, as gas sensor or like component in combustible batteries. Zirconia is translucent within the visible; it's high index of refraction and band gap values, perfect adhesion to substrates (glass, ceramics, silicon, polycor, and sapphire), high thermal stability, and corrosion and scratch resistance (N.T. Soo et al., 2012; K. Joy, S et al., 2012).

YSZ ceramic nano-clusters are interesting for several applications like high-for the high-temperature heat barrier coatings (TBCs), fuel cells, nanocatalysis, sensors, bio-separation, and chromatography (J. H. Shim et al., 2007; D. Chen et al., 2010; D. Lu et al., 2011; B. Yan et al., 2005).

Electrospray may be a curious spraying technique, in its ability to supply tiny, electrically charged droplets with high size uniformity at ambient conditions, during a wide size range, from 10's of nanometers to 100's of microns (Rosell-Llompart, 1994; Tang, 1994; Chen, 1995). Also, the ESD technique is straightforward, easily controllable, coldness process, rapid, cost effective and suitable for large-scale sensor production.

In the present work, AgNPs were produced by thermal chemical reaction between silver nitrate with ethylene glycol solution and trisodium citrate dehydrate solution as a reductant is administered. AgNPs were characterized by SEM and EDX. According to SEM results of six different concentrations of colloid AgNPs, it had been observed that the particles are homogenous and uniform in size within the particles range between 25–65 nm. The antimicrobial assay of AgNPs was investigated versus total nine differing types of microorganism; seven differing types of bacteria such as: *Escherichia coli*, *Klebsiella pneumoniae*, *Listeria monocytogenes*, *Staphylococcus aureus*, *Bacillus subtilis*, *Salmonella enterica* and *Enterococcus faecalis* and two sorts of fungi such as: *Aspergillus niger* and *Candida albicans*.

TiO₂, YSZ and TiO₂ –YSZ films was fabricated by using Electrospray Deposition process on stainless steel substrates, then sintered at a high temperature under argon gas. Fabricated coatings were characterized by using SEM, EDX, XRD and AFM.

In the final coating stage, colloidal silver nanoparticles were used as a coating solution over TiO₂, YSZ and TiO₂ –YSZ films by using Electrospray Deposition system. After coating the samples sintering was made at 450°C with the presence Ar gas as a shield for 20 minutes. The ultimate coated samples were characterized by SEM and EDX. TiO₂–Ag, YSZ–Ag and TiO₂ –YSZ–Ag thin films exhibited antimicrobial activity against micro-organism; bacteria and fungi two kinds of

bacteria such as: *Escherichia coli* and *Pseudomonas aeruginosa*, with *Candida albicans* fungi.



2. NANOCOATING

2.1. Definition

One of the most important nanotechnology branches is nanocoating, that which can be described as the series of steps for covering material with the support of a film on the nanoscale or to shield a nanoscale body. A nanocoating is a very fine microstructure where one or all of the constituents (boundaries, crystals, phases, etc.) are on the size less than 100 nm. Nanocoatings also can be constructed up by layers with a thickness lower than 100 nm (Schaefer and H.-E, 2010; Yousaf, S et al., 2015). They require a high density of interphase boundaries, grain boundaries and dislocations, where the distance between the approach to interatomic distances. Hence, coatings within nanostructure offer various properties from the traditional coatings, which enabled them to get over the wear and corrosion properties of their competitors. Nanocoatings are often classified consistent with the coordinated materials, like ceramic and metallic nanocoatings, or composed of two or more materials that are within the nanometer scale, just like in nanocomposite coatings. They have one or more components that are within the nanometer scale. According to very fine particles sizes of the utilized in this nanocoating, stuffing the spaces and blocking the corrosives elements from diffusing into the surface of the substrate are going to be more effective. Additionally, the elevated densities of the nanocoatings' grain boundaries supply superior adhesion properties, which can rise the lifetime of the coating.

Nanostructured coatings advance excellent chemical and physical properties, which make them powerful, rigid (Schuh et al., 2003), and have finest resistance to environments with corrosion, scratch and wear (Sriraman et al., 2015). The addition of properties like self-healing (Andreatta et al., 2007), self-cleaning (Sriraman et al., 2012), and super scratch and wear resistance was enhanced due to the highly affected to the event of paints (Wang et al., 2016). Nanocoating allows the supply of surrogates for the toxicity of chromium coating (Ma et al., 2016; Hibbard et al., 2001). Smart nanocoatings extremely interest in decrease corrosion and biofouling damage. Nanocoatings are improved to return to exterior motivation like pH, humidity, heat, stress, coating distortion, electromagnetic wave, etc., that will be by liberation controlled quantities of inhibitors so as to renovation and recovery defects and damages (McGee et al., 2012).

According to exceptional properties that the nanocoating possesses, they're utilized in daily practice like clothing, computers, cell phones, and eyeglasses. within the building field, they're utilized in tiles, windows, flooring, walls, paints, air filters, etc. the use of the nanolayer in these appliances makes them flame-retardant, wear and scratch resistant, anti-graffiti, corrosion resistant, self-cleaning, and antimicrobial resistance. They even have perfect adhesion, optical clarity, anti-fogging and anti-fouling properties, and are convenient as a photovoltaic material (Boostani et al., 2016). Within the biomedical area, metallic nanocoatings are wont to moderate surface properties when needed. They're utilized in the drugs industry primarily for etch protection, surface covering, and anti-corrosion functions, additionally to other minor functions like drug delivery and biocompatibility (Mahapatro, A, 2015). For all of the aforesaid properties that the nanocoatings convene they're utilized in many other fields like the military, the car industry, energy efficiency, the environment, etc.

2.2. Classification of Nanocoating

Nanocoatings are commonly classified to four different types: metallic nanocoating, ceramic nanocoating, nanocomposite coating and polymeric nanocoating.

2.2.1. Metallic Nanocoating

Metallic nanocoating generally consist of metals that are includes at less one of the pure metals. Pure metals are the main building units in metallic nanocoating that are like Cadmium (Cd), Nickel (Ni), Tungsten (W), Zinc (Zn), Phosphorous (P), Cobalt (Co), Iron (Fe), Cupper (Cu), etc. Nanocoating are often consist of a pure metal (Wang et al., 2006; Wang et al., 2007), or alloyed of pure metals for reason of the reinforcement of properties. That reinforcement is reinforced with the use of nanocoating, as nanomaterials conduct variously than micromaterials. Metallic nanocoatings are often produced during quite one technique like sputtering (Lu et al., 2006) and multi-arc ion plating (Guan et al., 2015), additionally to electrodeposition, which was be seen to be the foremost used technique in depositing metals (Li et al., 2009).

They already have a vast range of applications in many fields, like automotive, aerospace (Sriraman et al., 2012), seawater condensers and tubes, electronic manufactures, water electrolysis, energy generation (Mosavat et al., 2012; Ghosh et al., 2006), etc.

2.2.2. Ceramic Nanocoating

Ceramic nanocoating consists of compounds among metallic and nonmetallic materials, which are called ceramic materials, compounds; the foremost customarily known ceramics are oxides, nitrides, and carbides. Ceramic oxide coatings have a preferable advantage across metallic or organic oxides; they equipping a remote superior coating, even with a minimum thickness, because their higher hardness and strength (Watchman et al., 1993). Ceramic nanocoatings are performed in a wide range of industrial fields because of their engaging thermal and electrical properties, which they're more immune to oxidation, corrosion, and wear than metals in heat environments (Callister et al., 2012).

2.2.3. Nanopolymer Coatings

Conducting polymers have triggered an excellent package of benefit according to their electrochemical properties and their mixed ionic/electronic conductivity properties (Rout et al., 2003). They have many been used as steward matrices in different composite films. Organic and inorganic particles are often mixed with or integrated within the conducting polymers to turn their morphology, conductivity and different physical properties building onto the appliance, like corrosion safeguard. A nanocomposite with Polycrystalline form that contains conductive polymers was occurring to provide unfamiliar properties. Basically conducting polymer (ICP) films including inhibiting anions because the dopant anions can liberate them when the film is connected to a breach within the coating.

2.2.4. Nanocomposite Coating

The suitable description of nanocomposite coating is a material composed of at the minimum of two unmixable phases, which are isolated by an interface zone. The matrix is the most employing component in nanocomposite coating, during which the filler is dispersed (Nguyen et al., 2018).

The controlling a part of the composite, which is usually the fabric that possesses properties to be reinforced can describe the matrix. The matrix is often metallic, ceramic, polymer or a mixture of them with a dimension bigger than nanoscale.

Nanomaterials involve important constituent called fillers which will be within the nanoscale (0D, 1D, and 2D), therefore the nanocomposite coating is categorized consistent with the filler dimension. Nanoparticles (0D); nanotubes, nanowires, or nanorods (1D); or nanoplatelets, nanosheets, or nanofilms (2D) can be considered as fillers. A two-dimension nanocomposite coating can have a sandwich or laminate shape. Laminate nanocomposite consists of thin layers at thickness within nanolevel of at least two diverse type materials (Li et al., 2015). The sandwich nanocomposite may be a large scale layer with thickness upper than 100 nm, deposited on both surfaces of a nanoscale layer (Wu et al., 2010). The major objective of composing two various materials in one coating are to possess a replacement nanocomposite material with unique characteristics and excellent properties confront to all material separately. Popular nanocomposites that are used for coating are matrix-enhanced. In various composite films, polymers used as host matrices, nanomaterials as a filler or pigment are combined within the polymer matrix. The hybrid organic and inorganic material is understood as a polymer nanocomposite while fillers are inserted into a polymer, (Mittal V., 2010; Oliveira et al., 2013). An enhancement within the mechanical properties is acquired by nanocomposite coating.

2.3. Nanocoating Applications

Nanocoating can be applicable in many environmental facilities and can also be used as an improvement in certain traits. We will review some of nanocoating application such as antimicrobial, anticorrosion, self- cleaning and biocidal, scratch and abrasion resistant and high thermal resistant and fire resistant nanocoatings.

2.3.1. Antimicrobial Coating

Microorganisms are delicate creatures that are among the most influential creatures in the environment and public health, like bacteria, fungi or viruses, which can appear the main probable menace for our modernistic healthy lifestyle.

The growth of microbes on coated surfaces perhaps have multiple negative impact, involving aesthetic problems (discoloration of the coating), hazards to health and hygienic, malodor, biofilm development or microbial corrosion within the condition of metallic surface. The microbial attack is very effective to the Organic coatings, and hence the coating properties, the nutrients existence on the surface and therefore the nature of substrates act the most parameters that determine the microorganisms types ready to colonize the coating as shown in figure. The classical biocides function is to either by inhibit the growth of bacteria (biostatic) or by kill them (biocidal) as shown in figure 2.1. The pressure of growing from the environmentalists concerted with new legislations and consequently the possibilities of bacterial mutation have coercive coating industrialists to tracking new alternate. In the present time, extra emphasis is placed on the case without killing, antibacterial coatings. A vast diversity of organic or inorganic biocides are obtainable commercially and these prove a vast diversity of biocidal and biostatic mechanisms (G. Yamauchi et al., 2004). Inorganic biocides involve silver (Ag), flowers of zinc (ZnO), oxide (CuO), TiO₂, and selenium (Se) (A.J. Trogolo et al., 2003; Wagener 2005). Biocides within microcapsules have been developed to enhancing the longevity and activity of antimicrobial coatings (Xu, C.S. Xie 2003; G. Borkow 2005).

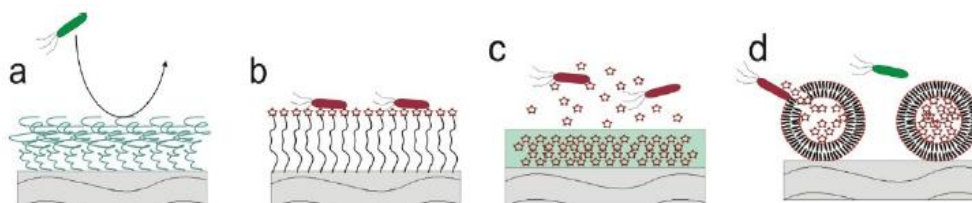


Figure 2.1. Classes of antibacterial coatings: (a) repelling bacterial attachment or biofilm development; (b) contact killing; (c) releasing of antibacterial agents; and (d) stimuli responsive release in the presence of bacteria (G. Yamauchi et al., 2004)

2.3.2. Anticorrosion Coatings

Corrosion can be defined as an important trouble for holders of trading equipments, installations, and plants. Corrosion is in fact an electrochemical procedure where the electrical cell be made up of an anode (the corrosion site), an electrolyte (the corrosive medium), and a cathode (part of the metal which is active within the corrosion process but doesn't itself corrode) (V.V. Verkholtantsev, 2003).

Corrosion usually refers to metals, though nonmetallic substrates like plastics, concrete or wood also damage within the environment. Because it may be a slow process it can vary, supposing a lot of forms and growing very quickly ever after it's triggered by environmental factors, like oxygen and water, which can't be removed.

Stop corrosion is conceivable, as well as nanocoatings are important as they will move the main base of the matter from the preservation versus corrosion to its protection. Nanocoatings can considerably increase the proportion of cost/benefit, supplying cost efficient solutions and improved performances (T. Rentschler and A. Claßen, 2002). The purpose of using Nanoparticles in organic coatings is to improve corrosion resistance. These nanomaterials have a really high area. Nanomaterials can deliver aloft loadings of organic as corrosion inhibitors, in case these surfaces have been activated. Thus, tailored nanoparticles are the valid carrier for delivery of the needed level of active corrosion inhibitors.

2.3.3. Self- Cleaning and Biocidal Coatings

There is an excellent advantage within the design and development of surfaces that not only supply biocidal activity but also are easy to wash and even self-cleaning. Most of such coatings acquire their biocidal/self-cleaning capacity by incorporating specific nanoparticles: basically silver (Ag) and titanium dioxide (TiO₂) (Li et al., 2005; Morrow et al., 2003) Nano TiO₂ is employed for developing anti-UV, anti-bacterial and self-cleaning paints. This possesses self-cleaning hydrophobic properties, which causes water droplets to bead-off of totally cured surface learning dirt and other surface contaminants along the way.

This self-cleaning action figure 2. 1 helps clean and maintain important surfaces and to accelerate drying, leaving the surface with minimal spotting.



Figure 2. 2. Self-cleaning action of nano coating (Li et al., 2005; Morrow et al., 2003)

2.3.4. Scratch and Abrasion Resistant Coatings

Coatings are vulnerable to damage caused by scratch and/or abrasion. Clearly, the buyer prefers to retain the aesthetic appearance of coated materials and for this reason clear coats used on automobiles must have good scratch and abrasion resistance. Another problem is that scratches can also cause damage to the underlying substrate. Many companies worldwide have undertaken the challenge of improving the scratch resistance of a coating without adversely affecting its other properties. Scratch resistance are often obtained by incorporating a greater number of cross links within the coating's binder but unfortunately highly cross linked (hard) films have poor impact resistance due to less flexibility. A less-cross linked (softer) film will show better performance with reference to other properties like antifingerprint and impact resistance but will have less scratch and abrasion resistance. Thus, so as to get optimal scratch resistance, the right combination of hardness and adaptability is required. During this context, organic-inorganic hybrid films are paving the way for scratch-resistant coating developments. Recent advances in nanotechnology plays a crucial role within the development of scratch-resistant coatings (T. Sawitowski, K. Schulte, 2005; D.R. Baer et al., 2003)

2.3.5. High Thermal Resistant and Fire Resistant Coatings

High thermal-resistant coatings are required for a vast sort of metallic substrates that we encounter in lifestyle, including nonstick cookware, barbecues and boilers. Fluorine or silicon-based products are wont to obtain a high thermal resistance for the above-mentioned products. Fluorinated coatings aren't suitable for high-temperature applications as they degrade above ~300 °C and produce toxic byproducts. Recent reports are made from innovative ways to style thermal-resistant coatings; for instance, titanium esters together with aluminum flakes are incorporated into binders that resist temperatures up to 400 °C. Above this temperature “burn off” occurs and a posh coating of titanium aluminum is made that deposits on the substrate and enhances thermal resistance up to 800°C (D.L. Gangotri and A.D. Chaware, 2004).

The devastating nature of fireside creates havoc and leads to great loss of lives and property. Thus, the necessity to develop fire retardant coatings is consistently growing.

Although protection against fire by the utilization of coatings for indefinite periods is impossible, the utilization of fireside -retardant coatings can delay the spread of fire or keep a structure intact against fire, thereby allowing sufficient time for safety measures to be taken.



3. NANOMATERIAL

3.1. Definition

Nanomaterials can be described as the basic units of nanotechnology, with dimensions not exceeding 100 nanometers over the shortest side or have structures which have such small dimensions but are constructing within larger materials. A nanometer mathematically can label as one millionth of a millimeter in the region of 100,000 smaller than the diameter of a person's hair (Bleeker et al., 2012). Nanomaterials are often fabricated from present chemical materials or totally rest chemical compounds, also synthesis from of one or more component. The distinctive features of nanomaterials come from its tiny size. Unique optical, magnetic, electrical, and other properties make it interest. These protrude properties have the potency for major influence in electronics, medicine, and rest of areas.

Nanomaterials exist in three essential classes promoted their origin:

1. Incidental nanomaterials, which are fabricated by accident as a by-product of commercial processes like nanoparticles produced from vehicle engine exhaust, welding fumes, combustion processes and even some natural action like forest fires; Engineered nanomaterials, which have been fabricated by human to have particular required properties for desirable applications.

2. Naturally produced nanomaterials, which may be found within the bodies of organisms, insects, plants, animals and human bodies. The more interests are engineered nanomaterials (ENs), which are designed for, and already getting used in many commercial products and processes. They will be found in such things as sunscreens, cosmetics, sports equipment, stain-resistant clothing, tires, electronics, also as many other everyday items, and are utilized in medicine for purposes of diagnosis, imaging and drug delivery.

ENs are resources designed at the molecular (nanometer) level to require advantage of their small size and novel properties which are generally not seen in their conventional, bulk counterparts. The two main reasons why materials at the nano scale can have different properties are increased relative area and new quantum effects. Nanomaterials have a way greater area to volume ratio than their conventional forms, which may cause greater chemical reactivity and affect their strength.

Also, at the nano scale, quantum effects can become far more important in determining the materials properties and characteristics, resulting in novel optical, electrical and magnetic behaviors (Wagner et al., 2014).

Most current nanoparticles and nanomaterials are often organized into four material-based categories:

1. Carbon-based nanomaterials: Generally, these nanomaterials contain carbon, and are found in morphologies like hollow tubes, ellipsoids or spheres. Fullerenes (C₆₀), carbon nanotubes (CNTs), carbon nanofibers, lampblack, graphene (Gr), and carbon onions are included under the carbon-based nanomaterials category. (Kumar et al., 2016).

2. Inorganic-based nanomaterials: These nanomaterials include metal and metal oxide NPs and nanomaterials. These nanomaterials are often synthesized into metals like Au or Ag NPs (Zhang et al., 2011), metal oxides like TiO₂ and ZnO NPs, and semiconductors like silicon and ceramics.

3. Organic-based nanomaterials: These include nanomaterials made mostly from organic matter, excluding carbon-based or inorganic-based nanomaterials. The use of noncovalent (weak) interactions for the self-assembly and style of molecules helps to rework the organic nanomaterials into desired structures like dendrimers, micelles, liposomes and polymer nanoparticles.

4. Composite-based nanomaterials: Composite nanomaterials are multiphase nanoparticles and nanomaterials with one phase on the nanoscale dimension which will either combine NPs with other nanoparticles or nanoparticles combined with larger or with bulk-type materials (e.g., hybrid nanofibers) (Badrossamay M. R et al., 2010) or more complicated structures, like a metalorganic frameworks. The composites could also be any combinations of carbon-based, metal-based, or organic-based nanomaterials with any sort of metal, ceramic, or polymer bulk materials.

Moreover, nanomaterials are often classified into four main different dimensions such as:

- 1- Zero dimensional (0-D): nanomaterials during this category have all of the three dimensions within the nanoscale. These can have different shapes like cubes and polygons, like nanoparticles and quantum dots.

2- One dimensional (1-D): nanostructures have two dimensions in nanoscale. These include nanowires, nano-rods, and nanotubes. These materials are long (several micrometer in length), but with diameter of only a couple of nanometer.

3- Two dimensional (2-D): this sort of nanomaterials have one dimension within the nanoscale. These include nano-films, nano-sheets or nano-walls. The world of the nano films are often large (several micrometer), but their thickness is extremely small (within nanometers scale).

4- Three dimensional (3-D) this sort of nanomaterials aren't confined to the nanoscale in any dimension. This class can contain bulk powders, dispersions of nanoparticles, bundles of nanowires, and nanotubes also as multi-nanolayers (pokropivny V. V. and Skorokhod V. V, 2007). Classification of nanomaterials illustrated in figure 3.1.

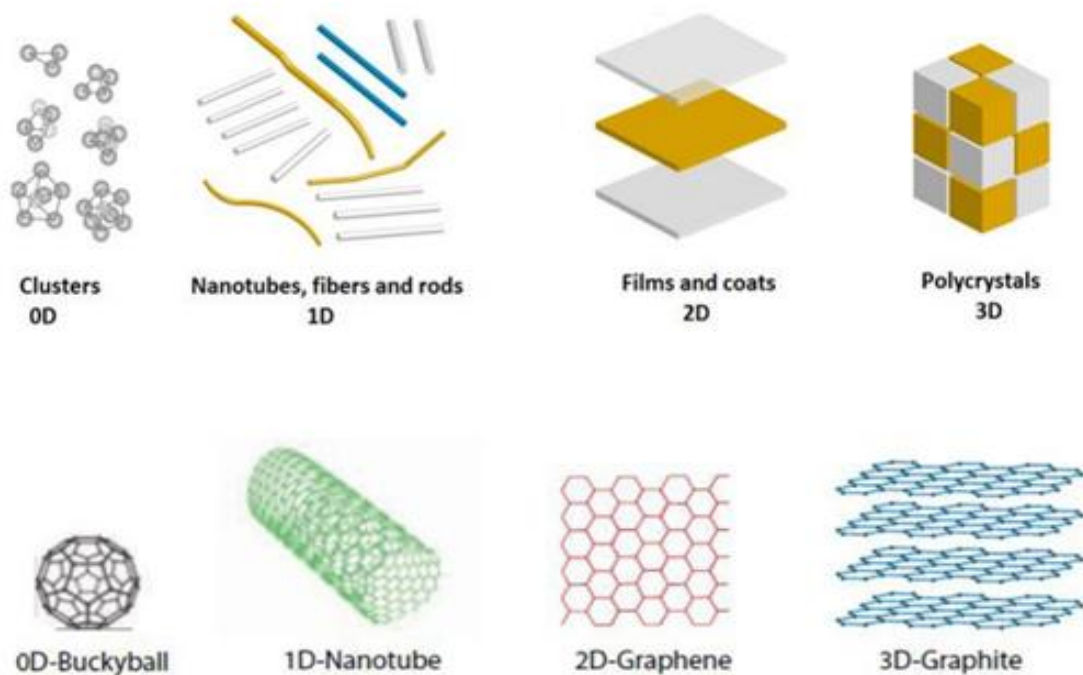


Figure 3.1. Classification of Nanomaterials (a) 0D spheres and clusters, (b) 1D nanofibers, wires, and rods, (c) 2D films, plates, and networks, (d) 3D nanomaterials (pokropivny V. V. and Skorokhod V. V, 2007)

3.2. Silver Nanoparticles (AgNPs)

AgNPs can be describe as a soft white lustrous element with relative molecular mass 107.87 g/mol freezing point 961.78 °C and boiling point 2162 °C. A crucial utilize of AgNPs is to offer a production a silver finish. AgNPs are generally within the size of 100 nm and includes approximately 20-15,000 silver atoms (J and C.X.a.S.H, 2008). Additionally, tubes, wires, multifactes or films are the production of nanostructure. Within the nanoscale, the Ag particles show deviating physicochemical properties (like pH dependent dividing to solid and dissolved particulate substance) and biological activates compared with the uniform metal (C and L, 2006).This is because the upper area per mass, allowing a huge quantity of atoms to react with their surroundings. attempts are made to investigate their attractive properties and utilize them in functional usage, like antibacterial, antifungal and anticancer curatives, diagnostics and optoelectronics, water disinfection, and other pharmaceutical applications (Chen D et al., 2009; Sun Y et al., 2002; Haes A.J et al., 2002; Zhang et al., 2016). Ag has attractive material properties and may be a low cost and bountiful natural resource. The foremost widespread chemical approximation, involves chemical reduction employing a assortment of organic and inorganic reducing agents, electrochemical techniques, physicochemical reduction, and radiolysis are vastly employed for the production of AgNPs. (El-Nour, K.M.M.A et al., 2010).

3.2.1. Antibacterial Activity of AgNPs

AgNPs have the power to anchor to the bacterial cell membrane and then penetrate it, thereby lead to structural changes within the cell wall just like the permeability of the cell wall and death of the cell. There's formation of "pits" on the surface of the cell, and there's cumulating of the nanoparticles on the cell surface (Sondi I and Salopek-Sondi B, 2004). The formation of free radicals by the AgNPs could also be considered to be other mechanism by which the cells die. There's formation of free radicals by the silver nanoparticles when in touch with the bacteria, and these free radicals have the power to wreck the cell wall and make it spongy which may in the end cause necrobiosis (Danilcauk et al., 2006; Kim et al., 2007). It's also been proposed that there are often release of silver ions by the nanoparticles (Feng, Q. et al., 2008), and these ions can interact with the thiol groups of the many vital enzymes and inactivate them (Matsumura, Y. et al., 2003).

The bacterial cells in touch with silver absorb silver ions, which inhibit several functions within the cell and damage the cells. Then, there's the generation of reactive oxygen species, which are produced possibly through the inhibition of a respiratory enzyme by silver ions and attack the cell itself. Silver may be a soft acid, and there's a natural tendency of an acid to react with a base, during this case, a soft acid to react with a soft base. Figure 3. 2 are often describing the mechanisms of antimicrobial activity of AgNPs. The cells are mainly made from sulfur and phosphorus which are soft bases. The action of those nanoparticles on the cell can cause the reaction to require place and then cause necrobiosis. Another fact is that the DNA has sulfur and phosphorus as its main components; the nanoparticles can act on these soft bases and damage the DNA which might decidedly cause necrobiosis (Morones, J. et al., 2005).

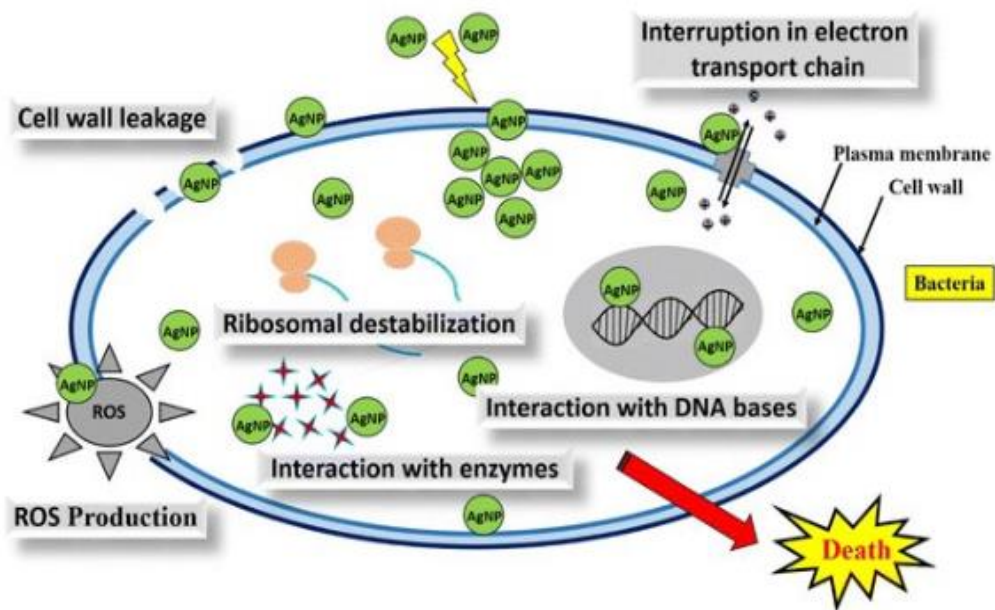


Figure 3.2. Schematic representation of mechanisms of antimicrobial activity of AgNPs (Morones, J. et al., 2005)

3.3. Titanium Dioxide TiO₂

Titanium dioxide (TiO₂) powder describe as a fine, white, crystalline, odorless powder, which exhibits relatively low toxicity (Zhang et al., 2010) with a relative molecular mass of 79.9 g/mol, boiling point of 2972°C, freezing point of 1843°C, and density of 4.26 g/cm³ at 25°C. TiO₂ may be a poorly soluble. Anatase and rutile are two crystal structures of TiO₂, with anatase being more chemically reactive. Nanosized TiO₂ particles belong to the foremost widely manufactured NPs on a worldwide scale due to its photo-catalytic properties and therefore the related surface effects. From Figure 3.3 are often see the formula and cubic structure of TiO₂. TiO₂ NPs are within the top five NPs utilized in consumer products (Hashimoto et al., 2005; Shukla et al., 2011). TiO₂ nanoparticles have many merits viz., high specific-surface area, proper electronic band structure, high quantum efficiency, chemical innerness and stability (Lai Y et al., 2015). TiO₂ NPs are widely utilized in number of applications, like a white pigment in paint, ceramics, as an artificial additive, in food packaging material, in sunscreens, in cosmetic creams, and as a component of surgical implants. Recently, the nano-form of TiO₂ has been also applied in paints as an antimicrobial agent, thanks to its hydroxyl generative property (Kaiser et al., 2013). They're also broadly utilized in the environmental decontamination of air, water, and soil by destruction of pesticides (Shi et al., 2013). Self-cleaning and anti-fogging materials also as coatings and paints for sanitization and disinfection products utilized in hospitals against a spread of various microbes.

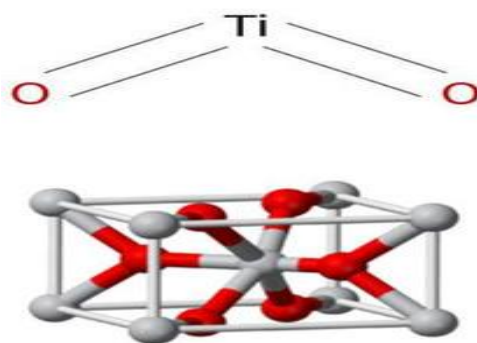


Figure 3.3. Chemical formula of TiO₂ (Hashimoto et al., 2005; Shukla et al., 2011)

3.4. Zirconium Dioxides (ZrO₂)

ZrO₂ (zirconia) can be describe as a white crystalline oxide of zirconium with a relative molecular mass of 123.218 g/mol, boiling point of 4,300 °C, freezing point of two ,715 °C, and density of 5.68g/cm³ at 25°C. Zirconia can be described according to its properties as a material of high importance in multiple technological applications, as it can be described as a substance of a natural color with a high degree, high hardness, high convertibility, chemically stable, corrosion resistance, chemical and microbial resistance. (J. C. Ray et al., 2006). ZrO₂ is a wide band gap semiconductor that offers bountiful oxygen spaces upon its surface. The reason is that it is useful in catalysis due to the high ability to ion exchange as well as the oxidation effectiveness (J. L. Gole et al., 2006). ZrO₂ is also an extremely important dielectric material for applications requiring dielectric transistors in non-electrical future devices (G. Dutta et al., 2006). ZrO₂ nanoparticles have produced utilizes in solid oxide fuel cells (S. Park et al., 2000) and in oxide, gas sensors (J E. C. Subbarao and H. S. Maiti, 1988). Also, the highly stable ZrO₂ nanoparticles are of great importance for high temperature systems such as energy transfer systems, due to the high oxygen transport capacity and long-term stability.

ZrO₂ (zirconia) may be a refractory and chemically inert metal oxide which exists in several phases counting on temperature. Monoclinic phase is stable below 1000°C, tetragonal phase exists above 1170°C and transform to cubic phase after 2370°C.

ZrO₂ is characterized by many properties of high importance, such as the distinctive mechanical properties, fracture resistance, hardness, strength, high thermal impact resistance, poor thermal conductivity, super elastic deformation, stable phase, and resistance against chemicals, this led to zirconia entering many industrial and engineering fields such as the medical industry, catalytic agents, jewelry industry, cutting tools, high density grinding media and nose cones (Zhang Q et al., 2000; Wright PK and Evans AG, 1999; Piconi C and Maccauro G., 1999; Salas P et al., 2003; Kumari L et al., 2009). It also enters the manufacture of ceramic dental materials because of its distinctive performance in this field (Park S et al., 2000). ZrO₂ that is highly stable can be applied in high temperature energy transfer systems that due to its low thermal conductivity, thermal resistance and its high oxygen ion transport capabilities.

Pure zirconia ceramics as developed structural materials using is restricted because the unprompted tetragonal to monoclinic phase conversion over cooling from improvement temperature to temperature.

The foremost common system is yttria stabilized zirconia (YSZ). Two phenomena are often wont to explain those mechanical properties and therefore the behavior of the YSZ material can thus be describe as ‘convertible’ or ‘not convertible. The convertible tetragonal YSZ phase (called t) is of great advantage while utilized as engineering ceramic material since it shows high amount of strength and hardness. This hardening mechanism is because the transformation of the tetragonal phase into the monoclinic phase which means a volume change related to pseudo plasticity (P. M. Martin, 2010). The amount of yttrium is a crucial parameter since it's an effect on the grain size, the temperature of the martensitic transition, strength and degradation action, particularly in humid environment (J. George and M. Dekker, 1992; H. J. Lee et al., 2007; E. C. Subbarao, 1988).

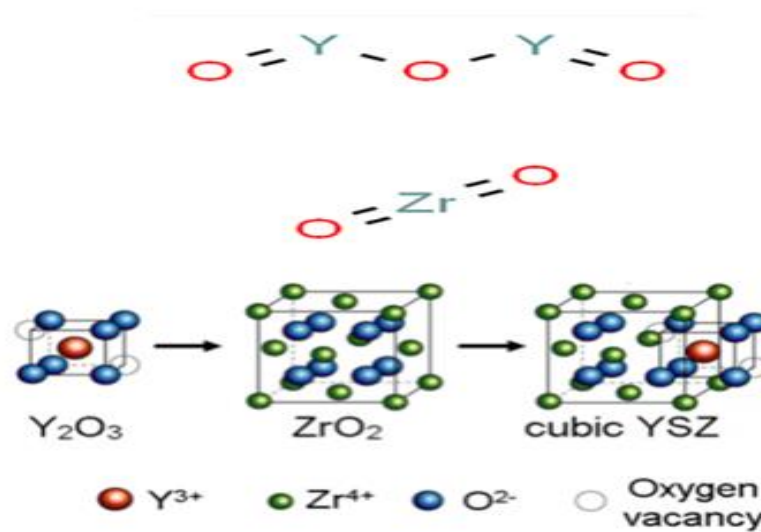


Figure 3.4. Chemical structures of ZrO_2 and YSZ (Yashima et al., 1995)

4. THIN FILMS

4.1. Definition

The thin film can be defined as an amazing art of nanoscience which plays a dominant role altogether persistent field of science and technology. A thin film is nothing but a small dimensional material formed by precipitating, one by one, molecular/atomic/ionic species of matter. A thin film may be a layer of fabric starting from fractions of a nanometer (monolayer) to many micrometers in thickness. The term thin film is employed for coatings that are wont to modify and increase the functionality of a bulk surface or substrate. They're wont to protect surfaces from wear, improve lubricity, corrosion and chemical resistance. In many cases thin films don't change the properties of the majority material. However, they will totally change the optical, electrical transport and thermal properties of a surface or substrate, additionally to providing an enhanced degree of surface protection. The event of novel materials is that the future prospect of thin film technology. The varied structures like superlattices, nanolaminates, nanotubes, nanocomposites, smart materials, photonic band gap materials, molecularly doped polymers and structured materials have the capacity to extend the functionality of thin films. New advanced and hybrid deposition processes are getting used and developed to deposit novel thin film materials and structures, which isn't possible with conventional techniques (P. M. Martin, 2010).

Thin films exhibit unique properties, which are creating from the atomic growth process. Size effects, including quantum size effects, characterized by the thickness, crystalline orientation and multilayer aspects. The technology of thin films covers a broad spectrum spanning the thickness from a couple of nanometers to at least one micron. One considers thin films to act because the bridge between monolayer and bulk structure. The forces acting upon the atoms at the surface are different from those of the majority. As a two-dimensional system thin films are of great importance to several world problems. The value of thin film materials is a smaller amount as compared to the corresponding bulk material when it involves surface processes. So as to develop new technologies for future application, it's important to utilize knowledge and determination of the character, functions and new properties of thin films.

A number of the important applications of thin films are in technology of industries, including microelectronics, optoelectronics, communication, sensors, catalysis, coating (for examples mirror in lasers and in telescopes) also as in energy generation and conservation strategies. Therefore, the impact of thin film science and technology in our modern life is gigantic. Within the other word, thin films are currently utilized in various aspects of both lifestyle and complicated also as hi-tech applications (Ohring Milton, 2002).

The basic properties of thin film, like composition, crystal phase, orientation, thickness and microstructure are controlled by the deposition conditions (M. Ohring, 1992; J. George et al., 1992).

4.2. Thin Film Deposition Techniques

An emerging technology needs thin films of latest materials for a special promising application. The thin film is often a single/multi component, multilayer coating on substrates of various shapes and sizes. The properties of the thin film are required for specific applications are often caused by using various deposition techniques (K. L. Chopra et al., 1988; S. Mohan, 1994; W. Schockley et al., 1961). The optical absorption, crystal structure, morphology, composition and electrical properties of thin films are extremely sensitive to the synthesis techniques and preparative parameters. Several methods are employed for the synthesis of metals, alloys, ceramic, polymer, semiconductors and superconductors on different substrate materials. Each method has its advantages and drawbacks. There is no technique is right to deposit the thin films covering all the specified aspects like cost of equipment, deposition parameters and nature of the substrate material. The performance and fabrication cost of thin film material depend upon synthesis methods, which are wont to produce devices. The vast sorts of thin film synthesis techniques are wont to fabricate thin film devices. It's possible to classify these techniques in two ways physical and chemical techniques (A. R. West et al., 2003; K. L. Chopra, 1961).

Herein we will explain some thin film deposition methods such as Sol-gel deposition, Spin Coating, and electrospray deposition (ESD)

4.2.1. Sol-Gel Deposition

The sol-gel method can be described as a well-known chemical route for the preparation of various materials such as glass and ceramic (Brinker C. J. and G. W, 1990). From the start, the foremost important applications of the sol-gel route were found within the preparation of metal oxide thin films (Dislich H, 1989). Essentially, the sol-gel process may be a wet chemistry method during which molecular precursors transform into an oxide network during hydrolysis-condensation reactions. Sol-gel process includes the growth of oxide networks during the formation of a sol (sol) and gelation of the sol to make a network during a continuous liquid phase (gel). The technique enables the processing of powders, ceramics, and thin films directly from mixture solution. Figure 4.1 allowed us to see the varied routes within the sol-gel process providing differing types of materials.

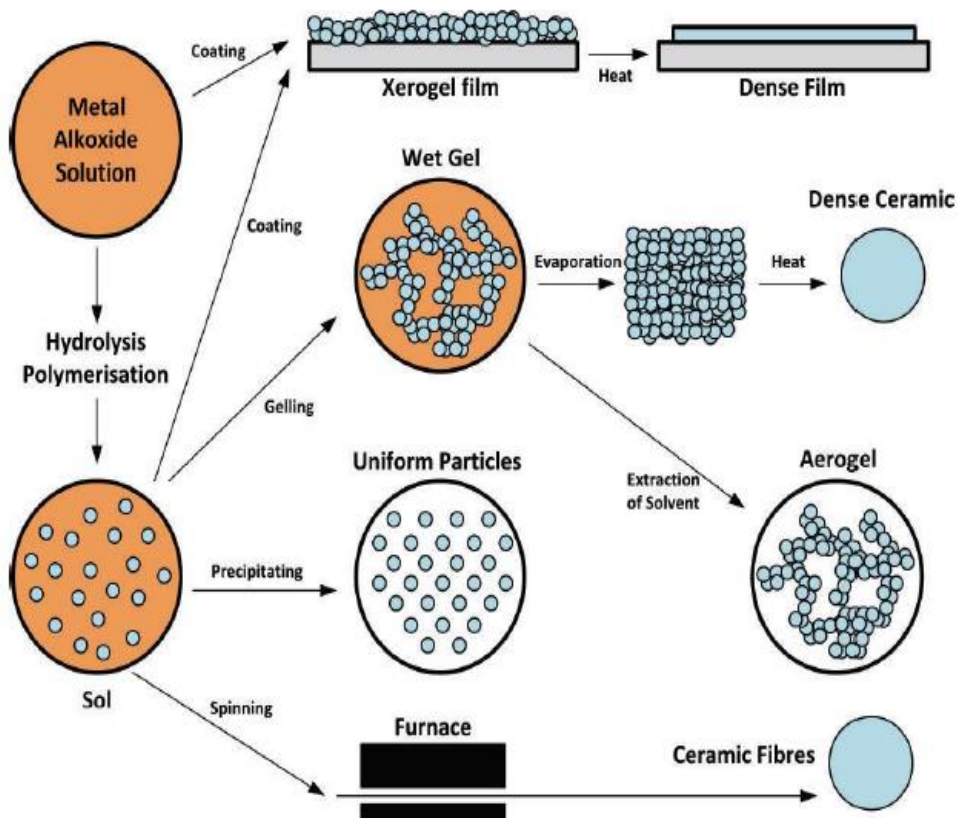


Figure 4.1. Schematic of various routes in the sol-gel process (Dislich H, 1989)

4.2.2. Spin Coating

Spin coating is one among the foremost common techniques for preparing of thin films on substrates and it's utilized in a good industries and technology application. The benefits of spin coating method are the power to supply uniform films from a couple of nanometers to a couple of microns in thickness quickly and simply. Additionally, it's simplicity and cheap in compare with other method, there are many parameters related with this method like the answer concentration the amount of rotation per minute (rpm) and interval time, Spin Coating process are often shown in figure 4.2. While, the disadvantage is an inherently batch (single substrate) process and thus relatively low throughput compared to roll-to-roll processes. The fast-drying times also can cause lower performance for a few particular nanotechnologies, which require time to self-assemble and/or crystalline. Finally, the fabric usage is usually very low at around 10% or less with the remainder being flung off the side and wasted. Whilst this is often not usually, a problem for research environments it's clearly wasteful for manufacturing (Aegerter and Mennig, 2004; Kohli, 2007).

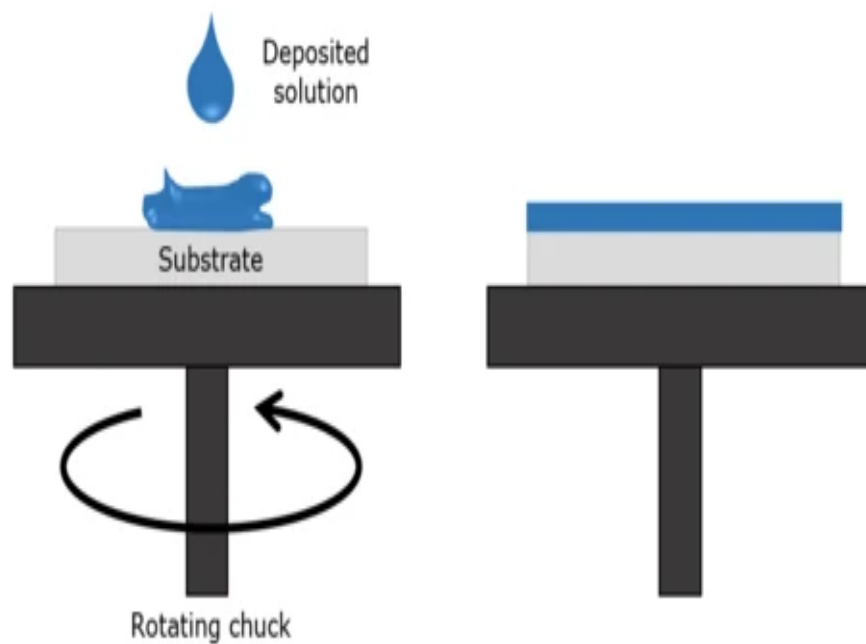


Figure 4.2. Schematic illustration of Spin Coating process (Aegerter and Mennig, 2004; Kohli, 2007)

4.2.3. Electrospray Deposition (ESD)

Electrospray deposition system can be described as a nanofabrication process for the spraying of natural polymers, synthetic polymers, and composite solutions. This system is employed to make nanostructured coatings (either fibers or particles) deposited on a conductive substrate using electrostatic force. Electrospray may be a simple method for liquid atomization under the electrical field force. The system can be established by supplying viscous liquid through a capillary nozzle which is maintained at high electrical potential as shown in figure 4.3. The diameters of atomized droplets and particles are often ranged from many micrometers right down to several tens of nanometers with nearly monodisperse distribution (Jaworek A. and Sobczyk, A.T, 2008). During conventional electrospray with an outsized distance between the nozzle and substrate, the charge repulsion force makes the charged particles step into instable movement and increases the deposition area, which is a barrier for micropattern deposition and system integration application of electrospray particles.

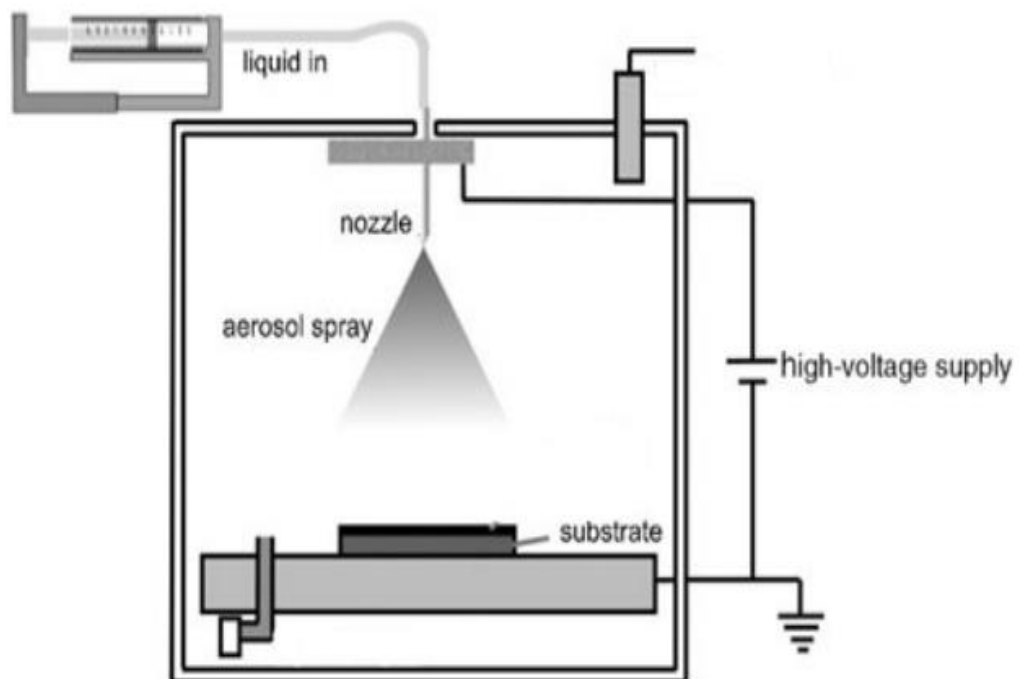


Figure 4.3. Schematic diagram of Electrospray deposition (Jaworek A. and Sobczyk, A.T, 2008)

4.3. Sintering

Sintering are often defined as a processing technique want to produce density-controlled materials and components from metal or ceramic powers by applying thermal energy. Sintering is that the method involving consolidation of powder grains by heating the “green body” to a heat below the freezing point, when the fabric of the separate particles diffuses to the neighboring powder particles. Sintering process are often explained as shown in Figure 4.4 below. Solid state sintering is occurring when the compact is densified wholly during a solid state at sintering temperature while liquid phase sintering occurs when a liquid phase is present within the compact during sintering (Kang and Suk-Joong L., 2005). Other sorts of sintering are vapor phase sintering, transient liquid phase sintering and viscous flow sintering.

The purpose of sintering is to supply sintered parts with reproducible and if possible designed microstructure through control of sintering variables. This process consolidates the fabric, increases its strength and typically causes it to shrink.

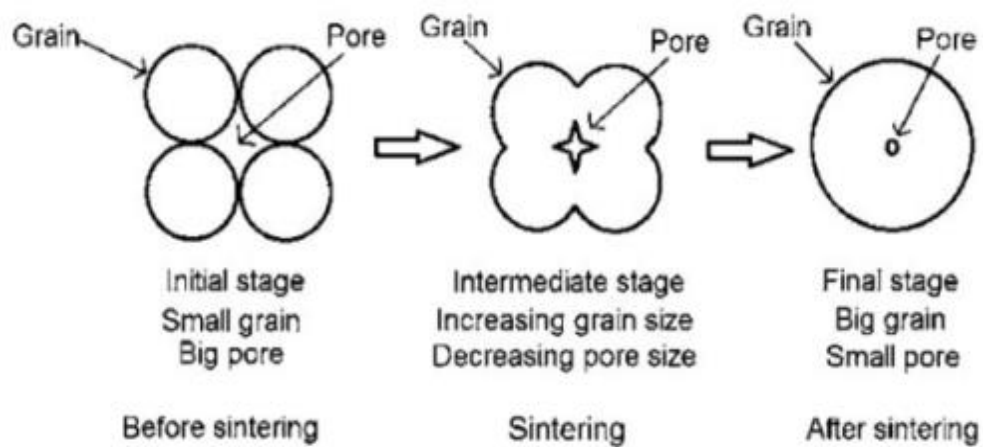


Figure 4.4. A model explaining the sintering process (Kang and Suk-Joong L., 2005)

4.4. Agar Diffusion Test

Agar diffusion test is that the primary method to work out the antimicrobial activity of the nanofibrous scaffolds. It's important to say here that it's only suitable for the diffusive test materials. The agar diffusion test is qualitative, easy to perform, and straightforward. The methodology includes the inoculation of bacterial cells on agar Petri dishes and test samples are laid over these dishes. Afterward, the dishes are incubated for 18–24 h at 37°C and thereafter, the expansion of bacteria is decided below the nanofibrous scaffolds (zone of inhibition) which may be seen in figure 4.5. The presence of antimicrobial activity is indicated by the absence of bacterial growth directly below the test sample (Bauer et al., 1966).

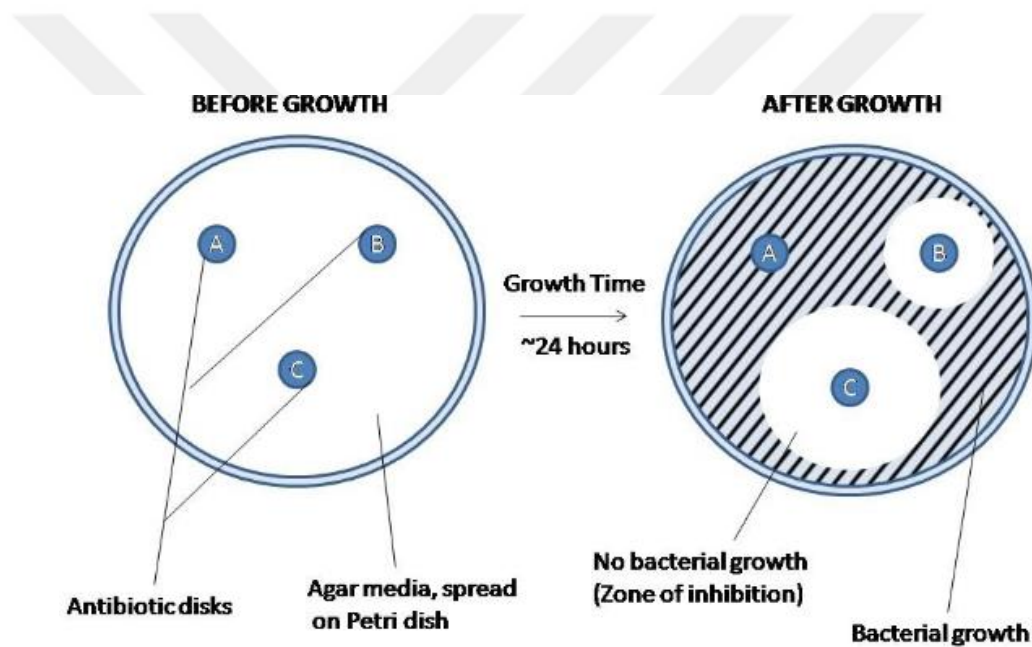


Figure 4.5. Agar diffusion method (Bauer et al., 1966)

5. LITERATURE REVIEW

(Balu S. S. et al., 2012) produced colloidal silver nanoparticles with 1mM concentration by using chemical reduction process, and made antimicrobial activity against five different kinds of bacteria. Silver nitrate and trisodium citrate was used as raw material. AgNPs were characterized by using UVS and STM. Particle size is observed by SEM upper than 10nm. They conclude that silver nanoparticles were successfully produced by chemical reduction process. AgNPs showed a good antimicrobial assay against clinical pathogens.

(T. Pavliashvili. et al., 2014) succeeded to produce AgNPs by using chemical reduction method. Tannin, sodium carbonate and silver nitrate was used as raw materials. UVS and SEM were used to characterize the obtained AgNPs. They conclude that the particle size is upper than 15 nm. Using tannin as a reductant and sodium carbonate as a solution stabilizer proved to be a favourable method for the preparation of AgNPs.

(F. A. Al-Marhaby and R. Seoudi, 2016) prepared colloidal AgNP with 0.25mM by using chemical reduction process. They used Silver nitrate, trisodium citrate and sodium borohydride as preparing material. Synthesized collide AgNPs were characterized by using UVS spectrometry and transmission electron microscopy (TEM). They conclude that the positions of the surface plasmon resonance bands depend on the size of the AgNP particles. Highest catalytic activity is observed by the smallest nanoparticles.

(E.G. Zemtsova et al., 2016) produced TiO₂-based nanocoating with two-level relief organization by sol-gel method. Dip coating was used as a coating process. SEM and AFM were used to characterize the TiO₂ nanocoating. They developed the method of production of nanostructured titanium matrix (nanotitanium) with enhanced strength without plasticity loss. They conclude that the nanotitanium with titan-organic nanostructures on the surface was developed. Biomedical studies showed that the composite coating with surface roughness between 75 and 200 nm with mean pore size of 120 nm demonstrates high surface adhesion properties.

(Sinan Salman Hamdi, 2016) published that Sol-gel technique prepared Ag–TiO₂ nano-composite thin films, which were deposited onto a glass substrate by the spin coating process. The microstructures and chemical ingredients of the obtained thin films were characterized by UVS, (SEM) and (XRD). They discovered that the silver nano-particles completely joined to the TiO₂ matrix, where those nanoparticles are distributed uniformly. In this way, the molar percent of the silver nitrate aqueous solution dominated the morphology of the thin film. Ag-TiO₂ nanocomposite is very useful for expanding antibacterial of prepared nanomaterials.

(Y. Adraider et al., 2013) have been successfully produced Zirconia coatings on a stainless steel surface using a sol–gel technology and fibre laser irradiation under continuous wave. (SEM), EDS, FTIR and (XRD) were used to characterize the surface monograph, chemical composition and crystal structure. They conclude that Zirconia coatings zirconia coatings crystallised in tetragonal structure in tetragonal structure are formed after laser irradiation, coating was uniform during low r laser energy density.

(I. Ferreri et al., 2015) were successfully prepared Ag–ZrCN thin film (11% of Ag) for antimicrobial usage. Physical Vapor Deposition (PVD) was used as a coating technique. Glow Discharge Optical Emission Spectroscopy (GDOES), SEM and X-ray photoelectron spectroscopy (XPS) was used for the characterization of the coated sample. They conclude that the coating process was good for distribution particles and shape. Antimicrobial activity was made with E. coli. Silver coating can be used as antimicrobial agent for medical devises.

(Ramona-Crina Suci et al., 2011) successfully produced TiO₂ thin film by using spin coating technique. They use X-ray diffraction and Fourier-transform infrared spectroscopy (FTIR) was used to characterized TiO₂ powder and thin film. They conclude that XRD analysis of titanium precursor powder shows that starting from 450°C annealing temperature where the TiO₂ anatase is the main crystalline phase. The diffraction pattern of the TiO₂/ITO thin film shows a low crystallinity of the anatase phase.

(Krylova, et al., 2009) published that variety of Ag nanoparticles/oxide mesoporous films with templated silica, titania, and zirconia was synthesized by sol-gel method at glass, aluminum, and silicon substrates using metal alkoxides. The microstructures and chemical ingredients of the obtained thin films were characterized by UVS, SEM and XRD. They discovered that in treated films pore structure undergoes smaller damages for silica due to its amorphous structure. In titania and zirconia films, silver can retard the crystallization of the matrices. Matrix crystallization promotes silver embedding into the outer layer of the film. At a higher silver content (10%) and higher calcination temperature (873 K), silver nanoparticles could be distributed more uniformly along the film.

(Sinem Cevik and Mevlüt Gürbüz, 2018) was successfully produced YSZ thin film by using electrospray deposition technique. Phase analysis of the YSZ coating was carried out by XRD, Surface morphology and film thickness were characterized by SEM. First they approved that YSZ had a lowest sedimentation ratio in isopropanol. They proved that YSZ film produce highly dense coatings with enhanced mechanical properties.

(Rudacova, et al., 2018) focused on the fundamental study of self-cleaning properties of ZrO₂ films, including photoinduced alteration of surface hydrophilicity, photocatalytic and photoinduced bactericidal activities. They conclude that the ZrO₂ thin films reveal self-cleaning properties and can be successfully used as biomedical or construction material. The antibacterial properties are investigated against *Escherichia coli* and associated with the activity of formed ion-radicals in the air and the poor adhesion of bacteria on the ZrO₂ surface due to high hydrophilicity of its membrane.

6. MATERIALS AND METHODS

6.1. Synthesis of AgNPs

6.1.1. Materials:

Silver nitrate (AgNO_3), trisodium citrate dihydrate ($\text{Na}_3\text{C}_6\text{H}_5\text{O}_7$), ethylene glycol ($\text{C}_2\text{H}_6\text{O}_2$), absolute ethyl alcohol ($\text{CH}_3\text{CH}_2\text{OH}$) and distilled water were used, all analytical grades without further purification. Collide AgNPs were prepared by using AgNO_3 with a purity of 99.5%, trisodium citrate dihydrate ($\text{C}_6\text{H}_5\text{Na}_3\text{O}_7 \cdot 2\text{H}_2\text{O}$) with a purity of 98% from Aldrich Chemical Co.

6.1.2. Methods

Chemical reduction method was used as a AgNPs production method. Silver nitrate solution (A) was prepared by dissolving a certain weight of silver nitrate in a mixture of (10 ml. ethylene glycol, 45 ml ethanol and 45 ml distilled water). Sodium citrate dihydrate solution (B) was prepared by dissolving a known different weight of sodium citrate in 100 ml (distilled water). Details of used weights and molar concentrations of the six samples are listed in table 1. After preparing the solutions, we put the solution (A) on a heating element until boiling and then solution (B) was added drop wise to solution (A). With the presence of stirring and heating together and after the completion of the addition process this distillation process took a few minutes as illustrated in figure 6.1.



Figure 6.1. chemical preparation of collidal AgNPs

We noticed that the solution color changed, at first it was light yellow and after a period of time it became pale yellow and may turn brown, gray, green or yellowish gray as shown in figure 6.2. After the changes in colour, solution was stirred in magnetic stirrer until it cooled down to room temperature.



Figure 6.2. Colors of synthesized colloidal AgNPs

Table 1. The weights and molar concentrations of the materials that are used in preparing the collidal AgNPs

Sample	Wt. of AgNO ₃ in (g)	Molar Con. in (M)	Wt. of trisodium citrate in (g)	Molar Con. in (M)
A	0.017	0.001	0.295	0.01
B	0.050	0.003	0.882	0.03
C	0.085	0.005	1.470	0.05
D	0.118	0.007	2.058	0.07
E	0.152	0.009	2.650	0.09
F	0.304	0.018	5.300	0.18

6.1.3. Antimicrobial Test of Colloidal AgNPs

The antimicrobial activity of synthesized colloidal AgNPs was tested on nine different types of pathogenic bacteria and fungi such as *Escherichia coli*, *Staphylococcus aureus*, *Bacillus subtilis*, *Klebsiella pneumoniae*, *Listeria monocytogenes*, *Salmonella enterica*, *Enterococcus faecalis*, *Aspergillus niger* and *Candida albicans* which were cultured on agar plates supplemented with different concentrations of AgNPs (1 mM, 3 mM, 5 mM, 7 mM, 9 mM and 18 mM) by Diffusion Method with incubation for 24 hr at 37 °C.

6.2. Synthesis of TiO₂ Thin Film

6.2.1. Material

TiO₂ powder with particle size of 25 nm, distilled water, ethyl alcohol (CH₃CH₂OH), ethylene glycol (C₂H₆O₂) and ammonia (NH₃) are used in synthesis.

6.2.2. Method

TiO₂ thin film solution was prepared by dissolving 1g of TiO₂ powder in a mixture of 5 ml ethylene glycol, 45 ml distilled water, 50 ml ethyl alcohol and few drops of ammonia. The mixture was stirred in magnetic stirrer for 60min. under 45°C, then sonicated for 30min. the mixture was stirred for 30 min. after these processes. The solution is left in dark place for 24 hr to use it in the next coating stage. In order to coat in stainless steel substrate, coating process was made by using ESD technique.

TiO₂ suspension was pumped by using an injector pump at 0.05 mL/min flow rate through the nozzle. Stainless steel 304 (1×1 cm²) was used as a substrate material. The suitable distance between the nozzle and the substrate was kept at 7 cm. The voltage was fixed at 10.5 kV for 45 min at room temperature during the deposition processes.

After deposition, high-frequency induction heat sintering system (MTI, EQ-SP-15VIM) was used to sinter the coating. The system was deflated to a vacuum level of 1x10 – 5 mbar, then Ar gas was used as a shield and current was activated and maintained until densification. Fabricated TiO₂ film was heated in the system up to 900°C for 90 min under Ar gas. Then, the samples were gradually cooled to room temperature.

6.3. Synthesis of YSZ Thin Film

6.3.1. Material

YSZ ($\text{ZrO}_2\cdot\text{Y}_2\text{O}_3$) powder with a particle size of 25 nm was purchased from Shenzhen Co. China, isopropyl alcohol ($\text{C}_3\text{H}_7\text{OH}$) and glacial acetic acids (CH_3COOH) were bought from Merck.

6.3.2. Method

YSZ suspension as a coating solution was prepared by dissolving 1g of YSZ powder in a mixture of 95 ml isopropyl alcohol and 5 ml glacial acetic acid. This mixture was sonicated for 15 min then stirred at 45°C for 30 min to get a homogenous solution. YSZ suspension was pumped by using an injector pump at 0.05 mL/min flow rate through the nozzle. Stainless steel 304 ($1\times 1\text{ cm}^2$) was used as a substrate material. The suitable distance between the nozzle and the substrate was kept at 7 cm. The voltage was fixed at 7.5 kV for 30 min at room temperature during the deposition. Coated samples were sintered under Ar gas at 1150°C for 90 min by using high-frequency induction heat sintering system (MTI, EQ-SP-15VIM). After 90 min, the samples were gradually cooled to room temperature.

6.4. Synthesis of TiO₂–YSZ Thin Film

6.4.1. Materials and Method

50% of prepared TiO₂ solution and 50% of prepared YSZ solution were mixed together. This mixture was then sonicated for 10 min and stirred for 30 min under 45°C to be ready for the coating stage. TiO₂–YSZ suspension was pumped by using an injector pump at 0.05 mL/min flow rate through the nozzle. Stainless steel 304 (1×1 cm²) was used as a substrate material. The suitable distance between the nozzle and the substrate was kept at 7 cm. The voltage was fixed at 9.2 kV for 45 min at room temperature during the deposition. The coated samples were sintered at 1000°C for 90 min under Ar gas. Then the samples were gradually cooled to room temperature.

6.5. Synthesis of Ag Thin Films

From the previous method of synthesis of silver nanoparticles, 5 mM of colloidal AgNPs was used for coating the second layer on TiO₂, YSZ and TiO₂–YSZ films. Colloidal AgNPs was pumped by using an injector pump at 0.02 mL/min flow rate through the nozzle. TiO₂, YSZ and TiO₂–YSZ fabricated films (1×1 cm²) was used as a substrate material. The distance between the nozzle and the substrate was kept at 7 cm. The voltage was fixed at 12.5 kV for 45 min at room temperature during the deposition. Coated samples sintered at 450°C for 20 min under argon gas.

6.5.1. Antimicrobial Test of Ag Thin Films

The antimicrobial activities of fabricated TiO₂–Ag, YSZ-Ag and TiO₂–YSZ-Ag films were tested on three different types of pathogenic bacteria and fungi two kinds of bacteria such as: *Escherichia coli* and *Staphylococcus aureus*, with one kind of fungi: *Candida albicans*. Coated samples were cultured on agar plates supplemented by Diffusion Method. The plates were incubated for 24 hr at 37 °C.

6.6. Chemical, Physical and Biogecal Characterization

6.6.1. SEM and EDX Characterization

Jeol JSM-7001F SEM is equipped with energy-dispersive X-ray spectroscopy (EDX), wavelength-dispersive X-ray spectroscopy (WDX), secondary electron (SE) detector, backscatter electron detector (BSD) and electron backscatter diffraction (EBSD). SEM was used to characterize the synthesized AgNPs. Surface morphology and film thickness of fabricated films. SE images and EDX elemental maps are used to determine the elemental composition and the ratios of elements of the synthesized AgNPs and fabricated films.

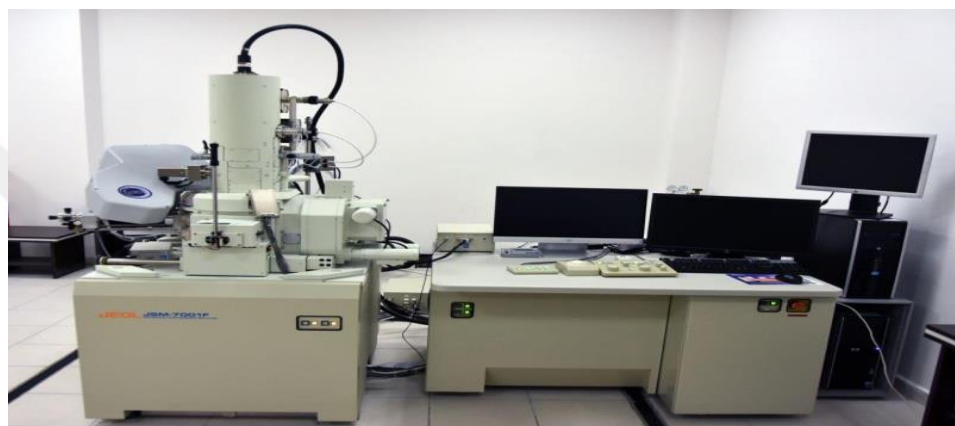


Figure 6.3. Scanning electron microscope (Jeol JSM7001F model)

6.6.2. XRD characterization

Rigaku Smart Lab XRD was used to characterize composition and crystal structure of the TiO_2 , YSZ and TiO_2 –YSZ coatings. The measurements were performed at 40 kV and 40 mA, with $\text{CuK}\alpha$ radiation.

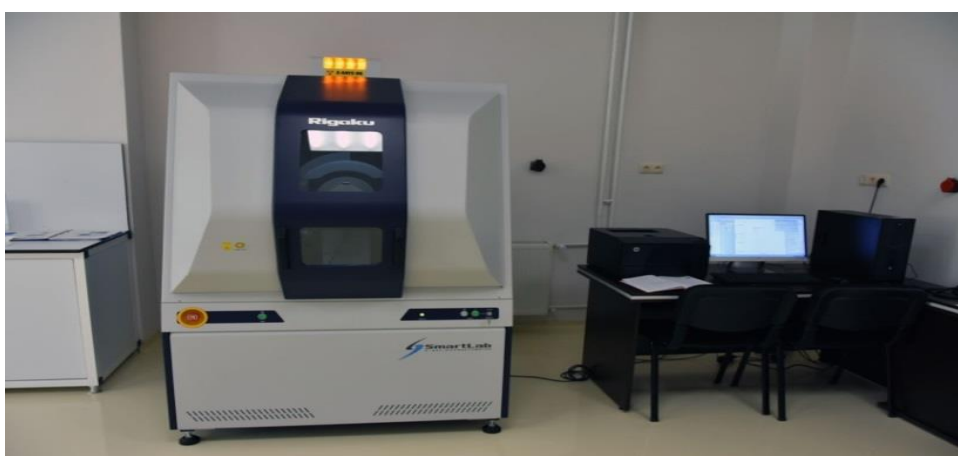


Figure 6.4. X-ray diffraction device (Rigaku. SmartLab model)

6.6.3. AFM Characterization

SOLVER NEXT SPM AFM was used to characterize the surface roughness and morphology of the fabricated TiO_2 , YSZ and TiO_2 –YSZ coatings.



Figure 6.4. Atomic force microscopy (SOLVER NEXT)

6.6.4. Antimicrobial Test

Agar diffusion test was used to verify the antimicrobial assay of produced colloidal AgNPs, TiO_2 –Ag, YSZ–Ag and TiO_2 –YSZ–Ag coatings against different kinds of pathogenic; bacteria and fungi.

6.6.5. Image J Program

Image J Program was used to measure the particle size of the synthesized AgNPs and fabricated thin films. These measurements are done through the use of images captured by SEM

7. RESULT AND DISCUSSION

7.1. Characterization of AgNPs

7.1.1. Antimicrobial Assay of Synthesized AgNPs

AgNPs synthesized by chemical methods have been found highly toxic against pathogenic bacteria and fungi. Herein, the synthesized nanoscale particles exhibited antibacterial activity against *Escherichia coli*, *Staphylococcus aureus*, *Bacillus subtilis*, *Klebsiella pneumoniae*, *Listeria monocytogenes*, *Salmonella enterica*, *Enterococcus faecalis*, *Aspergillus niger* and *Candida albicans*, as it is shown in figure 7.1.

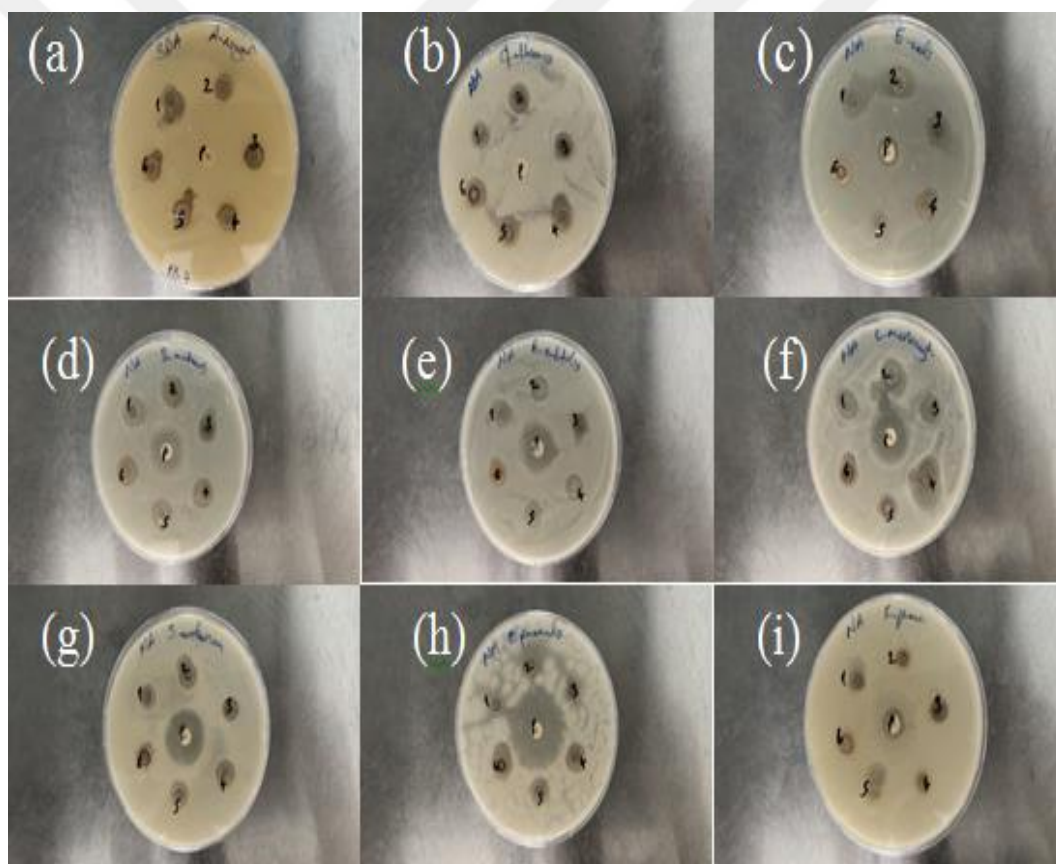


Figure 7.1. Result of Antimicrobial activity of AgNPs in (a) *Aspergillus niger* (b) *Candida albicans* (c) *Escherichia coli* (d) *Staphylococcus aureus* (e) *Bacillus subtilis* (f) *Listeria monocytogenes* (g) *Salmonella enterica* (h) *Enterococcus faecalis* and (i) *Klebsie*

Table 2. below shows the toxic effect of nanoscale silver particles in all concentrations that were prepared on all bacteria and fungi on which the antimicrobial effect was examined. And it shows the relation between the effect of colloidal silver nanoparticles concentration in mM and the inhibition zone diameter in mm.

Table 2. Concentration of colloidal silver nanoparticles vs Inhibition zone diameter on microorganisms

Con. Of AgNO ₃	<i>Aspergillus niger</i>	<i>Candida albicans</i>	<i>Escherichia coli</i>	<i>Staphylococcus aureus</i>	<i>Bacillus subtilis</i>	<i>Listeria monocytogenes</i>	<i>Salmonella enterica</i>	<i>Enterococcus faecalis</i>	<i>Klebsiella pneumoniae</i>
1	8 mm	12 mm	11 mm	12 mm	8 mm	9 mm	9 mm	11 mm	8 mm
3	8 mm	10 mm	11 mm	13 mm	8 mm	9 mm	9 mm	11 mm	-----
5	6 mm	11 mm	11 mm	13 mm	8 mm	9 mm	10 mm	12 mm	7 mm
7	-----	7 mm	10 mm	9 mm	7 mm	9 mm	7 mm	8 mm	7 mm
9	-----	11 mm	7 mm	12 mm	7 mm	8 mm	10 mm	10 mm	-----
18	7 mm	11 mm	7 mm	12 mm	7 mm	8 mm	8 mm	10 mm	-----

*----- = means no inhibition zone of AgNPs.

mm = means diameter of inhibition zone of AgNPs.

The antimicrobial test allowed us to discover and make sure that almost of prepared solutions had a good antimicrobial assay agent all kinds of microorganisms' bacteria and fungi. AgNPs solution with a concentration of 5 mM had a perfect toxicity in all pathogenic that were under test as shown in figure 7.1.

7.1.2. SEM and EDX Analysis

An image was taken with the scale of 100 nm and 50KX magnification, the nanoparticles could be clearly noticed at this level in Figure 7.2. (a). With 50K X magnification, the dimensions of the synthesized 1mM AgNPs particles can be seen randomly. The particles were selected and the diameters seemed to be as follows: 27.8 nm, 39.5 nm, 51.6 nm and 65 nm. In shown in Figure 7.2. (b) with the same magnification, the dimensions of the synthesized 3 mM AgNPs particle diameters seemed to be as follows: 17.8 nm, 23 nm, 31.9 nm and 54.1 nm.

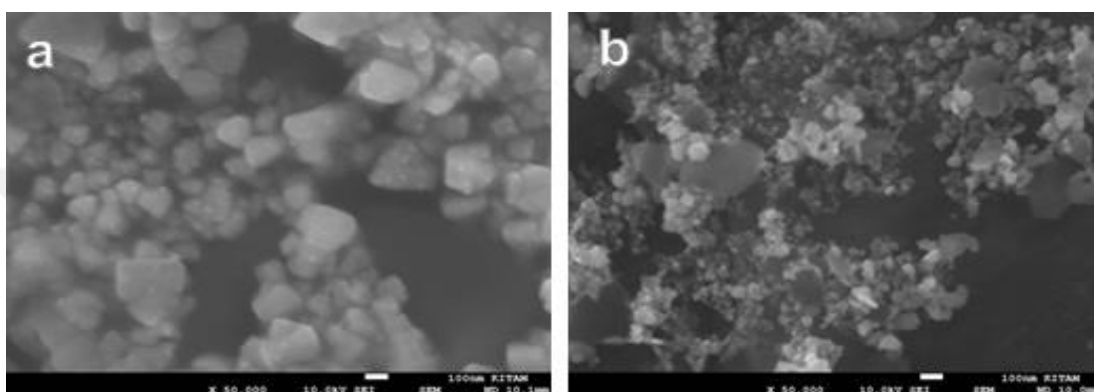


Figure 7.2. SEM images of synthesized AgNPs in (a) 1 mM and (b) 3 mM

SEM image with a scale of 100 nm and 40KX magnification in figure 7.2(a), the nanoparticles could be clearly noticed at this level. The dimensions of the synthesized 5mM AgNPs particle which be seen were randomly selected and the diameters appeared to be as follows: 15.1nm, 36.8nm, 40.1 nm and 61.7nm. In figure 7.2(b) 30K X magnifications, the nanoparticles were calculated as follows: 16 nm, 19 nm, 23 nm and 52 nm.

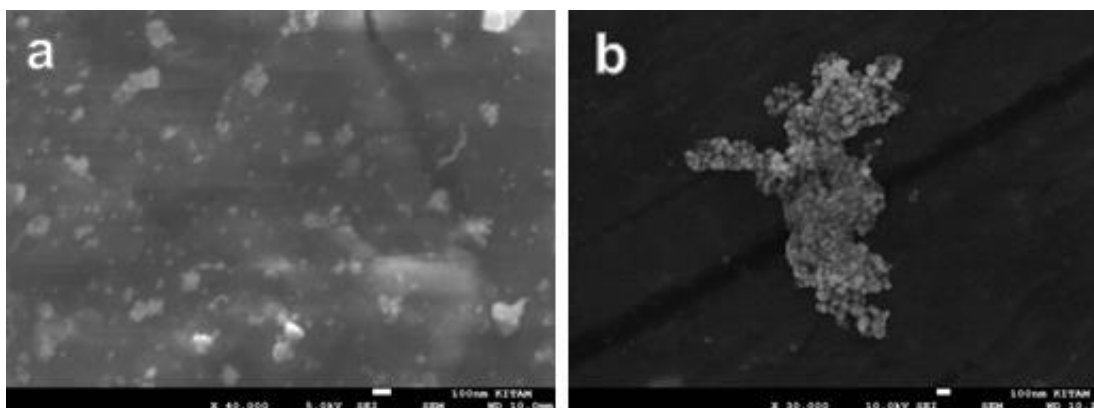


Figure 7.3. SEM images of synthesized AgNPs in (a) 5 mM and (b) 7 mM

In figure 7.4(a), SEM image with a scale of 100 nm and 150kX magnification, the nanoparticles could be clearly noticed at this level. The dimensions of the synthesized 9mM AgNPs particle diameter were calculated as follows: 11nm, 12.7nm, 24.7 nm and 45.1nm. Although in Figure 7.4(b) the image was taken with a scale of 100 nm with 50k X magnification, but the nanoparticles diameter were obtained as follows: 13.8 nm, 19.4 nm, 39.7 nm and 66.5nm.

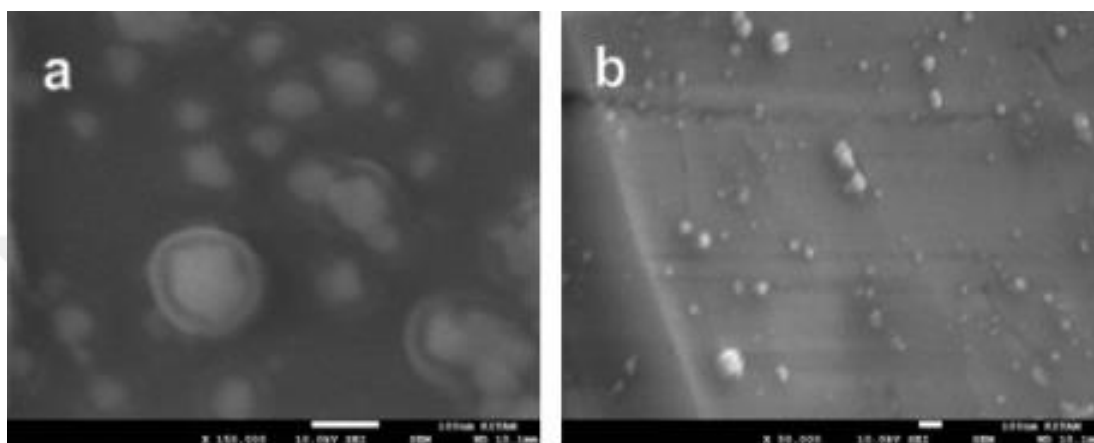


Figure 7.4. SEM images of synthesized AgNPs in (a) 9 mM and (b) 18 mM

We have measured the practical size of all prepared solutions then calculated the average particle size as shown in table 3 below

Table 3. The average practical size of AgNPs in AgNO₃ solution

Sample	Con. of AgNO ₃ in (mM)	Average particles size in (nm)
A	1	55.4
B	3	44.7
C	5	33
D	7	28.8
E	9	33.5
F	18	34.8

EDX analysis was conducted to ensure the production of AgNPs in our prepared solution. EDX analysis was made with a scale of 1 μ m for the prepared AgNPs. SEM images in figure 7.5. shows synthesized AgNPs, all the chemical compounds in the prepared solution and the percentage of chemical compounds in the solution as shown in figure 7.5 (a), (b) and (c).

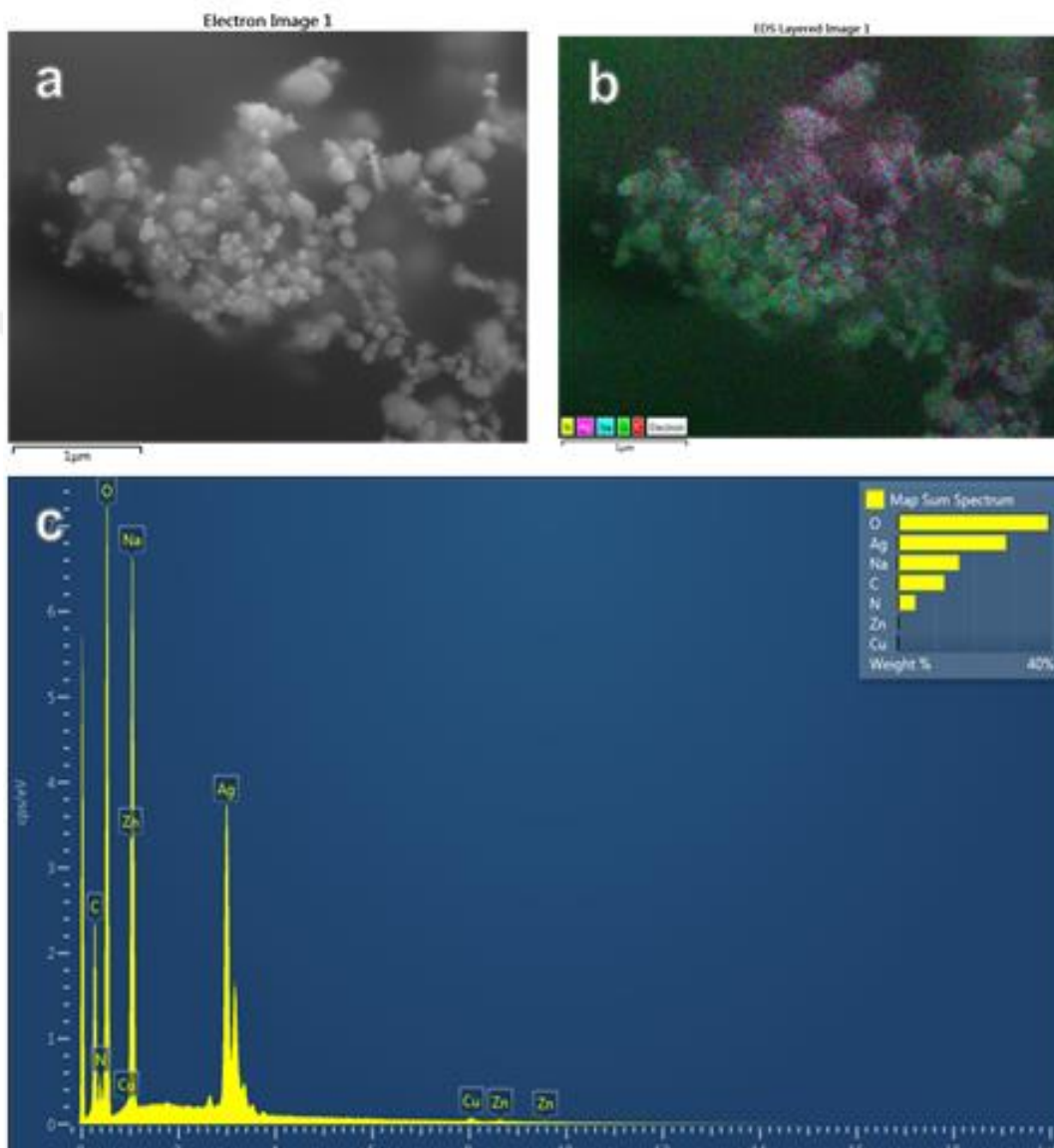


Figure 7.5. EDX analysis of fabricated solution in (a) synthesized AgNPs, (b) chemical composition of colloidal AgNPs and (c) elemental analysis of colloidal AgNPs.

SEM images enable us to calculate the particle size of fabricated AgNPs in all solutions. All prepared solutions included AgNPs within the nanoscale with a good amount. (T. Pavliashvili. et al., 2014) produced AgNPs with particle size upper than 15 nm in 1mM of AgNO₃ solution. And we produced AgNPs in several solutions with a particle size up to 11nm.

The composition of the prepared solution with 5 mM is further examined by EDX measurement. EDX result shown in figure 7.5(c) explains that the peak of Ag can be clearly seen in the survey spectrum. Also, the other elements as O, Na, Zn, and Cu are the components of the prepared solution.

(Balu S. S. et al., 2012) prepared collide AgNPs with 1mM with antimicrobial activity against five different kinds of bacteria. We prepared six solutions with a different concentration (1 mM, 3 mM, 5 mM, 7 mM, 9 mM, and 18 mM) and made the antimicrobial activity against seven different kinds of bacteria and to kinds of fungi.

Due to the good antimicrobial activity of 5 mM solution and the particle size of synthesized AgNPs, we used this solution as a coating solution in the final coating stage.

7.2 .Characterization of TiO₂, YSZ and TiO₂–YSZ Coatings

7.2.1. XRD Analysis

XRD analysis of crystalline phases was performed by using a Rigaku Smart Lab diffractometer at 40 kV and 30 mA (Cu K α radiation with a Ni filter) with Bragg-Brentano registration geometry ($2\theta = 0-80$).

The spectrum shows three major diffraction intensity peaks of stainless steel substrate were at 44.011° , 44.588° and 55.580° which corresponding to the peaks (1 1 1), (1 1 0) and (2 2 0) for stainless steel crystal planes as shown in figure 7.6.

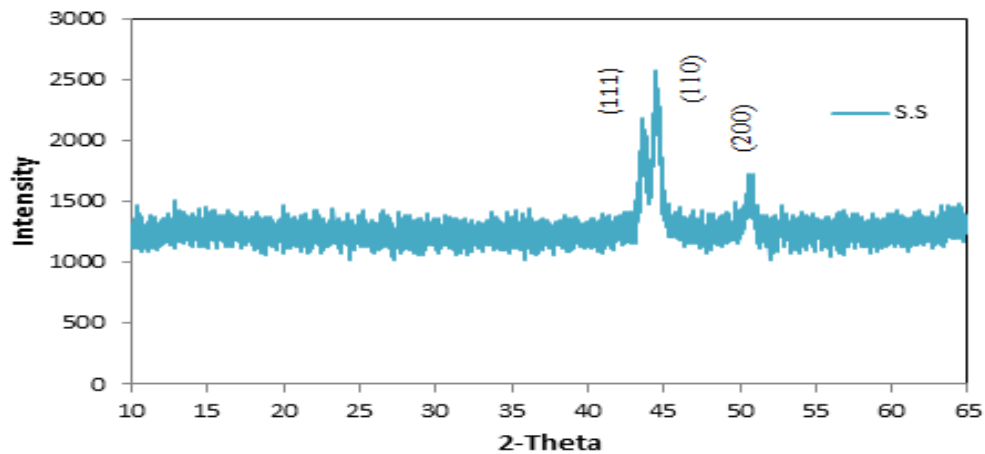


Figure 7.6. XRD patterns of the stainless steel substrate

XRD patterns of the TiO₂ powder detect that the peak at the different diffraction angles.

Figure 7.7(a) show that the five diffraction peaks of TiO₂ nanoparticle were at 25.428° , 38.00° , 48.066° , 54.06° and 55.21° , which corresponding to the orientations of (101), (002), (200), (102) and (105).

Figure 7.7(b) show The spectrum for four major diffraction intensity peaks of YSZ nanoparticles were at 28.284° , 35.224° , 50.241° and 59.88° which corresponding to the orientations (111), (200), (220) and (311) for YSZ powder crystal planes.

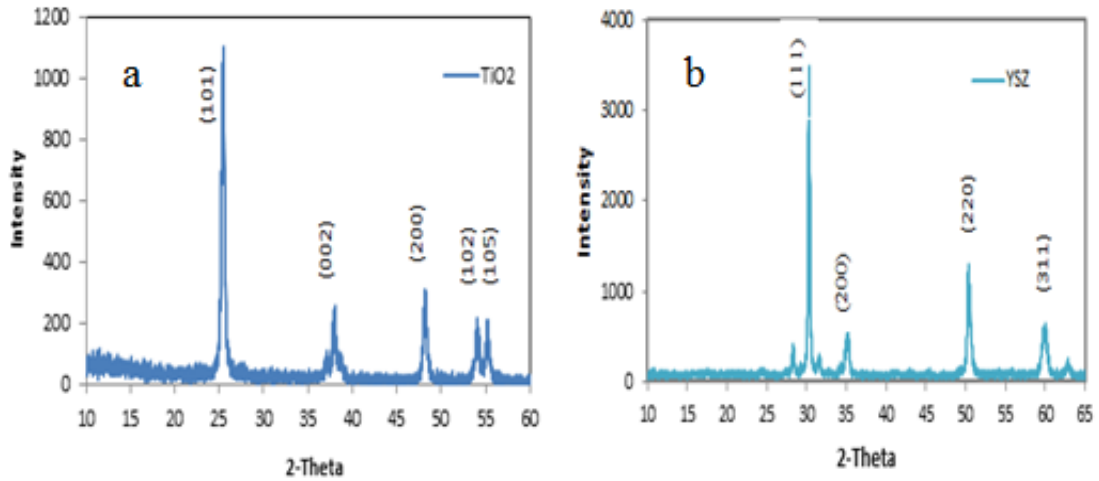


Figure 7.7. XRD patterns of the (a) TiO₂ powder and (b) YSZ powder

The comparison between XRD patterns of both TiO₂ powder, YSZ powder, TiO₂-YSZ coatings, YSZ coating and TiO₂ coating are represented in figure 7.8. All fabricated coatings were coated by using ESD in different deposition conditions with different temperatures in the sintering stage.

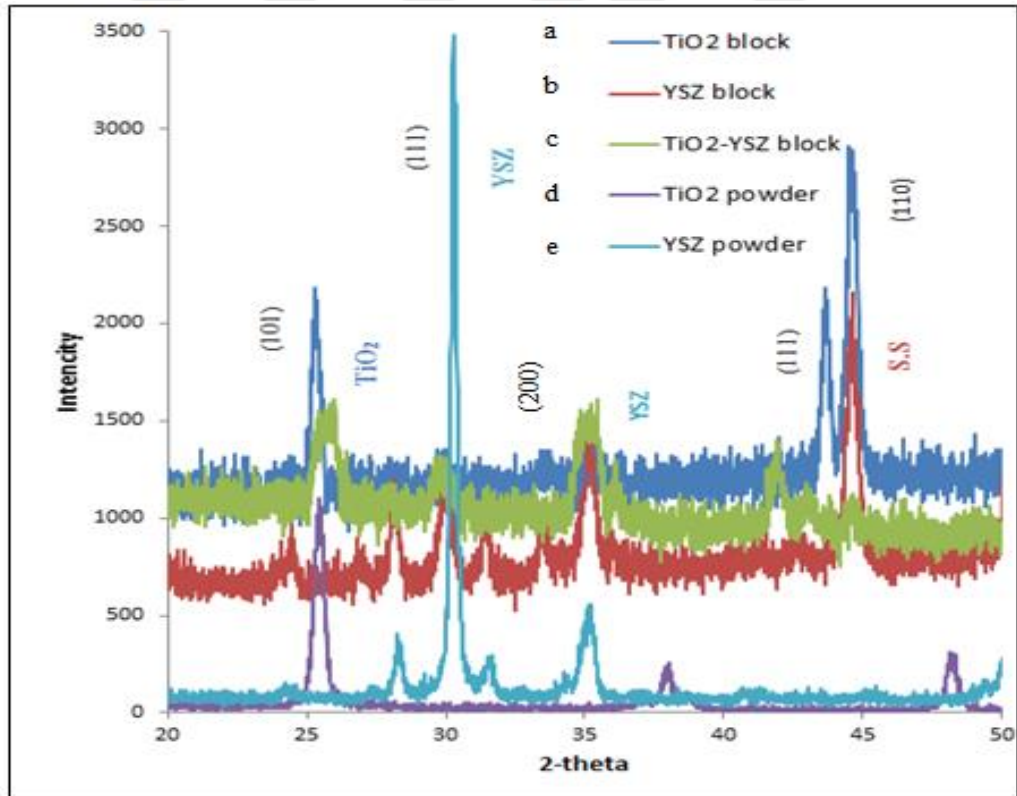


Figure 7.8. Evolution of diffraction patterns of (a) YSZ powder, (b) TiO₂ powder (c) TiO₂-YSZ coating, (d) YSZ coating and (e) TiO₂ coating.

XRD patterns of all fabricated coatings which were made on a stainless-steel substrate by using ESD process after sintering. According to the XRD results, we found that the diffraction angle of the stainless-steel substrate was $2\theta = 44.588^\circ$ as shown in Figure 7.6. XRD patterns of the TiO_2 powder detect that the peak at the diffraction angle $2\theta = 25.428^\circ$ with the orientation of (101) plane refer to TiO_2 powder which it similar to the diffraction peaks in figure 7.8 (a), (c) and (e) that which refers to TiO_2 powder, TiO_2 coating and TiO_2 -YSZ coating respectively. Figure 6.8(b), (c) and (e) show that the diffraction peaks of YSZ coating, TiO_2 -YSZ coating and YSZ nanoparticle were at 28.284° and 35.224° which corresponding to the orientations (111) and (200) plans and it is similar to the peaks in figure 7.7(b) for YSZ crystal planes. And YSZ powder with $2\theta = 28.284$ and 35.224 as shown in figure 7.7(a) and figure 7.7(b).

From XRD results for TiO_2 , YSZ and TiO_2 -YSZ coatings we found that it is clear that there is no change in Phases and it is refer to fabricated films.

The XRD plot of YSZ coating .on an Inconel 718 super alloy after sintering. There are no other diffractions from the substrate due to enough thickness of YSZ coating (Sinem Cevik & Mevlüt Gürbüz 2018).

XRD pattern of TiO_2 coating and powder showed a similar behavior, so characteristic peaks correspond to the crystallization of anatase and brookite phases of the TiO_2 coating and TiO_2 powder as shown in figure 7.8 (b) and (e). XRD analysis of our titanium precursor powder shows that starting from 450°C annealing temperature the TiO_2 anatase is the main crystalline phase. The diffraction pattern of the TiO_2 /ITO thin film shows a low crystallinity of the anatase phase (Ramona-Crina Suciú et al. 2011).

TiO_2 -YSZ coating was fabricated by ESD method and sintered at 1000°C . The Crystalline structure of TiO_2 -YSZ coating was characterized by using XRD. In accordance with XRD result TiO_2 -YSZ, composite coating microstructure is a mixture of amorphous and crystalline phases. From the peak's comparison of TiO_2 , YSZ and TiO_2 -YSZ coatings we found that the peaks at the same diffraction angle as shown in figure 7.8.

7.2.2. SEM and EDX Analysis

7.2.2.1. TiO₂ Coating

TiO₂ coating surface morphology was characterized by SEM. Images were taken with the scale of 1 μm with 5K X magnification as shown in figure 7.9(a), 100 nm with 50K X magnification as shown in figure 7.9(b). Particles could be seen randomly on fabricated TiO₂ coating. The particles were selected and the diameters appeared to be as follows: 36.4 nm, 39.5 nm, 64.4 nm and 72 nm.

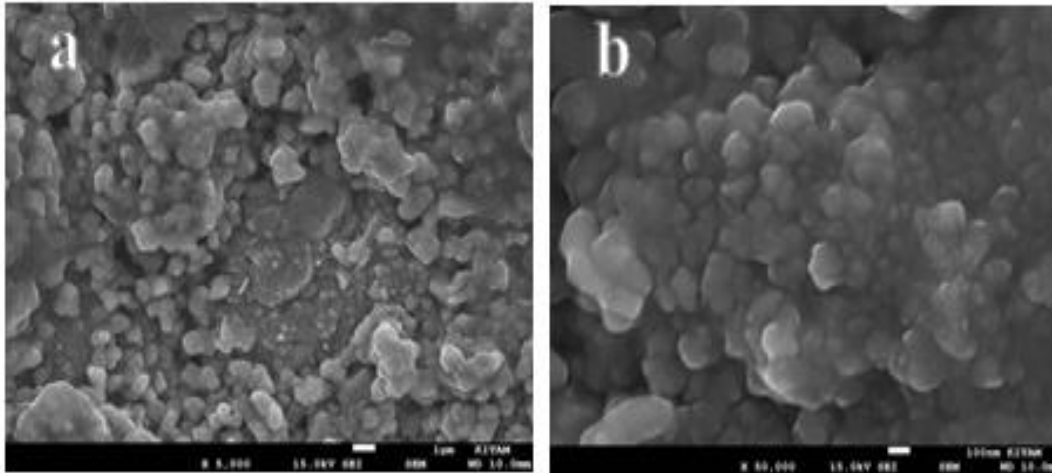


Figure 17.9. SEM images of TiO₂ coating surface in (a) microscale (b) nanoscale

Particle size of nanoscale TiO₂ was found as 36.4 nm, 39.5 nm, 64.4 nm and 72 nm. It has been observed that the regular distribution of titanium nanomaterials was observed on the stainless-steel surface. Nanomaterial assemblies were also observed on mineralogy due to the effect of high temperatures in the sintering stage as shown in figure 7.9 (a) and (b), which may lead to an increase in the hardness of the coating layer. (E.G. Zemtsova et al. 2016) produced TiO₂ nanocoating by using dip-coating method. By using SEM they found that the average size of nanostructures is 120 nm. We found that the average size of the TiO₂ nanostructure is 53 nm.

EDX analysis for TiO_2 coating was made at a microscale to calculate the elemental amount for the coated samples. EDX analysis was made with scale of $10\mu\text{m}$ for the fabricated TiO_2 coating. The elemental amount of TiO_2 coating was shown in figure 7.10 (a), (b) and (c).

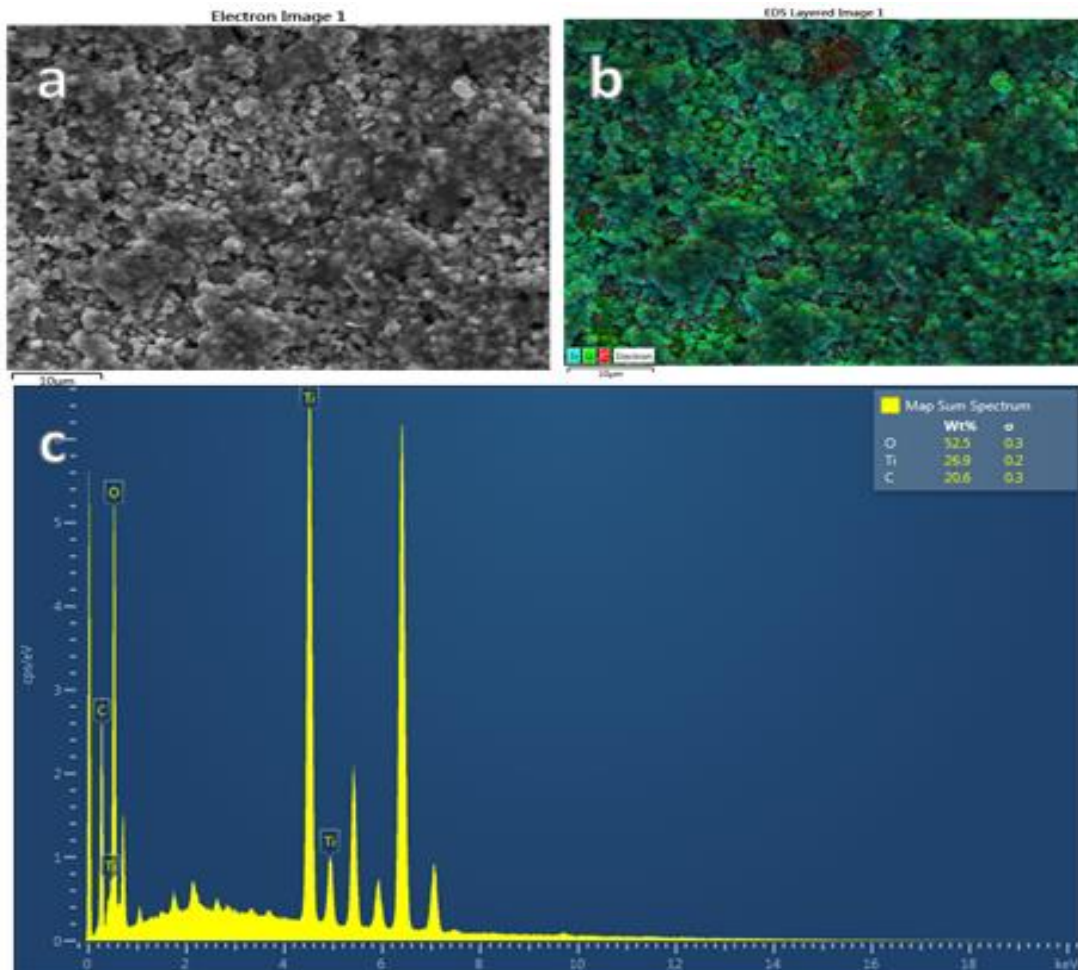


Figure 7.10. EDX analysis of fabricated TiO_2 coating in (a) SEM image of TiO_2 coating surface morphology at $10\mu\text{m}$ (b) chemical composition of TiO_2 coating and (c) elemental analysis of TiO_2 coating

The surface composition of TiO_2 films is further identified by EDX measurement. EDX results shown in figure 7.10 (a), (b) and (c) demonstrate that the peaks of Ti and O can be clearly seen in the survey spectrum. While the C element is the element of the stainless-steel substrate.

7.2.2.2. YSZ Coating

Surface morphology of the fabricated YSZ coating was checked by SEM. SEM images were taken with the scale of 1 μm with 5K X magnification as shown in figure 7.11(a) and 100 nm with 50K X magnification as shown in figure 7.11(b). Particles could be seen randomly on fabricated YSZ coating. The selected particles have diameters as follows: 35.5 nm, 59.9 nm, 64.3 nm and 76.1 nm.

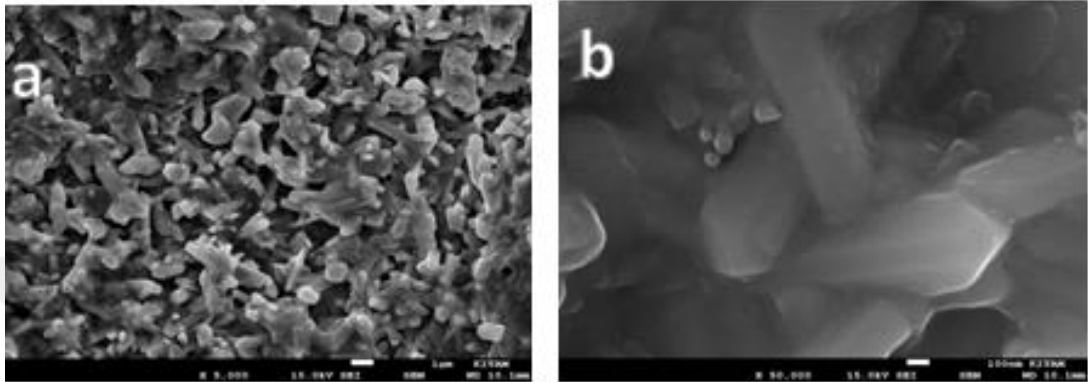


Figure 7.11. SEM images of YSZ coating surface in (a) microscale (b) nanoscale

YSZ thin layer was coated by using electrospray deposition as a coating technique on the surface of the 304 stainless-steel substrate. The ideal deposition set up for the coating device (ESD) was 0.05 ml as a flow rate and voltage of 7.5 KV with 7cm as the distance between the nozzle and the substrate. These parameters control the nanostructure of the thin film. We found the nanoparticle size of the YSZ coating as follows 35.5 nm, 59.9 nm, 64.3 nm and 76.1 nm. An agglomeration of nanomaterials in the form of large blocks was noticed on the target surface of the coating, was noticed as shown in figure 7.11. The reason for this large agglomeration of nanomaterials on the surface of the metal might be due to the high temperatures for a long period of time in the sintering process or due to electrostatic attraction of nanoparticles. This agglomeration or adhesion may give a cohesive structure that had a positive effect in improving the physical properties. YSZ thin film was successfully produced via the electrospray deposition technique. They demonstrated that YSZ film suggested producing highly dense coatings with enhanced mechanical properties. We used approximately the same coating conditions (Sinem CEVIK and Mevlud GÜRBÜZ 2018).

EDX analysis for YSZ coating was made at a microscale to calculate the elemental amount for the coated samples. EDX analysis was made with scale of 10 μ m for the fabricated YSZ coating. The elemental amount of YSZ coating was shown in figure 7.12 (a), (b) and (c).

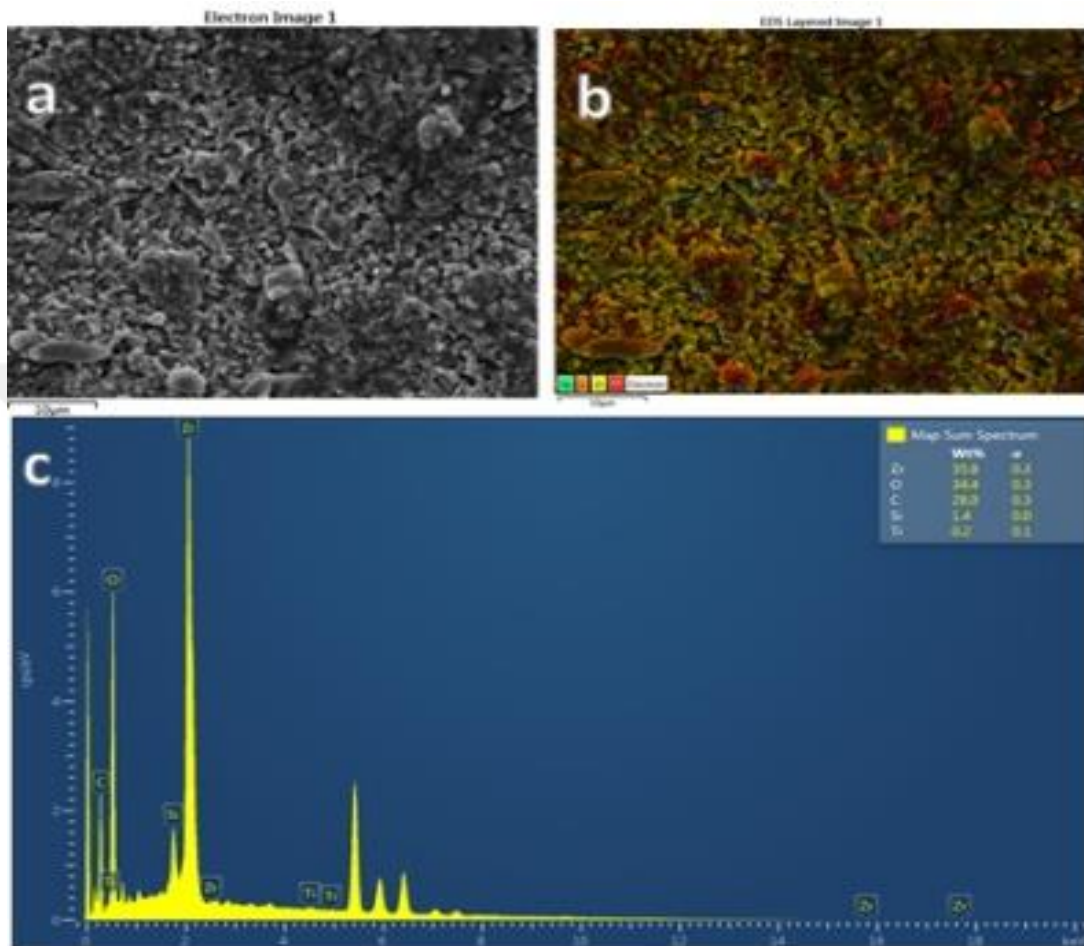


Figure 7.12. EDX analysis of fabricated YSZ coating in (a) SEM image of YSZ coating surface morphology at 10 μ m (b) chemical composition of YSZ coating and (c) elemental analysis of YSZ coating

The surface composition of YSZ films is further determined by EDX measurement. EDX results shown in figure 7.12 (a), (b) and (c) demonstrate that the peaks of Zr and O can be clearly seen in the survey spectrum. While C and Fe elements, are the elements of stainless-steel substrate. The YSZ thin film had a highly amount of YSZ on the surface of substrate. EDX analysis approved that we have a good deposition and distribution on the substrate.

7.2.2.3. TiO₂ –YSZ Coatings

TiO₂ –YSZ coating Surface morphology and film thickness was characterized by using SEM. SEM images was taken with the scale of 1µm with 5K X magnification as shown in figure 7.13(a) and 100 nm with 50K X magnification as shown in figure 6.13(b). Particles can be seen randomly seen on fabricated TiO₂ –YSZ coating surface. The particle sizes were selected and the diameters appeared to be as follows: 66.6 nm, 82.6 nm, 111.1 nm and 113.1 nm. And the thickness of film was measured in the limit of (2.72-3.77) µm as shown in figure 7.13(c).

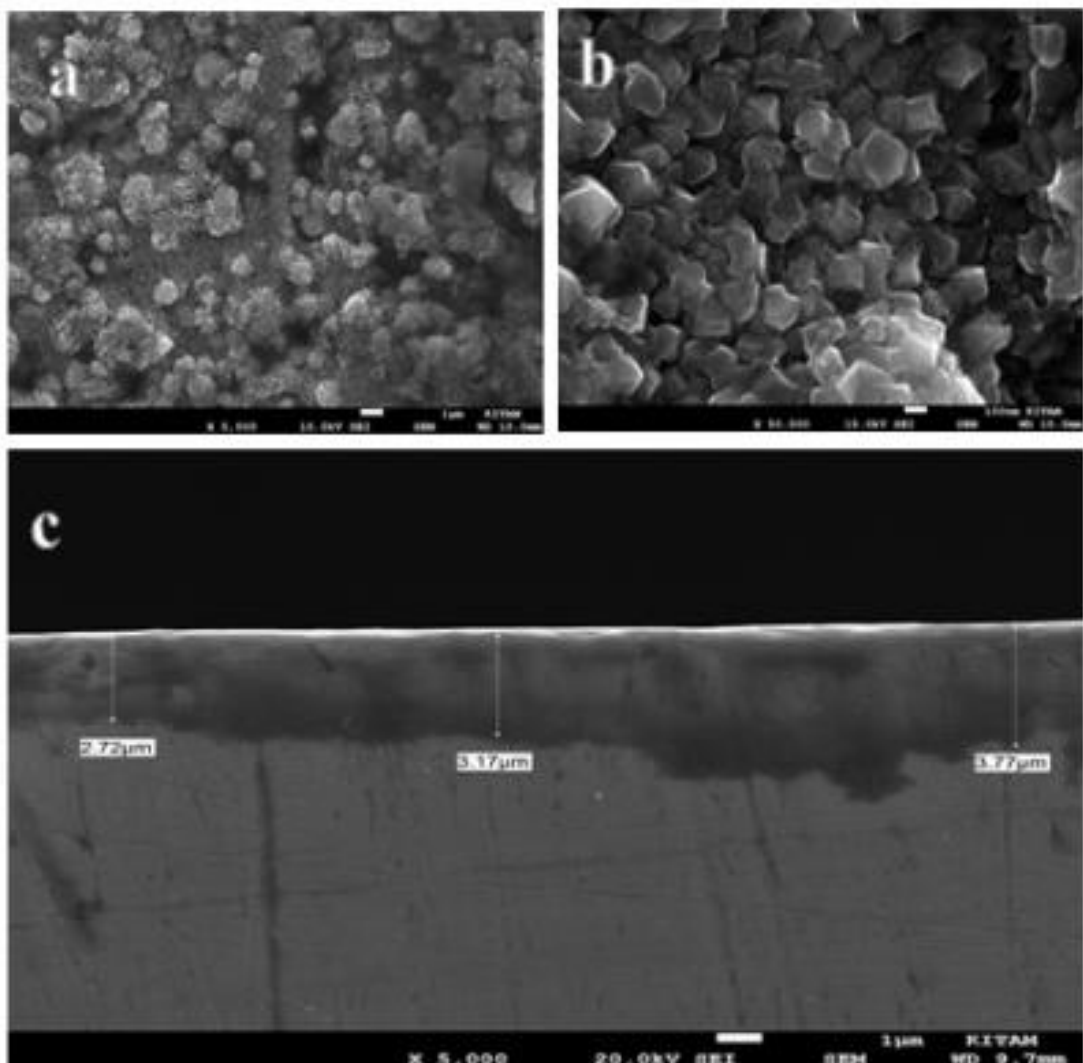


Figure 7.13. SEM images of (a) TiO₂ –YSZ coating surface in microscale (b) TiO₂ –YSZ coating surface in nanoscale and (c) TiO₂ –YSZ film cross section

TiO₂ –YSZ coating has been done by electrospray deposition as a coating technique on the surface of the stainless-steel substrate 304. Many parameters control the nanostructure of thin film just like spray flow rate, voltage intensity and distance between the nozzle and the substrate. The optimum deposition's parameters for the coating device (ESD) were 0.05ml as a flow rate and voltage of 9.2 kV for 45min with 7cm as the distance between the nozzle and the substrate. Surface topography and particles size was characterized by SEM. SEM measurement allowed us to observe and calculate the presence of nanoparticle YSZ minutes as follows 66.6 nm, 82.6 nm, 111.1 nm and 113.1nm. An agglomeration of nanomaterials on the target surface of the coating was noticed as shown in figure 7.13 (b). The synergistic work of the YSZ with TiO₂ gave a homogenous distribution in the form of islands of nanocomposites on the target surface. The reason for this agglomeration of nanomaterials on the surface of the metal may occur due to the high temperatures for a long period of time in the sintering process or due to electrostatic attraction of nanoparticles in the TiO₂ –YSZ solution preparation stage. This agglomeration or adhesion may give a cohesive structure that had a positive effect in improving the physical properties.

TiO₂ –YSZ coating thickness was observed by SEM. With SEM characterization we found that the film thickness of TiO₂ –YSZ coating was ranged as (2.72-3.77) μm and it's within the range of thin film thickness as shown in figure 7.13(c). Moreover, a good interaction and high adhesion between film and substrate was observed.

EDX analysis for TiO_2 – YSZ coating was made at a microscale to calculate the elemental amount for the coated samples. EDX analysis was made with scale of $1\mu\text{m}$ for the fabricated TiO_2 – YSZ coating. The elemental amounts of TiO_2 – YSZ coating was shown in figure 7.14(a), (b) and (c).

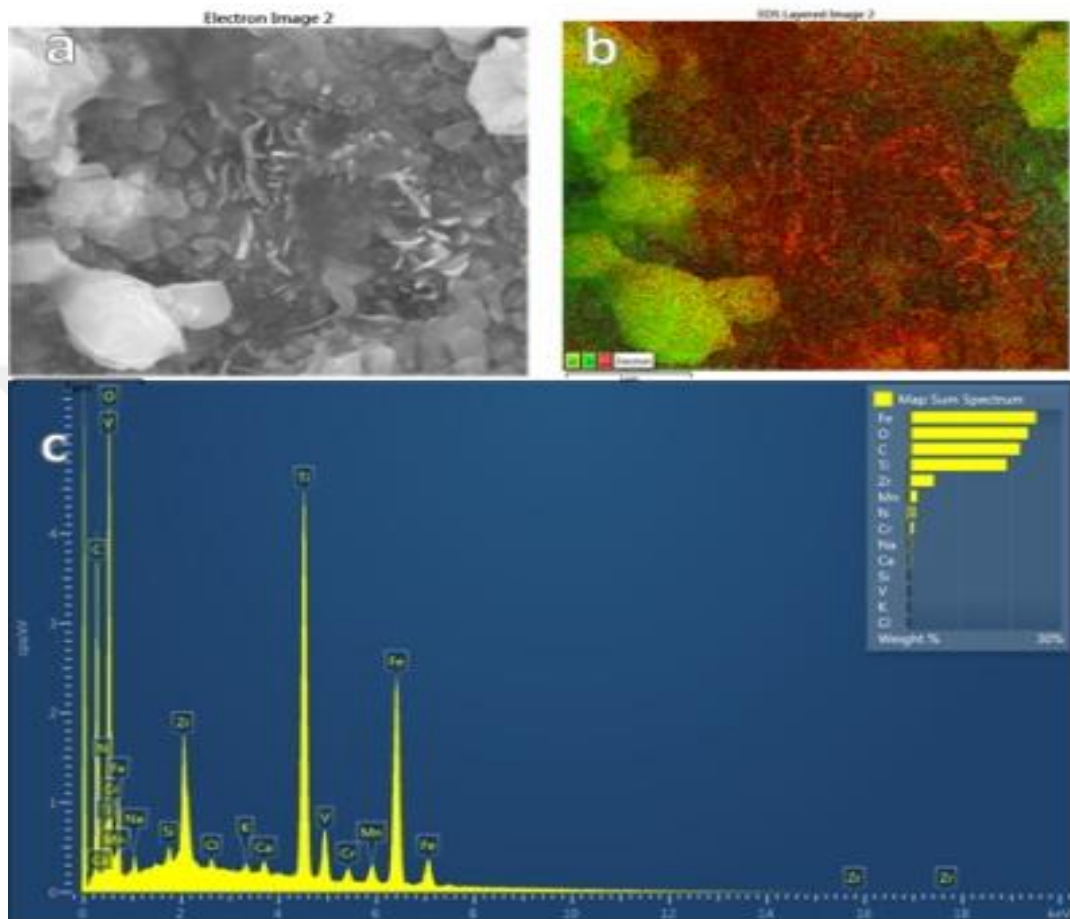


Figure 7.14. EDX analysis of fabricated TiO_2 – YSZ coating in (a) SEM image of TiO_2 – YSZ coating surface morphology at $1\mu\text{m}$ (b) chemical composition of TiO_2 – YSZ coating and (c) elemental analysis of TiO_2 – YSZ coating

On the other hand, the surface composition of TiO_2 – YSZ coating is determined by EDX measurement. EDX results that shown in figure 7.12 (b) and (c) demonstrate that the peaks of Ti, Y, Zr and O can be clearly seen in the survey spectrum. While C, Fe, Mn, N, Cr and Ca elements, are the elements of stainless-steel substrate. The YSZ thin film had a highly amount of TiO_2 and YSZ on the surface of the substrate. EDX results gave us a real impression of the distribution and presence of TiO_2 and YSZ nanomaterials on the surface of the stainless-steel substrate.

7.2.3. AFM Analysis

7.2.3.1. TiO₂ Coating Analysis

Average Roughness (Ra) of the TiO₂ coating surface and Root mean square (Rms) were characterized by using AFM. AFM images are all in the nanometer scale as shown in figure 6.15(a) and (b). We found that the Average Roughness (Ra) of the TiO₂ coating equals to 51.809 nm and (Rms) was found as : 61.522 nm.

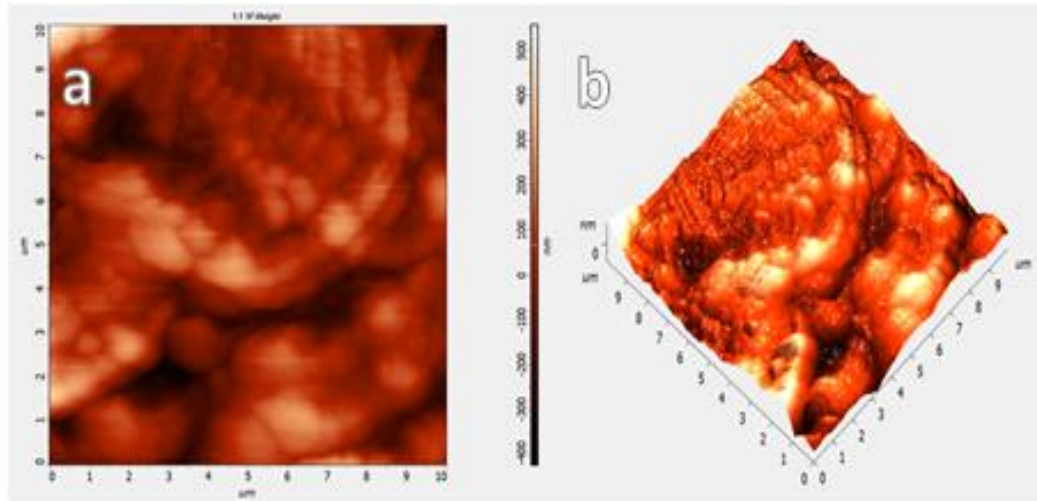


Figure 7.15. AFM images of the TiO₂ coating samples: (a) 2D image and (b) 3D image

The (Ra) value of the monolayer coated samples over areas of 10x10 μm is presented in figure 7.15(a) and (b). From AFM measurement It was found that the distribution of nanoscale TiO₂ particles in the thin film was uniform across the entire surface of the stainless steel the color of the image represents the height of the material. The lighter parts of the image are higher. We found that the (Ra) is equal to 51.809 nm and (Rms) was found as : 61.522 nm. Due to AFM results, we can conclude that the surface is a highly smooth and the structures were more compact with lower porosity. Some agglomerations were observed on the films. This agglomeration may be caused by TiO₂ solution preparation, deposition conditions or sintering temperature and time. The surface roughness is important for tribology of surface, homogenous surface causes less scratch ability (Kozuka and Hirano 2000).

7.2.3. 2. YSZ Coating Analysis

The surface topography of YSZ coating was characterized by using AFM. AFM images are all in the nanometer scale as shown in Figure 7.1 (a) and (b). We found that the (Ra) of YSZ coating equals to 59.465 nm and (Rms) was found 76.130 nm.

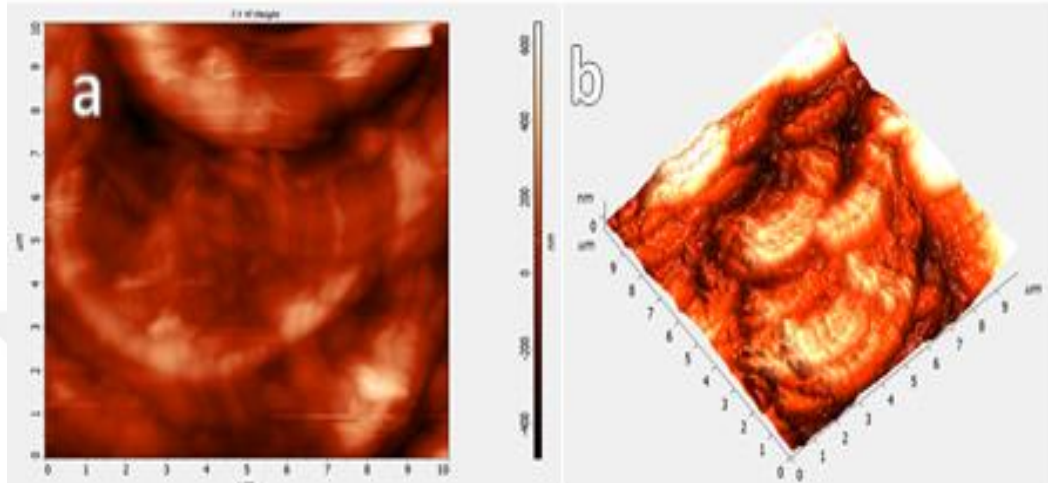


Figure 7.16. AFM images of the YSZ coating samples: (a) 2D image and (b) 3D image

The (Ra) value of the monolayer coated samples over areas of $10 \times 10 \mu\text{m}^2$ is elaborated in figure 6.16. Figure 7 (a) and (b) show the 2D and 3D AFM micrographs of the coated samples, suggesting uniform and dense films. From AFM measurement it was found that the distribution of nanoscale YSZ particles in the thin film was almost uniform across the entire surface of the stainless-steel. The color regions in the image represent the height of the material. We found that the (Ra) equal to 59.465 nm and (Rms) a highly smooth and the structures were more compact with lower porosity. The surface roughness is important for the surface tribology of the fine surface causes less scratch and corrosion ability and high thermal resistance.

7.2.3.3. TiO₂ –YSZ Coatings Analysis

AFM used for the characterization of TiO₂ –YSZ coating surface topography. All TiO₂ –YSZ coating images that obtained by AFM were in nanoscale as shown in figure 7.17(a) and (b). (Ra) of TiO₂ –YSZ surface was found as: 47.138 nm while Rms was equal to 63.718 nm.

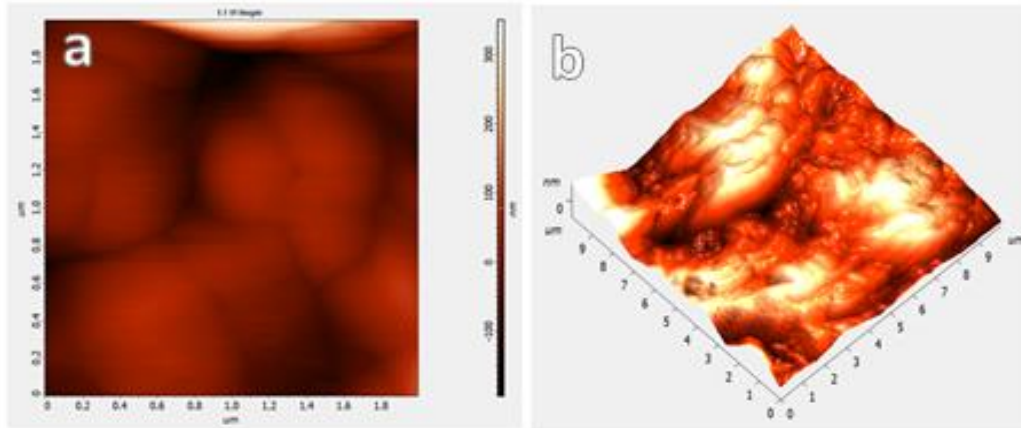


Figure 7.17. AFM images of the TiO₂ –YSZ coating samples: (a) 2D image and (b) 3D image

TiO₂ –YSZ coating was coated by ESD method in the stainless-steel substrate. AFM was used to determine (Ra) and (Rms) for the fabricated TiO₂ –YSZ coating surface. The (Ra) of the monolayer coated samples over areas of 10x10 μm² is presented in figure 7.17. Figure 7.17 (a) and (b) show the two and three-dimensional AFM micrographs of the coated samples, suggesting uniform and dense films. The distribution of nanoscale TiO₂ –YSZ particles in the thin film was uniform across the entire surface of the stainless steel. According to AFM results we found that the average roughness equal to 47.138 nm and (Rms) was found as 63.718 nm. AFM results allowed us to conclude that the surface is a very smooth and the structures were more compact with lower porosity. This type of uniform coating can be advantageous in different applications, including pharmaceutical and food equipment as well as medical and surgical tools.

According to the AFM result for the fabricated films, we find that the (Ra) of TiO₂ film is 51.809 nm, YSZ film is 59.465 nm and 47.138 nm for TiO₂ –YSZ coating. Due to these results gave us an impression that the TiO₂ –YSZ coating surface had the lowest (Ra) from the other coating, and thus the surface will be smoother.

7.3. Ag Thin Films Analysis

7.3.1. SEM and EDX Analysis

Ag thin film was coated by using ESD method by same conditions for TiO₂, YSZ and TiO₂-YSZ films samples as a second layers.

7.3.1.1. TiO₂-Ag Coating

Surface morphology and film thickness of the fabricated TiO₂-Ag coating were characterized by using SEM. SEM images was taken with the scale of 1μm with 5K X magnification as shown in figure 7.18(a) and at 100 nm with 50K X magnification as shown in figure 6.18(b). Particles can be seen random on fabricated TiO₂-Ag coating particles were selected and the diameters appeared to be as follows: 38.8 nm, 62.9 nm, 67.9 nm and 72.9 nm. And the thickness of film was measured in the limit of (1.48-2.27) μm as shown in figure 7.18(c).

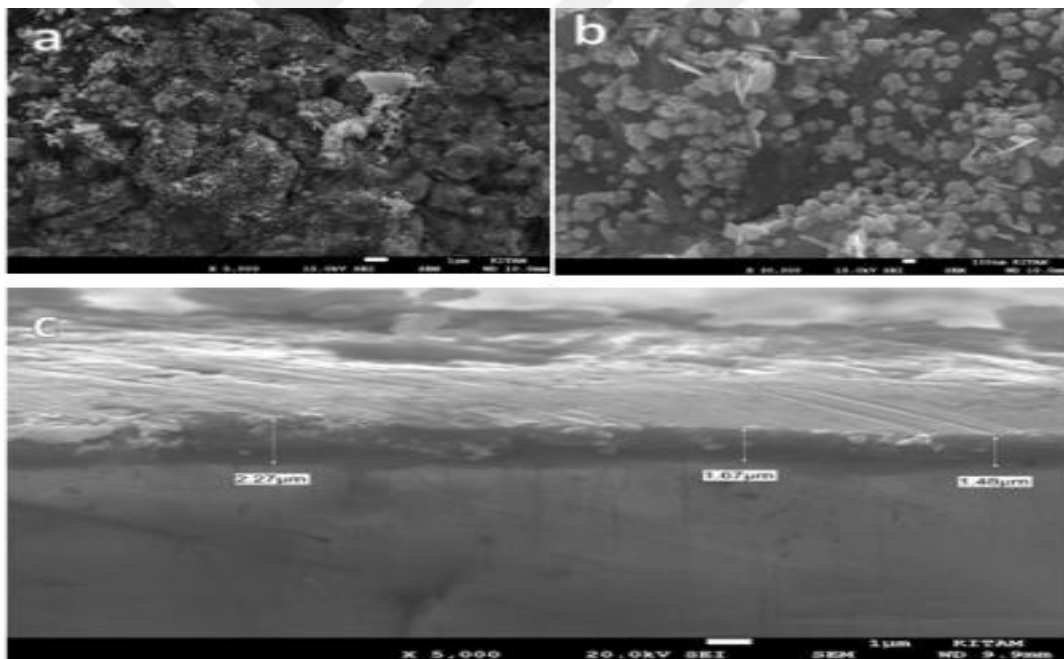


Figure 7.18. SEM images of (a) TiO₂-Ag coating surface in microscale (b) TiO₂-Ag coating surface in nanoscale and (c) TiO₂-Ag film cross-section

As we explained earlier in chapter six, Ag coating was coated by using ESD as a coating technique over the surface of the TiO₂ film. Many parameters control the nanostructure of Ag thin film just like spray flow rate, voltage intensity and distance between the nozzle and the substrate. The optimum deposition's set up for the coating device (ESD) was 0.02ml as a flow rate and voltage of 12.5 kV for 45min

with 7cm as distance between the nozzle and the substrate. Surface topography and particles size was characterized by SEM. SEM measurement allowed us to observe and calculate the presence of nanoparticle Ag minutes as follows: 38.8 nm, 62.9 nm, 67.9 nm and 72.9nm. We notice that a homogenous distribution of AgNPs in the TiO₂ matrix as shown in figure 7.18 (a).

Ag–TiO₂ nanocomposite thin films were prepared by using sol-gel method, which were deposited onto a glass substrate by the spin coating process. Fabricated Ag–TiO₂ nanocomposite is more agglomerate, growth and regularly distributed. the morphology of the produced thin film might be controlled via different proportion of AgNO₃ in the direction of TiO₂ in the solution of which prepared previously(Sinan Salman Hamdi., 2016).

TiO₂ –Ag coating thickness was observed by SEM. By SEM characterization we found that the film thickness of TiO₂ –Ag coating was ranged as (1.48-2.27) μm and it's within the range of thin film thickness as shown in figure 7.18(c).

EDX analysis for Ag coating was made at a microscale to calculate the elemental amount for the coated samples. EDX analysis was made with scale of 1μm for the fabricated TiO₂ – Ag coating. The elemental amounts of TiO₂ – Ag coating was shown in figure 7.19 (a), (b) and (c).

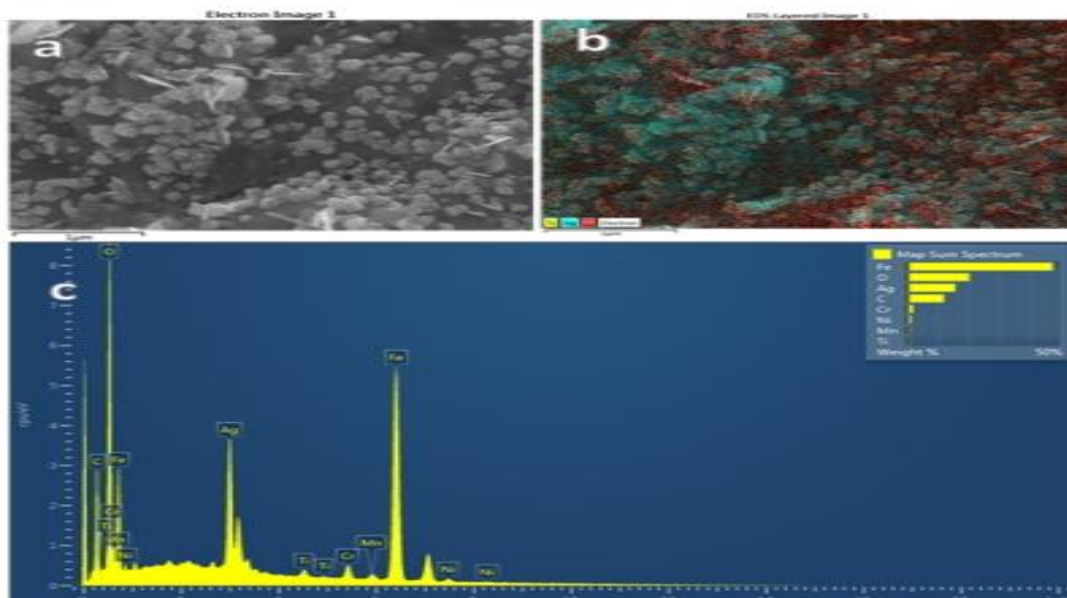


Figure 7.19. EDX analysis of fabricated TiO₂–Ag coating in (a) SEM image of TiO₂–Ag coating surface morphology at 1μm (b) chemical composition of TiO₂ –YSZ–Ag coating and (c) elemental analysis of TiO₂–Ag coating

Surface composition of $\text{TiO}_2 - \text{Ag}$ coating is determined by EDX measurement. EDX results that shown in figure 7.19 (a), (b) and (c) demonstrates that the peaks of Ag, Ti and O can be clearly seen in the survey spectrum. While C, Fe, Mn, N and Cr elements, are the elements of stainless-steel substrate. The $\text{TiO}_2 - \text{Ag}$ thin film had a highly amount of Ag on the surface of substrate. EDX results gave us a real impression about the distribution and presence of AgNPs on the TiO_2 film. We found that a high amount of AgNPs was occurred in the second layer. The EDX spectra indicated to presence a small amount of silver within the TiO_2 , that confirms individual silver ions interacted with the TiO_2 matrix (Sinan Salman Hamdi., 2016).

7.3.1.2. YSZ–Ag Coating

Surface morphology and film thickness of the synthesized YSZ-Ag coating was characterized by SEM. Images were taken with a scale of $1\mu\text{m}$, 5KX magnification as shown in figure 7.2(a) and 100 nm , 30KX magnification as shown in Figure 7.3(b). Particles could be seen randomly at YSZ-Ag coating. The selected particles had diameters as follows: 20 nm , 31 nm , 57 nm and 62 nm . The thickness of obtained film was measured between $(0.68\text{-}1.56)\mu\text{m}$ as shown in Figure 7.4(c).

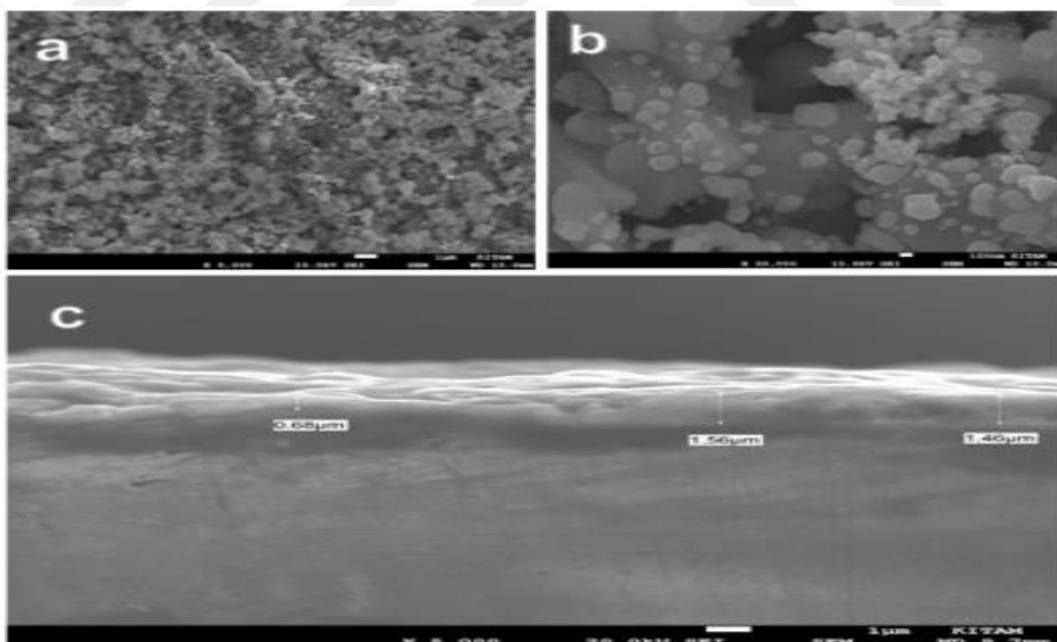


Figure 27.20. SEM images of (a) YSZ –Ag coating surface in microscale (b) YSZ – Ag coating surface in nanoscale and (c) YSZ Ag film cross section

Ag coating was conducted by using ESD as a coating technique over the surface of the YSZ film.

The nanostructure of Ag thin film is controlled by some factors during the coating process just like spray flow rate, voltage intensity and distance between the nozzle and the substrate or also by the preparation conditions of AgNPs. The optimum deposition parameters for the coating device (ESD) were 0.02 ml as a flow rate, voltage of 12.5 kV for 45min with 7 cm as the distance between the nozzle and the substrate. Surface topography and particle size were characterized by SEM. With SEM measurement, we found that the presence of Ag nanoparticle as follows: 38.8 nm, 62.9 nm, 67.9 nm and 72.9nm. AgNPs had a perfect distribution in the YSZ matrixes shown in figure 7.18(a). Matrix crystallization promotes silver embedding into the outer layer of the film.

SEM was used for the measurement of YSZ –Ag film thickness. By SEM characterization we found that the film thickness of YSZ –Ag coating was ranged as (0.68-1.56) μm shown in figure 7.20(c). Due to these results, it was confirmed that the coating layer manufactured by ESD technique is very thin layer. We noticed that there was a good interaction and High adhesion between film and substrate.

EDX analysis for Ag coating was made at a microscale to calculate the elemental amount for the coated samples. EDX analysis was made with scale of 1 μm for the fabricated YSZ – Ag coating. The elemental amounts of YSZ – Ag coating was shown in figure 7.21 (a), (b) and (c).

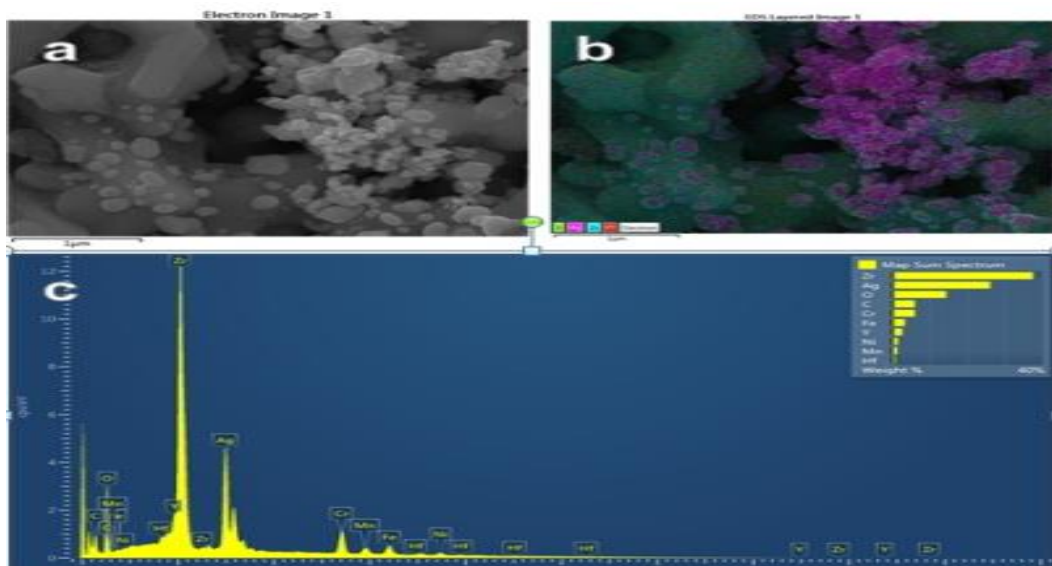


Figure 7.21. EDX analysis of fabricated YSZ – Ag coating in (a) SEM image of YSZ – Ag coating surface morphology at 1 μm (b) chemical composition of YSZ – Ag coating and (c) elemental analysis of YSZ – Ag coating

EDX technique was used for the analysis of YSZ – Ag coating Surface composition. EDX results exhibit that the peaks of Ag, Zr, Y and O can be clearly seen in the survey spectrum that shown in figures 7.21(a), (b) and (c).

Whilst C, Fe, Mn, N and Cr elements are the elements of stainless-steel substrate. The YSZ – Ag thin film had a high amount of Ag on its surface. An EDX result explains the distribution and presence of AgNPs on the YSZ matrix.

7.3.1.3. TiO₂ –YSZ–Ag Coating

SEM was used for the characterization of the surface morphology and the film thickness of the fabricated TiO₂ –YSZ–Ag coating. SEM images were taken with 1µm scale, 5KX magnification as shown in figure 7.22(a) and 100 nm with 30KX magnification as shown in figure 7.22(b). Particles could be seen randomly at fabricated TiO₂ –YSZ–Ag coating. The selected particles had diameters as follows: 24 nm, 25.9 nm, 28.5 nm and 38.9 nm. The thickness of obtained film was measured between (1.40-2.08) µm as shown in figure 7.22(c).

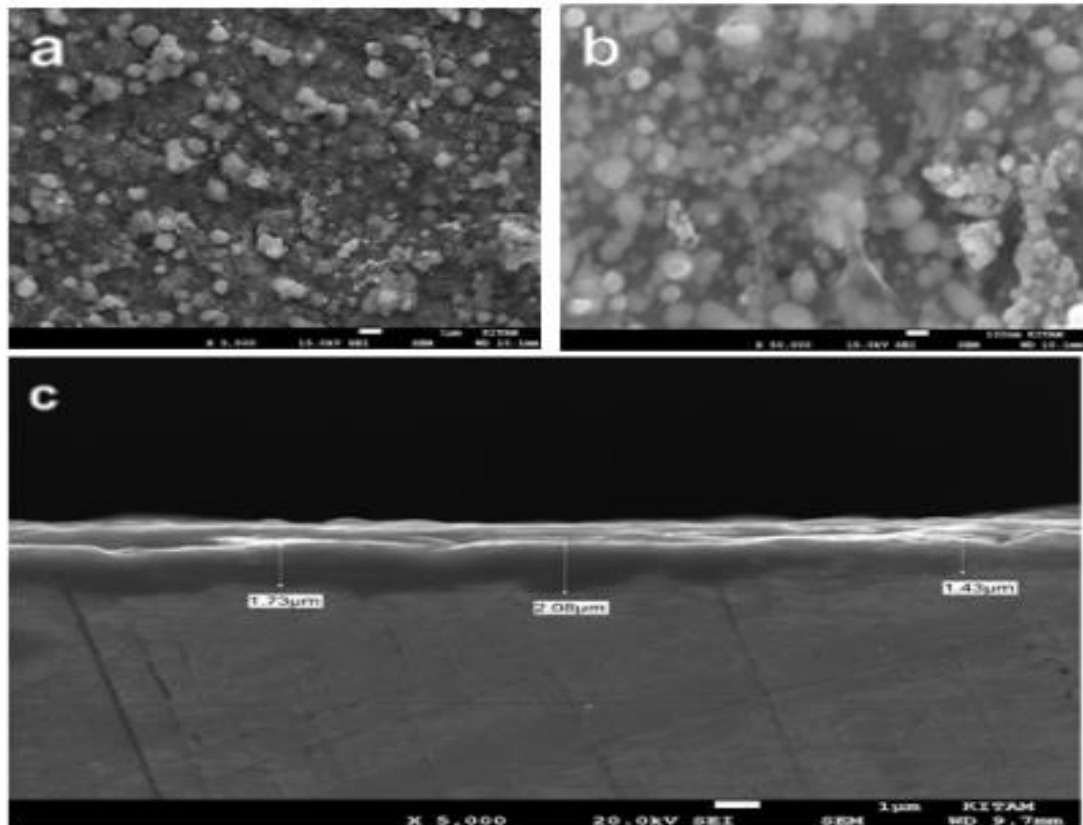


Figure 7.22. SEM images of (a) TiO₂ –YSZ–Ag coating surface in microscale (b) TiO₂ –YSZ–Ag coating surface in nanoscale and (c) TiO₂ –YSZ–Ag film cross section

Our work aims to produce TiO₂–YSZ–Ag thin film. 5 mM of colloidal AgNPs was used to be a coating solution in the final coating stage. ESD method is the coating process for coating Ag film over the surface of the TiO₂–YSZ film. The nanostructure of Ag thin film is controlled by spray flow rate, voltage intensity and distance between the nozzle and the substrate during the coating process, or also by the preparation conditions of AgNPs.

The optimum depositions set-up for the coating device (ESD) was 0.02 ml as a flow rate and voltage of 12.5 kV for 45 min with 7 cm as the distance between the nozzle and the substrate. Surface topography and particle size were characterized by SEM. By SEM measurement we found that the presence of Ag nanoparticle as follows: 24 nm, 25.9 nm, 28.5 nm and 38.9 nm. We noticed that small AgNPs (white and light gray) had a homogenous distribution in the TiO₂–YSZ matrixes shown in figure 7.22(b). The synergic work of TiO₂–YSZ matrix crystallization promotes silver embedding into the outer layer of the film.

The introduction of Ag ions into the oxide film precursor results in enhanced the damage of the mesostructure because of the formation of AgNPs within pores on thermal treatment. However, in the case of the TiO₂ and ZrO₂ films, Ag can retard the crystallization of the matrices. AgNPs form dominantly on the outer surface of the film under lower sintering temperature if the amount of loaded silver is low. Matrix crystallization promotes Ag embedding into the outer layer of the film. At a higher Ag content (10%) and higher calcination temperature (873 K), AgNPs could be distributed more uniformly along the film profile because of effective compensation of Ag droplets evaporation from the outer film surface by nucleation and migrating processes of Ag clusters within the film volume. (Krylova et al., 2009).

SEM was used to measure TiO₂–YSZ–Ag film thickness. By SEM characterization we found that the film thickness of TiO₂–YSZ–Ag coating was ranged as (1.40-2.08) μm shown in figure 7.22(c). Due to these results, it was confirmed that the coating layer manufactured by ESD technique is very thin.

The thickness of all fabricated films has been measured using a cross-section of SEM image as shown in figures 7.18(c), 7.20(c) and 7.22(c). The average film thickness of TiO₂-Ag coating is 1.806 μm, of YSZ-Ag coating is 1.233 μm and of the TiO₂–YSZ–Ag coating is 1.736 μm. These results are agreement with the theoretical calculation concerning the design of the thin layer.

As we mentioned previously, EDX analysis for Ag coating was made at a microscale to calculate the elemental amount for the coated samples. EDX analysis was made with scale of 1 μ m for the fabricated TiO₂–YSZ–Ag coating as shown in figure 7.23 (a), (b) and (c).

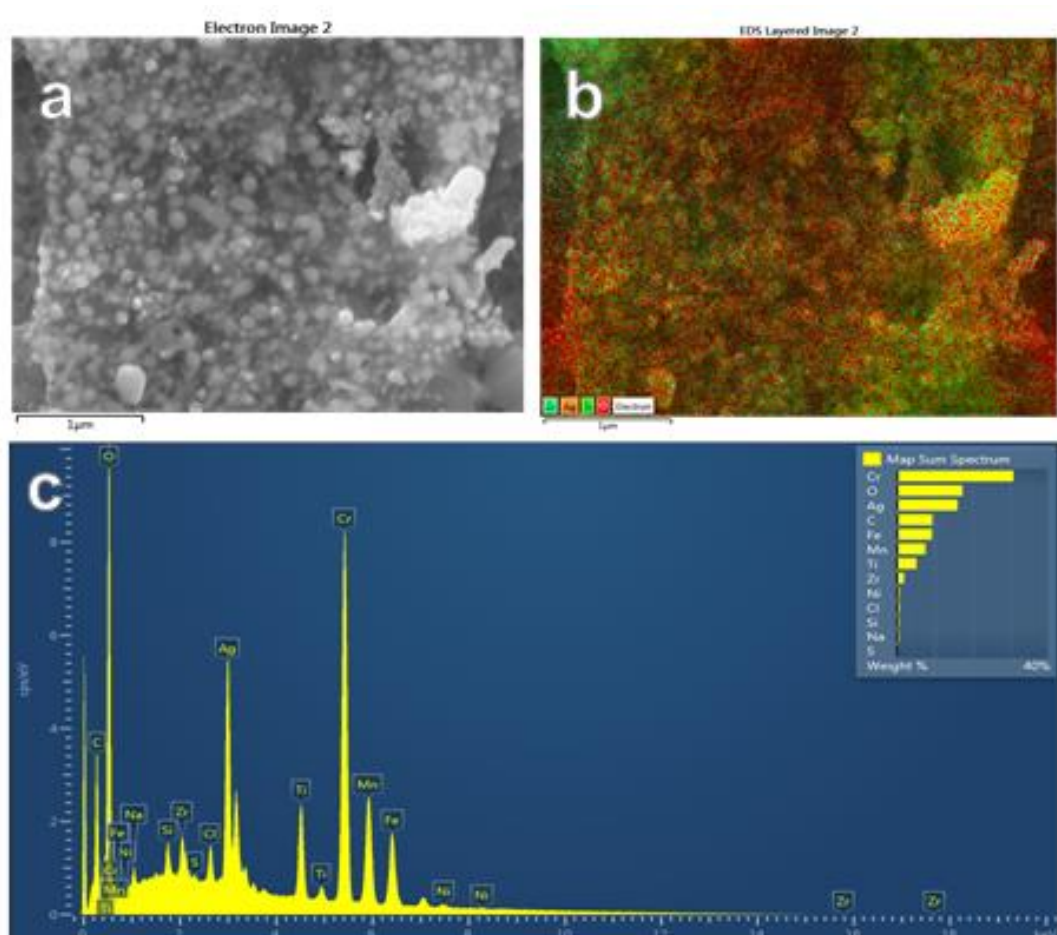


Figure 7.23. EDX analysis of fabricated TiO₂–YSZ–Ag coating in (a) SEM image of TiO₂–YSZ–Ag coating surface morphology at 1 μ m (b) chemical composition of TiO₂–YSZ–Ag coating and (c) elemental analysis of TiO₂–YSZ–Ag coating

EDX technique was used for the analysis of the TiO₂–YSZ–Ag coating Surface composition. EDX results exhibit that the peaks of Ag, Ti, Zr, Y and O can be seen in the survey spectrum shown in figures 7.23 (b) and (c). Whilst C, Fe, Mn, N and Cr elements represent the elements of stainless-steel substrate. The TiO₂–YSZ–Ag thin film had high amount of Ag on its surface. EDX results gave a real impression of the distribution and presence of AgNPs at the TiO₂–YSZ matrix.

7.3.2. Antimicrobial Assay of Fabricated Thin Films

TiO₂-Ag, YSZ-Ag and TiO₂-YSZ-Ag thin films fabricated by ESD method have been found highly toxic against pathogenic bacteria and fungi. The TiO₂-Ag, YSZ-Ag and TiO₂-YSZ-Ag thin films exhibited antimicrobial activity against pathogenic bacteria and fungi two kinds of bacteria such as: *Escherichia coli* and *Pseudomonas aeruginosa*, with *Candida albicans* fungi, it shown clear inhibition zone in figure 7.24.

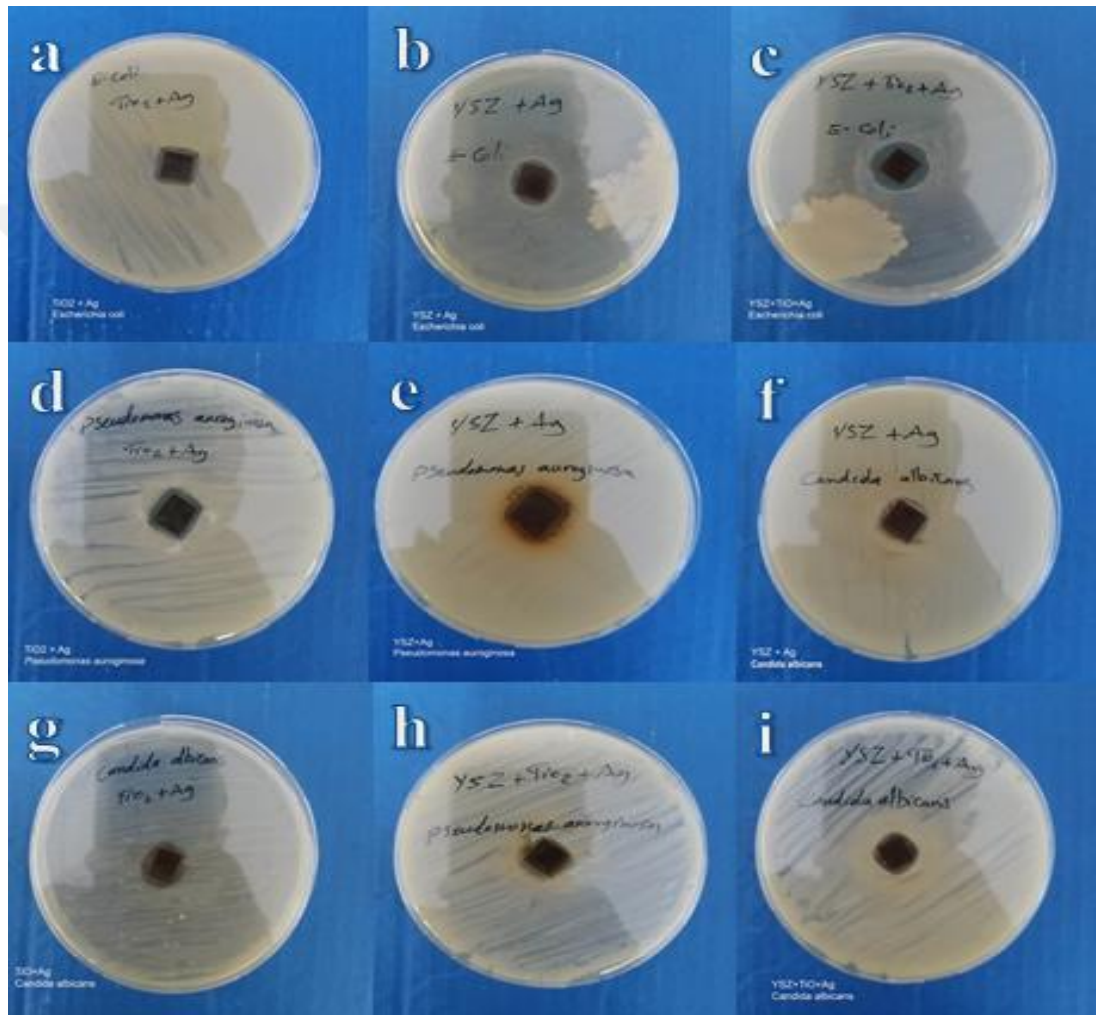


Figure 7.24. Result of Antimicrobial activity of (a) TiO₂-Ag coating in *Escherichia coli*, (b) YSZ-Ag coating in *Escherichia coli*, (c) TiO₂-YSZ-Ag coating in *Escherichia coli*, (d) TiO₂-Ag coating in *Pseudomonas aeruginosa*, (e) YSZ-Ag coating in *Pseudomonas aeruginosa*, (f) TiO₂-YSZ-Ag coating in *Pseudomonas aeruginosa*, (g) TiO₂-Ag coating in *Candida albicans*, (h) YSZ-Ag coating in *Candida albicans* and (i) TiO₂-YSZ-Ag coating in *Candida albicans*

Table 4. below shows the toxic effect of fabricated coatings on all bacteria and fungi on which the antimicrobial effect was examined. And it shows the relation between the effect of TiO₂-Ag, YSZ-Ag and TiO₂ -YSZ-Ag Thin films and the inhibition zone diameter in mm.

Table 4. Effect of thin films vs Inhibition zone diameter on selected microorganisms

sample	<i>Escherichia coli</i>	<i>Pseudomonas aeruginosa</i>	<i>Candida albicans</i>
TiO ₂ -Ag coating	20 mm	21 mm	19 mm
YSZ-Ag coating	18 mm	16 mm	15 mm
TiO ₂ -YSZ-Ag coating	23 mm	20 mm	16 mm

Due to the antimicrobial assay in figure 7.24, we conclude that all the fabricated films have a good antimicrobial activity against all types of microorganisms that was examined. The Inhibition zone shown in Table 4. indicates the tendency of the thin film to kill microbes on and around the coated sample. The TiO₂-Ag coating had the highest pathogenic effects against all the microorganisms, but we noticed that coating surface suffering from a huge damage because of the microbial corrosion which is caused by enzymatic secretions of microorganisms. YSZ-Ag coating had a normal antimicrobial effect as illustrated in table 4, but it had a high microbial resistance due to the perfect mechanical properties of YSZ.

It is worth noting that the fabricated TiO₂ -YSZ-Ag coating showed a perfect antimicrobial effect as well as the microbial corrosion resistance against the various kinds of microorganism that are examined. This perfect performance of TiO₂ -YSZ-Ag coating attributed to the synergistic work of TiO₂ and YSZ which in turn improves the surface properties such as corrosion and scratch resistance, it also improves the performance of nanoscale silver as anti-microbial growth.

8. CONCLUSION

Colloidal AgNPs were successfully synthesized by two step chemical reduction process using thermal reduction technique, reduction of aqueous silver nitrate using tri sodium citrate. The particle size of synthesized AgNPs was controlled by mixing time, temperature and silver nitrate concentrations. An AgNPs in all concentration show a good antimicrobial activity in almost kinds of bacteria and fungi. 5 mM concentration of colloidal silver nanoparticles had a perfect antimicrobial effect in all microorganisms that are used in this study.

Ammonia and ethylene glycol are a very useful choice to make high suspension solution suspension and to decrease the sedimentation ration of TiO₂ solution. The best TiO₂ nanopowder coating was performed at a flow rate of 0.05 mL/min and voltage of 10.5 kV for 45 min. ESD made a regular distribution of TiO₂ nanomaterials on the stainless-steel surface.

The optimum YSZ nanopowder coating was performed at a flow rate of 0.05 mL/min and an applied voltage of 7.5 kV for 30 min.

TiO₂ –YSZ coating was performed at a flow rate of 0.05 mL/min and an applied voltage of 9.2 kV for 30 min. The synergistic work of the YSZ with TiO₂ gave a homogenous distribution in the form of islands of nanocomposites on the target surface. The results clearly indicated that the coatings produced by ESD are very smooth surfaces and that the distribution of nanomaterials was regular on the surface of stainless steel.

The coating layer manufactured by ESD technique is a very thin layer. Moreover, a very good interaction and high adhesion between film and substrate was observed.

Low amount of AgNPs about (0.03 wt. %) was used in the final layer coating. For Ag film; the suitable deposition's set up for the coating device (ESD) was 0.02 ml as a flow rate and voltage of 12.5 kV for 45 min with 7 cm as a distance between the nozzle and the substrate surface. The synergic work of TiO₂ –YSZ matrix crystallization promotes Ag embedding into the outer layer of the film.

TiO₂–Ag coating had the highest pathogenic effects against all the microorganisms, but the coating surface suffering from a huge damage because of the microbial corrosion which is caused by enzymatic secretions of microorganisms. YSZ–Ag coating was not affected by the enzymatic secretions of microorganisms; on

the other side it had a normal antimicrobial activity. The fabricated TiO_2 –YSZ–Ag coating had a perfect antimicrobial effect as well as it showed a high microbial corrosion resistance against the various kinds of microorganism that which examined. This perfect performance of TiO_2 –YSZ–Ag coating attributed to the synergistic work of TiO_2 and YSZ which in turn improves the surface properties of corrosion and scratch resistance.



FEATURE WORK

1. Conducting physical and chemical tests of the fabricated films to determine their resistance in other industrial conditions.
2. Using different concentration of TiO_2 , AgNPs and YSZ as coating solution.
3. Using another nanomaterial as antimicrobial agent in the coating solutions.
4. Production of gold nanoparticles and use it as a coating material for biomedical devices and biosensor.



REFERENCE

- A. R. West, (2003). John Willy & Sons, Singapore.
- A.J. Trogolo, C.F. Rossitto, K.E. Welch, II, (2003). World Patent, WO 03/055941.
- Abou-Helal M.O, Seeber W.T, (2002). *Appl. Surf. Sci. j.* 195: 53.
- Aegerter, M.A., Mennig, M., (2004). Sol-Gel Technologies for Glass Producers and Users, *Springer*, pp. 193-202, ISBN 9781402079382.
- Aida V. Rudakova, Alexei V. Emeline, Kirill M. Bulanin, Lyudmila V. Chistyakova, Maria V. Maevskaya, Detlef W. Bahnemann, (2018). Self-cleaning Properties of Zirconium Dioxide Thin, *Journal of Photochemistry and Photobiology A: Chemistry* S1010-6030(18)31013-X.
- Aidla A, Uustare T, Kiisler A.A, Aarik J, Sammelseg V, (1997). *Thin Solid Films j.* 305: 270.
- Andreatta, F.; Aldighieri, P.; Paussa, L.; Di Maggio, R.; Rossi, S.; Fedrizzi, L. (2007). Electrochemical behaviour of ZrO₂ sol-gel pre-treatments on AA6060 aluminium alloy. *Electrochim. Acta*, 52, 7545–7555.
- Asta Sileikaite, Igoris Prosycevas, Judita Puiso, Algimantas Juraitis, Asta Guobienė, (2006). Analysis of Silver Nanoparticles Produced by Chemical Reduction of Silver Salt Solution. 1392–1320. *Materials Science*. Vol. 12, No. 4.
- Badrossamay M. R., McIlwee H. A., Goss, J. A., Parker K. K (2010). *Nano Lett.*, 10, 2257–2261. doi:10.1021/nl101355x.
- Balu S. S., Chittaranjan Bhakat, and Dr. Sanjay Harke, (2012). Synthesis of silver nanoparticles by chemical reduction and their antimicrobial activity *International Journal of Engineering Research & Technology (IJERT)* ISSN: 2278-0181 Vol. 1 Issue 6
- Bauer, A.W., Kirby, W.M., Sherris, J.C., Turck, M., (1966). Antibiotic susceptibility testing by a standardized single-disk method. *Am. J. Clin. Pathol.* 45 (4), 493–496.
- Beyene, F.G. (2016). A review on nanocoating of metallic structures to improve hardness and maintaining toughness. *I-Manager's J. Mater. Sci.*, 4, 32–41
- Besra L, Liu M, (2007). A review on fundamentals and applications of electrophoretic deposition (EPD). *Prog Mater Sci* 52:1–61
- Bleeker, E. A. J. Cassee, F. R. Geertsma, R. E. de Jong, W. H. Heugens, E. H. W. Koers-Jacquemijns, M. van De Meent, D. Oomen, A. G. Popma, J. Rietveld, A. G. Wijnhoven, S. W. P. (2012). Interpretation and implications of the

- European Commission's definition on nanomaterials; Letter report 601358001; RIVM: Bilthoven, Netherlands.
- Boostani, H.; Modirrousta, S, (2016). Review of Nanocoatings for Building Application. *Procedia Eng.*, 145, 1541–1548.
- Brinker C. J. and G. W. Scherer, (1990). Sol-gel science: the physics and chemistry of sol-gel processing., San Diego, CA, USA: vol. 8, academic Inc. Press.
- Brinker C.J, Frye G.L, Hurd A.J, Ashlet C.S, (1991). *Thin Solid Films j.* 97: 201.
- Brinker C.J, Scherer G.W, (1990). *Sol–Gel Science*, Academic Press, San Diego, CA.
- C, L., (2006). "Proteomic analysis of the mode of antibacterial action of silver nanoparticles". *J Proteome Res*, 5: p. 916-924
- Callister, W.D.; Rethwisch, D.G. , (2012). Fundamentals of Materials Science and Engineering an Integrated Approach, 3rd ed.; JohnWiley & Sons Inc.: Hoboken, NJ, USA.
- Chen, D. Qiao, X. Qiu, X. Chen, J, (2009). Synthesis and electrical properties of uniform silver nanoparticles for electronic applications. *J. Mater. Sci.* 44, 1076–1081.
- Choi Y, Yamamoto S, Umabayashi T, Yoshikawa M, (2004). *Solid State Ionics j.* 172:105.
- Choy, K.L., (2003). Chemical Vapour Deposition of Coatings, *Elsevier*, 48, p. 51–170.
- Chrysicopoulou P, Davazoglou D, Trapalis C, Kordas G, (1998). *Thin Solid Films j.* 323:188.
- D. Chen, L. Cao, F. Huang, P. Imperia, Y.-B. Cheng, and R. A. Caruso, (2010). *J. Am. Chem. Soc.* 132, 4438–4444. doi:[10.1021/ja100040p](https://doi.org/10.1021/ja100040p).
- D. Lu, J. Wang, L. Wang, D. Du, C. Timchalk, R. Barry, et al. (2011). *Adv. Funct. Mater.* 21, 4371–4378. doi:[10.1002/adfm.201100616](https://doi.org/10.1002/adfm.201100616).
- D.L. Gangotri, A.D. Chaware, (2004) *Paint India* September, 39–42.
- D.R. Baer, P.E. Burrows, A.A. El-Azab. (2003) *Prog. Org. Coat*, 47, 342–356.

- Danilcauk, M., Lund, A, Saldo, J, Yamada, H, Michalik, J, (2006). "Conduction electron spin resonance of small silver particles". *Spectrochimica. Acta. Part A.*, 63: p. 189-191.
- Dislich H., (1986) Sol-gel: science, processes and products. *Journal of Non-Crystalline Solids*. 80: p. 115-121.
- E. C. Subbarao and H. S. Maiti, (1988) "Science and technology of zirconia," *Advances in Ceramics*, vol. 24, pp. 731–737.
- Eduardo L. Crepaldi, Galo J. de A. A. Soler-Illia, David Grosso and Cle´ment Sanchez (2003) Nanocrystallised titania and zirconia mesoporous thin films exhibiting enhanced thermal stability *New J. Chem.*, , 27, 9–13 DOI: 10.1039/b205497n.
- El-Nour, K.M.M.A., Eftaiha, A, Al-Warthan, A, Ammar, R.A.A. (2010) Synthesis and applications of silver nanoparticles. *Arab. J. Chem.*, 3, 135–140.
- F. A. Al-Marhaby and R. Seoudi, (2016) Preparation and Characterization of Silver Nanoparticles and Their Use in Catalytic Reduction of 4-Nitrophenol *World Journal of Nano Science and Engineering*, 6, 29-37
<http://www.scirp.org/journal/wjnse>
<http://dx.doi.org/10.4236/wjnse.2016.61003>
- Feng, Q., Wu, J, Chen, GQ, Cui, FZ, Kim, TN, Kim, JO, (2008) "A mechanistic study of the antibacterial effect of silver ions on Escherichia coli and Staphylococcus aureus". *J. Biomed. Mater. Res.*, 52: p. 662-668.
- Ferreri , S. Calderon V. , R. Escobar Galindo, C. Palacio, M. Henriques , A.P. Piedade , S. Carvalho (2015) Silver activation on thin films of Ag–ZrCN coatings for antimicrobial activity *Materials Science and Engineering C* 55 (2015) 547–555.
- Fork D.K, Fenner D.B, Connell G.A.N, Phillips J.M, Geballe T.H (1990) Epitaxial yttrium-stabilized zirconia on hydrogen-terminated Si by pulsed laser deposition, *Appl. Phys. Lett.* j. 57: 1137.
- G. Borkow, (2005) Hygienic Coatings & Surfaces, PRA Coatings Technology Centre, Paris, 16–17 March, paper 20.
- G. Dutta, K. P. Hembram, G. M. Rao, and U. V. Waghmare, (2006) "Effects of O vacancies and C doping on dielectric properties of ZrO₂/ZrO₂: a first-principles study," *Applied Physics Letters*, vol. 89, no. 20, Article ID202904.

- G. Schimid, L. F. Chi. (1998) "Metal Clusters and Colloids," *Adv.Mater.*, 10 (7), 515).
- G. V. Krylova Yu. I. Gnatyuk N. P. Smirnova A. M. Eremenko V. M. Gun'ko (2009) Ag nanoparticles deposited onto silica, titania, and zirconia mesoporous films synthesized by sol-gel template method *J Sol-Gel Sci Technol* 50:216–228 DOI 10.1007/s10971-009-1954-x
- G. Yamauchi, Y. Riko, Y. Yasuno, T. Shimizu, N. Funakoshi, (2004), *Nano and Hybrid Coatings*, The Paint Research Association, Manchester, UK, 24–25 January 2005, paper 20.58. J. Ross, *Polymer Paint Color J.* 194(4479), 18–20.
- Ghosh, S.K. Dey, G.K. Dusane, R.O. Grover, A.K. (2006) Improved pitting corrosion behaviour of electrodeposited nanocrystalline Ni-Cu alloys in 3.0 wt.% NaCl solution. *J. Alloys Compd.*, 426, 235–243.
- H. J. Lee, D. Y. Kim, J. S. Yoo, J. Bang, S. Kim, S. M. Park, *Bull Korean Chem. Soc.*, 28, 953.
- H. Kozuka and M. Hirano, (2000) "Radiative striations and surface roughness of alkoxide-derived spin coating films," *Journal of Sol-Gel Science and Technology*, vol. 19, no. 1–3, pp. 501–504.
- Haes, A.J.; Duyne, R.P.V. (2002) A Nanoscale optical biosensor: sensitivity and selectivity of an approach based on the localized surface plasmon resonance spectroscopy of triangular silver nanoparticles. *J. Am. Chem. Soc.*, 124, 10596–10604.
- Hashimoto K, Irie H, Fujishima A, (2005). TiO₂ photocatalysis: a historical overview and future prospects. *Jpn J Appl Phys Part 1: Regul Pap Brief Commun Rev Pap*, 44, 8269-8285, <http://dx.doi.org/10.1143/JJAP.44.8269>
- Hibbard, G.; Aust, K.T.; Palumbo, G.; Erb, U. (2001). Thermal Stability of Electrodeposited Nanocrystalline Cobalt. *Scr. Mater.*, 44, 513–518.
- Hu L, Yoko T, Kozuka H (1992). *Thin Solid Films* j. 219: 18.
- Hu L, Yoko T, Kozuka H, Sakka S, (1992). *Thin Solid Films* j. 18: 219.
- J, C.X.a.S.H., 2008 "Nanosilver: A Nanoproduct in Medical Applications". *Toxicol Lett*, 176: p. 1-12.

- J. C. Ray, D.-W. Park, and W.-S. Ahn, (2006). "Chemical synthesis of stabilized nanocrystalline zirconia powders," *Journal of Industrial and Engineering Chemistry*, vol. 12, no. 1, pp. 142–148.
- J. George, M. Dekker, (1992). *Preparation of Thin Films*, New York
- J. H. Shim, C. Chao, H. Huang, and F. B. Prinz, (2007). *Chem. Mater.* 19, 3850–3854. doi:[10.1021/cm070913t](https://doi.org/10.1021/cm070913t).
- J. He, J. Chen, L. Ren, Y. Wang, C. Teng, M. Hong, et al., (2014). *ACS Appl. Mater. Interfaces* 6, 2718–2725. doi:[10.1021/am405202d](https://doi.org/10.1021/am405202d).
- J. L. Gole, S. M. Prokes, J. D. Stout, O. J. Glembocki, and R. Yang, (2006). "Unique properties of selectively formed zirconia nanostructures," *Advanced Materials*, vol. 18, no. 5, pp. 664–667.
- J.H. Yue, S. (2012). Tribological behavior of electrodeposited Zn, Zn–Ni, Cd and Cd–Ti coatings on low carbon steel substrates. *Tribiol. Int.*, 56, 107–120.
- Jaworek A., Sobczyk, A.T. (2008). Electro spraying route to nanotechnology: An overview. *J. Electrostat.*, 66, 197–219.
- K. Joy, S. Lakshmy, Prabitha B. Nair, Georgi P. Daniel. (2012). *Journal of Alloys and Compounds* 512, 149-155.
- K. L. Chopra, (1969). "Thin Film Phenomena" Mc. Graw Hill, New Delhi, ISBN: 978-0070107991.
- K. L. Chopra, L. K. Malhotra, (1984). "Thin Film Technology and Applications", (Ed.) K. L. Chopra, L. K. Malhotra TMH Publishing Co., New Delhi, India.
- K. Mallikarjuna, G. R. Dillip, G. Narasimha, N. John Sushma, B. Deva Prasad Raju, (2012). "Phytofabrication and Characterization of Silver Nanoparticles from Piper betle Broth", *Res. J. Nanosci. and Nanotech*, 2, 17-23.
- K.V. Anisimov et al. (eds.), (2016). Proceedings of the Scientific-Practical Conference "Research and Development -", https://doi.org/10.1007/978-3-319-62870-7_49
- Kaiser JP, Zuin S, Wick P, (2013). Is nanotechnology revolutionizing the paint and lacquer industry? A critical opinion. *Sci Total Environ* 442, 282-289. <http://dx.doi.org/10.1016/j.scitotenv.2012.10.009>
- Kang, Suk-Joong L. (2005). Sintering: Densification, Grain Growth, and Microstructure. *Elsevier Ltd.* pp. 9–18.

- Kim, D., Jeong, S. and Moon, J. (2006). Synthesis of Silver Nanoparticles Using the Polyol Process and the Influence of Precursor Injection. *Nanotechnology*, 17, 4019-4024. <http://dx.doi.org/10.1088/0957-4484/17/16/004>
- Kim, J., Kuk, E, Yu, K, Kim, JH, Park, SJ, Lee, HJ, Kim, SH, Park, YK, Park, YH, Hwang, C-Y, Kim, YK, Lee, YS, Jeong, DH, Cho, MH, (2007). "Antimicrobial effects of silver nanoparticles". *Nanomedicine*, 3(95-101).
- Kumar, N. Kumbhat, S. (2014). Carbon-Based Nanomaterials. *Essentials in Nanoscience and Nanotechnology*; John Wiley & Sons, Inc.: Hoboken, NJ, U.S.A., 2016; pp 189–236. doi:10.1002/9781119096122.ch5
- Kumari L, Du GH, Li WZ, Vennila RS, Saxena SK, Wang DZ. (2009). Synthesis, microstructure and optical characterization of zirconium oxide nanostructures. *Ceramics International*. ;35(6):2401–2408.
- L. Kumari, W. Li, J. Xu, R. Leblanc, D. Wang, Y. Li, H. Guo, and J. Zhang (2009). Controlled hydrothermal synthesis of zirconium oxide nanostructures and their optical properties. *Cryst. Growth Des.* 9, (9), 3874–3880.
- Lai Y, Wang L, Liu D, Chen Z, Lin C (2015) TiO₂-based nanomaterials: design, synthesis and applications. *J Nanometer* 2015:1–3
- Larson S.A, Falconer J.L (1994) *Appl. Catal. B: Environ.* j. 4: 149.
- Li, Q. Yang, X.; Zhang, L.; Wang, J.; Chen, B. (2009). Corrosion resistance and mechanical properties of pulse electrodeposited Ni-TiO₂ composite coating for sintered NdFeB magnet. *J. Alloys Compd.*, 482, 339–344.
- Li, R. and Chen, L., (2005). A paint containing nano titanium oxide and nano silver, and its preparation method. Chinese Patent, CN10027622.
- Li, X. Guerieri, P. Zhou, W. Huang, C. Zachariah, M.R. 2015 Direct deposit laminate nanocomposites with enhanced propellant properties. *ACS Appl. Mater. Interfaces*, 7, 9103–9109.
- Lu, H. Li, Y. Wang, F. (2006). Enhancement of the electrochemical behavior for Cu₇₀Zr alloy by grain refinement. *Surf. Coat. Technol.*, 201, 3393–3398.
- M. A. Meyers, A. Mishra, D. J. Benson, (2006). "Mechanical properties of nanocrystalline materials", *Prog. Mater sci.*, 51 (4), 427-556.

- M. C. Daniel, D. Astruc, (2004). "Gold nanoparticles: assembly, supramolecular chemistry, quantum-size-related properties, and applications toward biology, catalysis, and nanotechnology". *Chem Rev*, 104 (1), 293-346.
- M. Ohring, (1992) *The Materials Science of Thin Films*, Academic press limited.
- M. Willert, R. Rothe, K. Landfaster, M. Antonietti, (2001). "Synthesis of inorganic and metallic nanoparticles by miniemulsification of molten salts and metals", *Chem. Mater.*, 13 (12), 4681–4685.
- Ma, J.; Xu, J.; Jiang, S.; Munroe, P.; Xie, Z. (2016). Effects of pH value and temperature on the corrosion behavior of a Ta₂N nanoceramic coating in simulated polymer electrolyte membrane fuel cell environment. *Ceram. Int*, 42, 16833–16851.
- Mahapatro, A, (2015). Bio-functional nano-coatings on metallic biomaterials. *Mater. Sci. Eng. C*, 55, 227–251.
- Matsumura, Y., Yoshikata, K, Kunisaki, S, Tsuchido, T, (2003). "Mode of bacterial action of silver zeolite and its comparison with that of silver nitrate". *Appl. Environ. Microbiol.*, 69(4278-4281). Page | 63
- Mattox, D.M., (1998). *Handbook of Physical Vapor Deposition (Pvd) Processing: Film Formation, Adhesion, Surface Preparation and Contamination Control*, William Andrew, p.50-70, ISBN 9780815514220.
- McGee, J.D. Thomas, S.S. Bammel, B.D. Bryden, T.R. (2012). Release on Demand Corrosion Inhibitor Composition. U.S. Patent No. 8241524.
- Mittal, V. (2010). *Polymer Nanocomposites: Synthesis, Microstructure, and Properties*. In *Optimization of Polymer Nanocomposite Properties*; WILEY-VCH Verlag GmbH & Co. KGaA: Weinheim, Germany, pp. 1–19, ISBN 9783527325214.
- Morones, J., Elechiguerra, JL, Camacho, A, Holt, K, Kouri, JB, Ramirez, JT, Yacaman, MJ, (2005). "The bactericidal effect of silver nanoparticles". *Nanotechnology*, 16: p. 2346-2353
- Morrow, W. H. and McLean, L. J., (2003). Self-cleaning UV reflective coating, its applying methods, and UV irradiating device prepared therefrom. U.S. Patent, US 2003059549.

- Mosavat, S.H.; Shariat, M.H.; Bahrololoom, M.E. (2012). Study of corrosion performance of electrodeposited nanocrystalline Zn-Ni alloy coatings. *Corros. Sci.*, 59, 81–87.
- Mritunjai Singh, Shinjini Singh, S. Prasad, I. S.Gambhir, (2008). “Nanotechnology In Medicine And Antibacterial Effect Of Silver Nanoparticles”, Digest Journal of Nanomaterials and Biostructures Vol. 3, No.3, p. 115 – 122.
- N. Savithramma, M. Linga Rao, K. Rukmini and P. Suvarnalatha devi, (2011). “Antimicrobial activity of Silver Nanoparticles synthesized by using Medicinal Plants”, *International Journal, ChemTech Res.* 3(3).
- N.T. Soo, N. Prastomo, A Matsuda, G. Kawamura, H. Muto, A.F. Mohd Noor, Z. Lockman, K.Y. Cheong, (2012). *Applied Surface Science* 258(2012) 5250-5258
- Nguyen-Tri, P. Nguyen, T.A. Carriere, P. Ngo Xuan, C. (2018). Nanocomposite Coatings: Preparation, Characterization, Properties, and Applications. *Int. J. Corros.*, 2018, 4749501.
- Ohring, Milton (2002). “Materials Science of Thin Films Deposition and Structure” 2nd edition, Elsevier, Inc, ISBN: 978-0-12-524975-1.
- Oliveira, M. Machado, A. (2013). Preparation of polymer-based nanocomposites by different routes. *Nanocomp. Synth. Charact. Appl.*, 1–22.
- P. M. Martin, (2010). *Handbook of Deposition Technologies for Films and Coatings*.
- Piconi C, Maccauro G, (1999). Zirconia as a ceramic biomaterial. *Biomaterials.* 20(1):1–25.
- Pierson, H.O., (1999). Handbook of Chemical Vapor Deposition, 2nd Edition: Principles, Technology and Applications, William Andrew, p. 234-345, ISBN 9780815514329.
- Ponraj J. S., G. Attolini, and M. Bosi, (2013). Review on Atomic Layer Deposition and Applications of Oxide Thin Films. *Critical Reviews in Solid State and Materials Sciences*, 38: p. 203-233.
- Pokropivny V. V., Skorokhod V. V. 2007 *Mater. Sci. Eng., C*, 27, 990–993. doi:10.1016/j.msec.2006.09.023.

- Ramona-Crina SUCIU, Marcela-Corina ROȘU, Teofil-Dănuț SILIPAȘ, Alexandru Radu BIRIȘ, Ioan BRATU and Emil INDREA (2011). TiO₂ thin films prepared by spin coating technique *Rev. Roum. Chim.*, 56(6), 607-612
- Ratyakshi and Chauhan RP. (2009). Colloidal synthesis of silver nanoparticles *Asian journal of chemistry* Vol. 21, No 10. S113-116.
- Rosell-Llompart, J., and J. Fernandez de la Mora. (1994). "Generation of monodisperse droplets 0.3 to 4 μm in diameter from electrified cone-jets of highly conducting and viscous liquids." *Journal of Aerosol Science* 25: 1093-1119.
- Rout, T. K., Jha, G., Singh, A. K., Bandyopadhyay, N. and Mohanty, O. N., (2003). Development of conducting polyaniline coating: a novel approach to superior corrosion resistance. *Surf. Coat. Technol.*, 167, 16–24.
- S. Mohan, in (1994). "Proc. Advanced Course on Thin Film Processing", Instrumentation and Services unit, I. I. Sc. Bangalore, India.
- S. Park, J. M. Vohs, and R. J. Gorte, (2000). "Direct oxidation of hydrocarbons in a solid-oxide fuel cell," *Nature*, vol. 404, no. 6775, pp. 265–267.
- Salas P, de la Rosa-Cruz E, Diaz-Torres LA, Castaño VM, Meléndrez R, Barboza-Flores M. (2003). Monoclinic ZrO₂ as a broad spectral response thermoluminescence UV dosimeter. *Radiation Measurements.* ; 37(2):187–190.
- Schaefer, H.-E. (2010). Nanoscience; Springer: Berlin/Heidelberg, Germany; Stuttgart, Germany, Volume 1, ISBN 9788578110796.
- Schuh, C.A.; Nieh, T.G.; Iwasaki, H. (2003). The effect of solid solution W additions on the mechanical properties of nanocrystalline Ni. *Acta Mater.* 51, 431–443.
- Seshan K (2001). *Handbook of thin-film deposition processes and Techniques, Principles, Methods, Equipment and Applications*, Noyes Publications/William Andrew Publishing.
- Shukla RK, Sharma V, Pandey AK, Singh S, Sultana S, Dhawan A, (2011). ROS-mediated genotoxicity induced by titanium dioxide nanoparticles in human epithelial cells. *Toxicol in Vitro* 25, 231-241. <http://dx.doi.org/10.1016/j.tiv.2010.11.008>

- Sinan Salman Hamdi, (2016). Synthesis of Ag –TiO₂ Thin Films by Spin Coating Process *Eng. &Tech.Journal, Vol.34, Part (A), No.13*
- Sinem Cevik & Mevlüt Gürbüz (2018). Induction Heated Sintering and Mechanical Properties of Electrosprayed Nano YSZ, *Transactions of the Indian Ceramic Society, 77:1, 37-44*, DOI: 10.1080/0371750X.2018.1455537
- Sondi, I., Salopek-Sondi, B, (2004). "Silver nanoparticles as antimicrobial agent: a case study on E. coli as a model for Gram-negative bacteria". *J. Colloid Interface Sci., 275: p. 177-182.*
- Sun, Y.; Mayers, B.; Herricks, T.; Xia, Y. Polyol (2003). Synthesis of uniform silver nanowires: a plausible growth mechanism and the supporting evidence. *Nano Lett., 3, 955–960.*
- T. Pavliashvili, T. Kalabegishvili, M. Janjalia, E. Ginturi, and G. Tsertsvadze (2015). Preparation of silver nanoparticles in silver nitrate solution by using tannin *Section B-Short communication Eur. Chem. Bull., 4(1), 30-32*
- T. Rentschler, A. Claßen, (2002). *Eur. Coat. J., 9, 24–27.*
- T. Sawitowski, K. Schulte, (2005). *Nano and Hybrid Coatings, PRA Coatings Technology, 24–25 January, Manchester, UK, Paperno. 8.*
- Takeda S, Suzuki S, Odaka H, (2001). *Thin Solid Films j. 392: 338.*
- Takenobu, T., Miura, N., Lu, S.Y., Okimoto, H., Asano, T., Shiraishi, M. and Iwasa, Y. (2009). Ink-Jet Printing of Carbon Nanotube Thin-Film Transistors on Flexible Plastic Substrates. *Applied Physics Express, 2, 0250051-0250053.* <http://dx.doi.org/10.1143/APEX.2.025005>
- Tang, K., and A. Gomez. (1994). "On the structure of an electrostatic spray of monodisperse droplets." *Physics of Fluids 6: 2317-2332.*
- Thompson, D.G., Stokes, R.J., Martin, R.W., Lundahl, P.J., Faulds, K. and Graham, D. (2008). Synthesis of Unique Nanostructures with Novel Optical Properties Using Oligonucleotide Mixed-Metal Nanoparticle Conjugates. *Small, 4, 1054-1057.* <http://dx.doi.org/10.1002/sml.200700938>
- V. Colvin, M. Schlamp, A. Alivisatos, (1994). "Light emitting diodes made from cadmium selenidenanocrystals and a semiconducting polymer.". *Nature, 370, 354-357.*

- V.V. Verkholtantsev, (2003). *Eur. Coat. J.*, 10,32–37.
- Vyom Parashar, Rashmi Parashar, Bechan Sharma, Avinash C. Pandey, 2009 “Parthenium Leaf Extract Mediated Synthesis Of Silver Nanoparticles: A Novel Approach Towards Weed Utilization”, *Digest Journal of Nanomaterials and Biostructures* Vol. 4, No.1, p. 45 – 50.
- W. Schockley, H. J. Queissor, (1961). *J Appl Phys*, 32, 510.
- Wagener, (2005). *Hygienic Coatings & Surfaces*, PRA Coatings Technology Centre, Paris, 16–17 March, paper 14.
- Wagner, S. Gondikas, A. Neubauer, E.; Hofmann, T. von der Kammer, F, (2014). *Angew. Chem., Int. Ed.*, 53, 12398–12419. doi:10.1002/anie.201405050
- Wang M.T, Wang T.H, Lee J, (2005). Electrical conduction mechanism in high-dielectric constant ZrO₂ thin films, *Microelectron. Reliability* j. 45: 969.
- Wang, L. Zhang, J. Gao, Y. Xue, Q. Hu, L. Xu, T. (2006). Grain size effect in corrosion behavior of electrodeposited nanocrystalline Ni coatings in alkaline solution. *Scr. Mater.*, 55, 657–660.
- Wang, L.; Lin, Y.; Zeng, Z.; Liu, W.; Xue, Q.; Hu, L.; Zhang, J. (2007). Electrochemical corrosion behavior of nanocrystalline Co coatings explained by higher grain boundary density. *Electrochim. Acta*, 52, 4342–4350.
- Wang, Y.; Zhang, L.; Hu, Y.; Li, C. (2016). Comparative Study on Optical Properties and Scratch Resistance of Nanocomposite Coatings Incorporated with Flame Spray Pyrolyzed Silica Modified via in-situ Route and ex-situ Route. *J. Mater. Sci. Technol.*, 32, 251–258.
- Wasa K, Kitabatake M, Adachi H, (2004). Thin film materials technology: sputtering of control compound materials, *Springer Science & Business Media*.
- Watchman, J.D.; Haber, R.A. (1993). Ceramic Films and Coatings—An overview. In *Ceramic Films and Coatings*; Noyes Publications: New York, NY, USA, p. 1.
- Wendel H, Holzschuh H, Suhr H, Erker G, Dehnicke S, Mena M, (1990). Thin zirconium dioxide and yttrium oxide-stabilized zirconium dioxide films prepared by plasma-CVD, *Mod. Phys. Lett. B* j. 4: 1215.

- Wright PK, Evans AG. (1999). Mechanisms governing the performance of thermal barrier coating. *Current Opinion in Solid State and Materials Science.*; 4:25–30.
- Wu, J.; Shen, X.; Jiang, L.; Wang, K.; Chen, K. (2010). Solvothermal synthesis and characterization of sandwich-like graphene/ZnO nanocomposites. *Appl. Surf. Sci.*, 256, 2826–2830.
- Xiong, Y., Siekkinen, A.R., Wang, J., Yin, Y., Kimb, M.J. and Xia, Y. (2007). Synthesis of Silver Nanoplates at High Yields by Slowing Down the Polyol Reduction of Silver Nitrate with Polyacrylamide. *Journal of Materials Chemistry*, 17, 2600-2602. <http://dx.doi.org/10.1039/b705253g>
- Xu, C.S. Xie, (2003). *Prog. Org. Coat.*, 46,297–301.
- Y. Adraider, Y.X.Pang, F.Nabhani, S.N.Hodgson, M.C. Sharp, A.Al-Waidh, (2013). Fabrication of zirconium oxide coatings on stainless steel by a combined laser/sol–gel technique *Ceramics International* 39(2013)9665–9670
- Yakutik IM, Shevchenko GP, Rakhmanov SK. (2004). The Formation of Monodisperse Spherical Silver Particles *Colloids and Surfaces A: Physicochemical and Engineering Aspects* 242. pp. 175 – 179
- Yousaf, S.; Alhnan, M.A.; Abdallah, A.; Abdallah, B.; Khan, I.; Ahmed, W, (2015). Nanocoatings in medicine: Antiquity and modern times. In *Emerging Nanotechnologies for Manufacturing*; Ahmed, W., Jackson, M.J., Eds.; Elsevier Inc.: Oxford, UK, pp. 418–443, ISBN 9780323289900.
- Zelner M, Minti H, Reisfeld R, Cohen H, Tenne R (1997) Preparation and characterization of CdS films synthesized in situ in zirconia sol-gel matrix, *Chem. Mater. J.* 9: 2541.
- Zhang Q, Shen J, Wang J, Wu G, Chen L, (2000). Sol-gel derived ZrO₂-SiO₂ highly reflective coatings. *International Journal of Inorganic Materials*; 2(4):319–323.
- Zhang R, Niu Y, Li Y, Zhao C, Song B, Li Y, Zhou Y, (2010). Acute toxicity study of the interaction between titanium dioxide nanoparticles and lead acetate in mice. *Environ Toxicol Pharmacol* 30, 52-60.
- Zhang, J. Langille, M. R. Mirkin, C. A. (2011). *Nano Lett.*, 11, 2495–2498. doi:10.1021/nl2009789

Zhang, X.-F.; Liu, Z.-G.; Shen, W.; Gurunathan, S. (2016). Silver nanoparticles: Synthesis, characterization, properties, applications, and therapeutic approaches. *Int. J. Mol. Sci.*, 17, 1534

Zheng S.K, Wang T.M, Xiang G, Wang C, (2001). *Vacuum j.* 62: 361.



CURRICULUM VITAE



Name and Surname: Abdulmohsin AL AIROA

Place of Birth: IRAQ

Date of Birth: 06.10.1984

Foreign Language: English

Education Status

High School: SAMARAA

License: Tikrit University, Engineering Faculty, Chemical Engineering department (2007-2008).

Work Experience

- Pharmaceutical industry for 8 years (2006 -2014).
- 2 years in Pharmaceutical production (2006 -2008).
- 4 as a super visor of syrup analysis lab. (2008 -20012).
- 2 as an analyzer in antibiotic analysis lab. (2012 – 2014).

RELATED WORK

1. Production of Novel $\text{Tio}_2\text{-AgNP}$ - YSZ Thin Film for Antimicrobial and Multifunctional Usage by Electrospray Deposition System.
2. Preparation and Characterization of Colloid Silver Nanoparticles and Their Antimicrobial Activity.